Summer 2015

Hydrologic and hydraulic model development for flood mitigation and routing method comparison in Soap Creek Watershed, Iowa

Jingyun Sun
University of Iowa

HYDROLOGIC AND HYDRAULIC MODEL DEVELOPMENT FOR FLOOD MITIGATION AND ROUTING METHOD COMPARISON IN SOAP CREEK WATERSHED, IOWA

by

Jingyun Sun

A thesis submitted in partial fulfillment of the
requirements for the Master of Science degree in
Civil and Environmental Engineering
in the Graduate College of
The University of Iowa

August 2015

Thesis Supervisors: Professor Larry J. Weber
Professor Nathan Young

Graduate College
The University of Iowa
Iowa City, Iowa

CERTIFICATE OF APPROVAL

_____

MASTER'S THESIS

_____

This is to certify that the Master's thesis of

Jingyun Sun

has been approved by the Examining Committee
for the thesis requirement for the Master of Science
degree in Civil and Environmental Engineering at the
August 2015 graduation.

Thesis Committee: _____
Larry Weber, Thesis Supervisor

_____
Nathan Young, Thesis Supervisor

_____
Allen Bradley

ACKNOWLEDGMENTS

Firstly, I want to thank to my advisor, Dr. Larry Weber for giving me the opportunity to become a member of IIHR-Hydroscience and Engineering and work on the Iowa Watersheds Project. I want to thank him for the help and professional advice he has given to me. I also want to thank my co-advisor, Dr. Nathan Young for his intelligent guidance on the model development and my thesis development. Moreover, I want to thank Dr. Allen Bradley for his innovative thoughts on how to calibrate the model and performing the result analysis.

I would like to take this opportunity to thank the entire Iowa Watersheds Project team for their support throughout my time at IIHR. I have really enjoyed working in such a wonderful team with so many intelligent and responsible people. At the same time, I have also made a lot of friends at IIHR and they made my every minute at IIHR meaningful and colorful.

Finally, I want to thank my family for their love and support. None of my goals would have been achieved without their endless support.

I believe that coming to the University of Iowa is one of the best decisions I've ever made in my life.

ABSTRACT

The primary objective of this thesis is to develop hydrologic and hydraulic models for the Soap Creek Watershed, IA for the evaluation of alternative flood mitigation strategies and the analysis of the differences between hydrologic and hydraulic routing methods.

In 2008, the state of Iowa suffered a disastrous flood that caused extensive damage to homes, agricultural lands, commercial property, and public infrastructures. To reduce the flood damage across Iowa, the U.S. Department of Housing and Urban Development (HUD) awarded funds to the Iowa Flood Center and IIHR-Hydroscience & Engineering at the University of Iowa to conduct the Iowa Watersheds Project. The Soap Creek Watershed was selected as one of the study areas because this region has suffered frequent severe floods over the past century and because local landowners have organized to construct over 130 flood detention ponds within it since 1985.

As part of the Iowa Watersheds Project, we developed a hydrologic model using the U.S. Army Corps of Engineers' (USACE) Hydrologic Center's hydrologic Modeling System (HEC-HMS). We used the hydrologic model to evaluate the effectiveness of the existing flood mitigation structures with respect to discharge and to identify the high runoff potential areas. We also investigated the potential impact of two additional flood mitigation practices within the Soap Creek Watershed by utilizing the hydrologic model, which includes changing the land use and improving the soil quality. The HEC-HMS model simulated 24-hour design storms with different return periods, including 10, 25, 50, and 100 year. The results from modeling four design storms revealed that all three practices can reduce the peak discharge at different levels. The existing detention ponds were shown to reduce the peak discharge by 28% to 40% depending on the choice of observed locations

and design storms. However, changing the land use can reduce the peak discharge by an average of only 1.0 %, whereas improving the soil quality can result in an average of 15 % reduction.

Additionally, we designed a hydraulic model using the United States Army Corps of Engineers' (USACE) Hydrologic Engineering Center's River Analysis System (HEC-RAS) to perform a comparative evaluation of hydrologic and hydraulic routing methods. The hydrologic routing method employed in this study is the Muskingum Routing method. We compare the historical and design storms between HEC-HMS, HEC-RAS, and observed stage hydrographs and take the hydrograph timing, shape, and magnitude into account. Our results indicate that the hydraulic routing method simulates the hydrograph shape more effectively in this case.

PUBLIC ABSTRACT

In 2008, the state of Iowa suffered a disastrous flood that caused extensive damage to homes, agricultural lands, commercial property, and public infrastructures. To reduce flood damage across Iowa, the U.S. Department of Housing and Urban Development (HUD) awarded funds to the Iowa Flood Center and IIHR-Hydroscience & Engineering at the University of Iowa to conduct the Iowa Watersheds Project. The Soap Creek Watershed was selected as one of the study areas because this region has suffered frequent severe floods over the past century and because local landowners have organized to construct over 130 flood detention ponds within it since 1985.

Although the detention pond is a widely accepted flood control practice, its effectiveness as a system to reduce the peak flow rate has rarely been investigated. One primary objective of this thesis is to evaluate the benefits that these detention basins could bring to the downstream areas of the Soap Creek Watershed. The thesis also provides an overview of the physical characteristics of the watershed, which can help local residents gain a better understanding of their living environment with respect to streams, soil type, land use, and so on. In order to achieve this goal, we developed a numerical model that can mimic the process by which rainfall is converted into runoff. In addition, we developed a different numerical model that simulates how water flows through the channel. The second objective of the model is to compare these two models with respect to technology.

TABLE OF CONTENTS

LIST OF TABLES

LIST OF FIGURES

CHAPTER 1. INTRODUCTION

1.1. Description of the Iowa Watersheds Project

The state of Iowa suffered several significant floods during the past decades, which adversely affected the local residents' and communities' economic, social, and environmental livelihoods. The Great Flood of 1993, with its $15 billion in damages, was one of the most costly and devastating floods to ever occur in the United States (Larson, 1993). For Iowa, however, damages from the 2008 floods were locally much worse than the Great Flood of 1993, and 85 of Iowa's 99 Countries were declared disaster areas in the 2008 event. Due to the severity of flooding, the U.S. Department of Housing and Urban Development (HUD) awarded funds to the Iowa Flood Center (IFC), a unit within IIHR – Hydroscience & Engineering at the University of Iowa, to conduct the Iowa Watersheds Project in the spring of 2012. The goal of the project was to evaluate watershed-scale flood mitigation alternatives. Four watersheds were selected for this project: the Middle Raccoon River Watershed, Soap Creek & Chequest Creek Watersheds, Turkey River Watershed, and Upper Cedar River Watershed. Figure 1.1 illustrates the locations of these selected watersheds. During this project, the IFC worked closely with the Watershed Management Authorities (WMA), which consists of representatives from counties, cities, and soil and water conservation districts within each watershed.

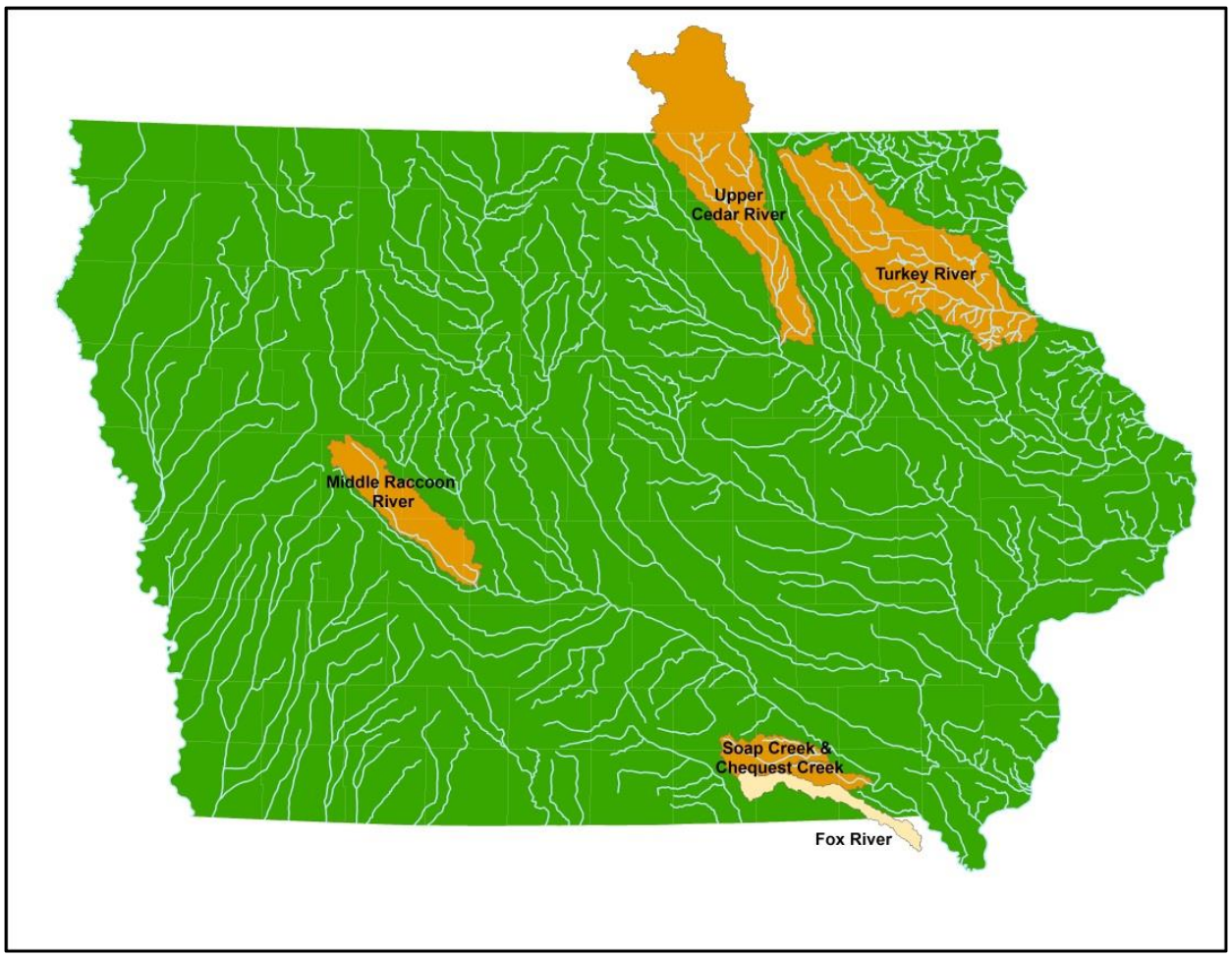

Figure 1.0.1 Iowa Watersheds Project Study Areas

The Iowa Watersheds Project aims to plan, implement, and evaluate watershed projects to lessen the severity and frequency of flooding in Iowa (IIHR, 2012). This large project is divided into two phases. Phase I includes a comparison of the four watersheds, data collection, hydrologic model development, and assessment of watershed scenarios that seek to reduce flood damages (Iowa Flood Center, 2012). Phase I began in June 2012 and concluded with the submission of a hydrologic assessment report to the WMA. Phase II focuses on the construction and implementation of flood mitigation projects. The Turkey River, Upper Cedar River, and Soap Creek Watersheds have been selected to receive $1.5 million each to fund the construction

of small-scale flood mitigation projects. Phase II began in the fall of 2013 and is projected to be completed in the summer of 2017.

One objective of this thesis is to complete Phase I of the Iowa Watersheds Project for the Soap Creek Watershed. In order to achieve this goal, we developed a hydrologic model (HEC-HMS) for the Soap Creek Watershed, which we used to simulate the effects of the existing pond system on peak discharge, to identify areas of high runoff potential where additional practices might have the greatest benefit, and to assess the potential impact of additional mitigation practices. Additionally, to better understand how differences between hydrologic and hydraulic routing methods affect runoff predictions, we developed a hydraulic model (HEC-RAS) for the Soap Creek Watershed's major tributaries. The hydrologic routing method employed in the hydrologic model is the Muskingum Routing Method. Therefore, the remainder of the thesis focuses on the comparison between the Muskingum Routing Method and the hydraulic routing method. We also compare the results generated from the two different model programs (HEC-HMS and HEC-RAS). Generally, the hydraulic routing method predicted lower peak discharges and a longer time base of the hydrograph than the hydrologic routing method.

1.2. Thesis Outline

This thesis is organized into 7 chapters. Chapter 2 contains a literature review, which is comprised of an introduction of detention basins, regionalization methodology used to calibrate rainfall-runoff models in ungaged watershed as well as hydrologic and hydraulic routing methods. Chapter 3 provides an overview of the physical characteristics throughout the Soap Creek Watershed, including its current land use, soil type, previous flood records, and so on. Chapters 4 and 5 introduce the development of hydrologic and hydraulic models, respectively. Chapter 4 presents the methodologies which are used to determine the inputs of the hydrologic

model, including rainfall data, initial base flow, and curve number (CN). The model calibration and validation are necessary before running any simulation. This part was completed in Chapter 4. Chapter 5 introduces more details about the hydraulic model's development, including treatment of the channel, junctions, and bridges. Chapter 5 also discusses the boundary and initial conditions used in the hydraulic model. Chapter 6 discusses the application of both the hydrologic and hydraulic models. For the hydrologic model, we discuss the benefits that existing ponds provide to downstream areas, how to identify the high runoff potential areas, and two hypothetical increased infiltration practices within the watershed. In addition, we compare the hydrologic and hydraulic routing method results. Chapter 7 presents a summary of the results and conclusions.

CHAPTER 2. LITERATURE REVIEW

2.1. Introduction

This chapter offers a literature review of three main topics related to this thesis: 1) detention basins; 2) the regionalization methodology used to calibrate rainfall-runoff models in ungaged watersheds; and 3) a description of the hydrologic and hydraulic routing methods. The literature review firstly provides recent studies relating to the evaluation of the effectiveness of a network of detention basins in reducing flood peak. It also introduces alternative methods to calibrate a hydrologic model for ungaged basins. This information prepares the reader for the calibration sections of the thesis. Finally, this chapter provides an overview of two different routing methods in order to help readers gain a more complete understanding of the results analysis in the following chapters.

2.2. Detention Basins

Flooding is a natural hazard that can cause devastating damage. To protect people and property from this hazard, many kinds of flood mitigation practices have been developed to lower either the damage caused by floods or the likelihood of their happening. Generally, flood mitigation practices involve various kinds of man-made structures such as dams, detention basins, levees, floodwalls, embankments, diversions, etc. One of the most commonly used practices is the detention basin, which was adopted by the Soap Creek Watershed, which is the study area of this thesis.

Detention basins are designed to reduce peak flow by temporarily storing the excess storm water and then releasing the water volume at allowable rates over an extended period (Ravazzani et al., 2014). Detention basins can be either wet or dry. Wet detention basins are designed to permanently retain some volume of water all the time, while dry detention basins are

not. It is very easy to investigate the hydrologic effectiveness of an individual detention basin. However, the effectiveness of a detention basin systems is not that easy to evaluate because they work simultaneously. The size, shape, and location of each detention basin may have a significant impact on their performance as a whole. Although the concept of a detention basin has been widely accepted, the questions regarding its effectiveness in managing stormwater runoff persist (Urbonas et al, 1981).

One study was conducted in the Valley Creek Watershed in Chester County, Pennsylvania to evaluate the effectiveness of an existing system of storm water detention basins operating at the watershed scale. The Valley Creek Watershed has a drainage area of 24 square miles. It has undergone rapid development from the westward spread of suburban Philadelphia and is now covered by approximately 17% impervious surfaces. In order to limit the postconstruction peak flow rate to or below its predevelopment level, a system of 111 detention basins has been constructed within the Valley Creek Watershed since the 1970s, and 82 of them ultimately were included in the hydrologic model which was developed using HEC-HMS. A storage-versus-outflow curve was created for each basin and used in the HEC-HMS model. The model was run with six measured events between September 2001 and August 2002, with rainfall depths ranging from 0.47 to 1.76 inches, which are lower than the storm event with a 2-year return period.

Comparisons of the output hydrographs at the furthest downstream point on the main stem of the creek were made between the models with and without detention basins for these six events. The results indicated that the computed peak flow rates were nearly identical between these two models for all input storm events, with the largest peak flow rate reduction of 4% and the average peak flow rate reduction for all six events of only 0.3% (Emerson et al., 2005). The

peak flow rates for two of these events were slightly increased with the presence of the basins. The study indicated that the detention basins in the Valley Creek Watershed are designed on a site-by-site basis. This was considered to be one reason for their slight effect since they may not work efficiently when operating simultaneously. This result points to the need to evaluate the detention basins at a watershed-scale instead of at a site scale. The study also supported the hypothesis that on-site detention basins do not affect watershed-wide storm hydrographs that result from frequent storm events (e.g., 2-years). When ponds are designed to control the peak flow from single recurrence events, the effectiveness of the system in controlling the flow rates along the major drainageways is limited to only that single event (Urbonas, 1981). Detention basins are traditionally designed for larger storm events (Emerson, 2003). Thus, simulating large storms, such as 24-hour 2-, 5-, 10-, 25-, 50-, and 100-year storms, should be a better choice for the assessment of the detention basins' effectiveness.

Another study was conducted in the Silver Creek Watershed, a subbasin of the larger Lower Kaskaskia watershed in Illinois. It has a total drainage area of 459 square miles, which consists primarily of cropland, grassland, and forest. Like the Valley Creek Watershed, this area is currently experiencing moderate to high levels of urbanization. The goal of this study is to identify the detention pond sizes that can best achieve our target peak flow reduction criteria. For the sake of this goal, the entire Silver Creek Watershed was delineated into 159 subbasins, and each basin is considered as a site for a detention pond. An optimal control model was constructed by coupling the distributed hydrologic model, SWAT (Soil and Water Assessment Tool) with a GA (Genetic Algorithm). The maximum daily flow reduction of 16.8% can be achieved by the optimum solutions found by the model. Although the results were generated from the hypothetical detention basins, they still proved that selecting, placing, and sizing the ponds at a

holistic, watershed-scale can more effectively and economically achieve the peak flow reduction goal (Kaini et al., 2007). Identifying the runoff potential distribution within a watershed is considered an important step in developing a runoff management practice.

2.3. Regionalization approach for hydrologic model calibration

Today, the hydrologic model, also known as the rainfall-runoff model, plays an important role in water resource management as well as in urban planning. The hydrologic model is a mathematic model that can translate incoming precipitation into runoff via routing, storage, and loss processes (Kult, 2013). This translation process is defined as the hydrologic response of a watershed.

Traditionally, the easiest calibration approach of the hydrologic model is to calibrate it with observed flow data. However, this approach only applies to the watershed, which is gaged. As the hydrologic model becomes increasingly popular and useful, other strategies need to be developed in order to extend their applicability to locations where they cannot be calibrated or validated because of insufficient observed data. The term regionalization has roots in the processes of regime classification and catchment grouping and was later extended to the rainfall-runoff modeling context to include the transfer of parameters from neighboring gaged catchments (also called donor catchments) to an ungaged catchment (Oudin, 2008). In the past decades, there have been numerous studies relating to different techniques of applying the regionalization methodology. There are three typical kinds of regionalization methodologies: 1) regionalization based on regression, 2) regionalization based on spatial proximity; and 3) physical similarity between ungaged and gaged watershed.

The first method establishes a regression relationship between model parameters and gaged watershed characteristics such as drainage area, land use, soil type, and topography. The

relationship can then be applied to the ungaged watershed in order to produce a new set of model parameters on the basis of its own characteristics. The hypothesis on which this method relies makes it impractical because it presumes that there is a close relationship between the observable watershed characteristics and model parameters (Oudin et al., 2008). However, model calibration can lead to non-unique optimal parameter sets since they depend on the models and the objective functions used to measure their performance (Bárdossy, 2007; Gupta et al., 1998; Madsen, 2003). The second regionalization approach is based on spatial proximity, which uses the parameter values calibrated for geographic neighbors. The justification for this is the assumption that because the physical and climatic characteristics are relatively homogeneous within a region, neighboring regions should behave similarly (Oudin et al., 2008). One can assume that watersheds with similar characteristics show a similar hydrologic behavior and can therefore be modeled using similar parameters (Bárdossy, 2007). The third regionalization method is based on spatial proximity. This method transfers the parameters from the gaged watershed, which is neither the geographic neighbor nor the one who shares similar physical characteristics. Instead, they use the catchment descriptors, which are the same as those used for the regression-based approach.

Each method has its own advantages and disadvantages, and there is agreement on which method is preferable. The Coweeta Hydrologic Laboratory used a conceptual rainfall-runoff model with six parameters to investigate the regression regionalization approaches to daily streamflow predictions for 13 catchments. The results reveal that high significance regression between model parameters and physical catchment descriptors does not guarantee a set of parameters with good predictive power (Kokkonen et al., 2003). It also points out that it may be worthwhile to adopt the entire set of calibrated parameters from the gauged catchment instead of

deriving a quantitative relationship between catchment descriptors and model parameters when a gauged catchment resembles the ungauged catchment in terms of hydrologic behavior. Another study which sought to regionalize 11 parameters of a lumped conceptual model was conducted on over 308 catchments in Australia. The results showed that the methods that are based on multiple regressions with catchment attributes perform significantly poorer; however, the regionalization based on spatial proximity performs better on the ungaged catchment (Merz et al., 2003). Moreover, a comparison of these three regionalization approaches was made based on the 913 French catchments. To ensure the generality of the conclusion, two lumped rainfall-runoff models were applied to the daily data over this large set of catchments. The results indicate that spatial proximity provides the best regionalization results, while the progression approach is the least satisfactory. However, this conclusion cannot be extended to other locations because it was predicted based on the presence of a dense network of gaging stations (Oudin et al., 2008).

2.4. Comparison of the hydrologic and hydraulic routing methods

Flow routing is a mathematical procedure for predicting the changing magnitude, speed, and shape of a flood wave as a function of time (i.e., the flow hydrograph) at one or more points along a watercourse (waterway or channel). The watercourse may be a river, stream, reservoir, estuary, drainage ditch, or storm sewer. Flow routing can be classified as either a hydrologic or hydraulic routing method. Routing by a lumped system method is called hydrologic routing, whereas routing by a distributed system method is called hydraulic routing (Maidment, 1993). The following sections provide detailed descriptions of the hydrologic and hydraulic routing method.

2.4.1. Hydrologic Routing Method

There are five hydrologic routing methods available for the HEC-HMS model: the Kinematic Wave Routing, Lag Routing, Modified Puls Routing, Muskingum Routing, and Muskingum-Cunge Routing methods. We selected the Muskingum method for the present study because it is commonly used and can provide reasonably accurate results for moderate to slow rising floods propagating through mild to steep sloping watercourses (Maidment, 1993). The Muskingum Routing method uses a simple expression of the continuity equation:

$$I - Q = \frac{dS}{dt} \qquad \text{Equation 2.1}$$

where I is the inflow rate, Q is the outflow rate, and S is the storage.

This method models the storage volume of flooding in a river channel as the sum of wedge and prism storage, as shown in Figure 2.3.1. The volume of prism storage is equal to KQ, where K is approximately the travel time of the flood wave through the reach. The volume of wedge storage is equal to $KX(I - Q)$, where X is the dimensionless weight factor between inflow and outflow.

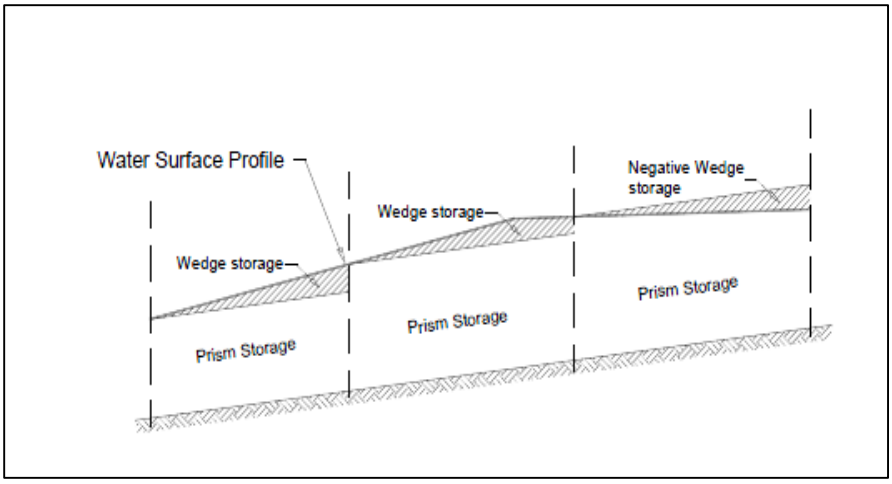

Figure 2.1 Prism and wedge storage (from Linsley et al., 1982).

The total storage, S, in the reach can be represented by:

$$S = KQ + KX(1 - Q) \qquad \text{Equation 2.2}$$

The values of X have the range $0 \ll X \ll 0.5$. If $X = 0.5$, the storage depends equally on inflow and outflow. If $X = 0$, the storage depends only on the outflow, as in the case of a large body of water such as a reservoir. In natural systems, X is between 0 and 0.3, with a mean value near 0.2 (Mays, 2010). Substituting Equation 2.2 in the Continuity Equation yields the routing equation for the Muskingum method:

$$Q_{j+1} = C_1 I_{j+1} + C_2 I_j + C_3 Q_j \qquad \text{Equation 2.3}$$

where $C_1 = \dfrac{\Delta t - 2KX}{2K(1 - X) + \Delta t}$

$$C_2 = \frac{\Delta t + 2KX}{2K(1 - X) + \Delta t}$$

$C_3 = \frac{2K(1-X)-\Delta t}{2K(1-X)+\Delta t}$, note that $C_1 + C_2 + C_3 = 1$.

As introduced previously, two parameters, K and X, need to be determined before using the Muskingum method. These two parameters are fitted to the HEC-HMS model by calibrating to observed hydrographs. It is not necessary to have great accuracy when determining the X values since the method results are relatively insensitive to the value of this parameter (Chow et al., 1988).

The hydrologic routing method greatly improves computational efficiency and speed and also reduces the amount and detail of field data traditionally needed for hydraulic routing (Weinmann and Lawrenson, 1979). However, the Muskingum routing method has some limitations that will affect the accuracy of the final result. Firstly, a basic assumption of Muskingum routing is that K remains constant at all flows. This assumption is convenient and may produce good results for some reaches. However, it may pose a challenge, as the travel time will obviously change with flow. Secondly, the method assumes a single stage-discharge relationship. In other words, for any given discharge, Q, there can be only one stage height. In fact, different stage heights could result from a given discharge since the geometry is changing along the channel. Additionally, the routing method is not suitable for rapidly rising hydrographs such as dam-break floods, and it neglects variable backwater effects due to downstream constrictions, bridges, dams, large tributary inflows, or tidal fluctuations (Maidment, 1993).

2.4.2. Hydraulic Routing Method

While the hydrologic routing method only uses the principle of continuity and a single stage-discharge relationship, the hydraulic routing method employs the full Saint-Venant

Equations, which consist of the continuity and the momentum equations. In this way, hydraulic routing methods can provide more accurate solutions by considering the effects of channel storage and wave shape (Bedient and Huber, 1988). The continuity equation describes conservation of mass for the one-dimensional system (HEC-RAS v4.1 Reference Manual, 2009) and can be written as follows:

$$\frac{\partial A}{\partial t} + \frac{\partial S}{\partial t} + \frac{\partial Q}{\partial x} - q_l = 0$$

where x = distance along the channel,

t = time,

Q = flow,

A = cross-sectional area,

S= storage from non-conveying portions of cross section,

q_l = lateral inflow per unit distance.

The momentum equation states that the rate of change in momentum is equal to the external forces acting on the system. The full momentum equation for a single channel is:

$$\frac{\partial Q}{\partial t} + \frac{\partial (VQ)}{\partial x} + gA(\frac{\partial z}{\partial x} + S_f) = 0$$

where g = acceleration of gravity,

S_f = friction slope,

V = velocity.

Several important assumptions are applied to the hydraulic routing method. First, the water level at each cross section is flat. Second, the fluid is incompressible, which means its density is constant. Third, the channel bottom is fixed. Fourth, the vertical accelerations are negligible so that the vertical pressure distribution is hydrostatic. The application of the momentum equation allows the hydraulic routing method to account for more physical characteristics, including the bed slope, roughness, geometry and length of channel. Compared to hydrologic routing methods, the hydraulic routing method can compute not only the water depth but also the flow rate with respect to time at each cross section. In addition, hydraulic routing methods can better represent many special flow conditions, including dam breach and tidal effects.

CHAPTER 3. CURRENT CONDITIONS IN THE SOAP CREEK WATERSHED

3.1. Introduction

This chapter provides an overview of the current Soap Creek Watershed conditions, including hydrology, geology, topography, land use, and hydrologic/meteorologic instrumentation, as well as a summary of previous floods on record. These datasets are either from the government authorities or investigations in the field. With the aid of these high resolution and more recent datasets, the HEC-HMS and the HEC-RAS models perform accurately.

3.2. Hydrology

The Soap Creek Watershed, as defined by the boundary of ten-digit Hydrologic Unit Code (HUC-10, 071000907), has a drainage area of approximately 258 square miles. It is located in Southeast Iowa and is a sub-watershed within the Lower Des Moines River's eight-digit Hydrologic Unit Code (HUC8, 0710009).

The Soap Creek Watershed falls within a portion of Appanoose, Davis, Monroe, and Wapello Counties. Soap Creek flows from west to east and has two headwater branches, North and South Soap Creek. These two branches converge in Davis County, and flow continues eastward. Little Soap Creek traverses southern Wapello County and enters Soap Creek northeast of Floris, Iowa. Soap Creek then continues to its outlet, discharging into the Des Moines River approximately 12 miles southeast of Ottumwa. Two large recreational lakes are located in the watershed: Lake Sundown, a 470 acre private lake situated on South Soap Creek, and Lake Wapello, a 287 acre state-owned lake situated on Pee Dee Creek. Flow conditions are classified as intermittent in the lower 18 miles of Little Soap Creek, Soap Creek below Mormon Creek, South Soap Creek below Lake Sundown, and the lower end of the larger tributaries. Flow

conditions in other channels are classified as ephemeral (United States Department of Agriculture, 1988). Intermittent streams generally have flow that occurs only during the wet season (50 percent of the time or less). Ephemeral streams generally have flow that occurs during and shortly after storms (Mays, 2010).

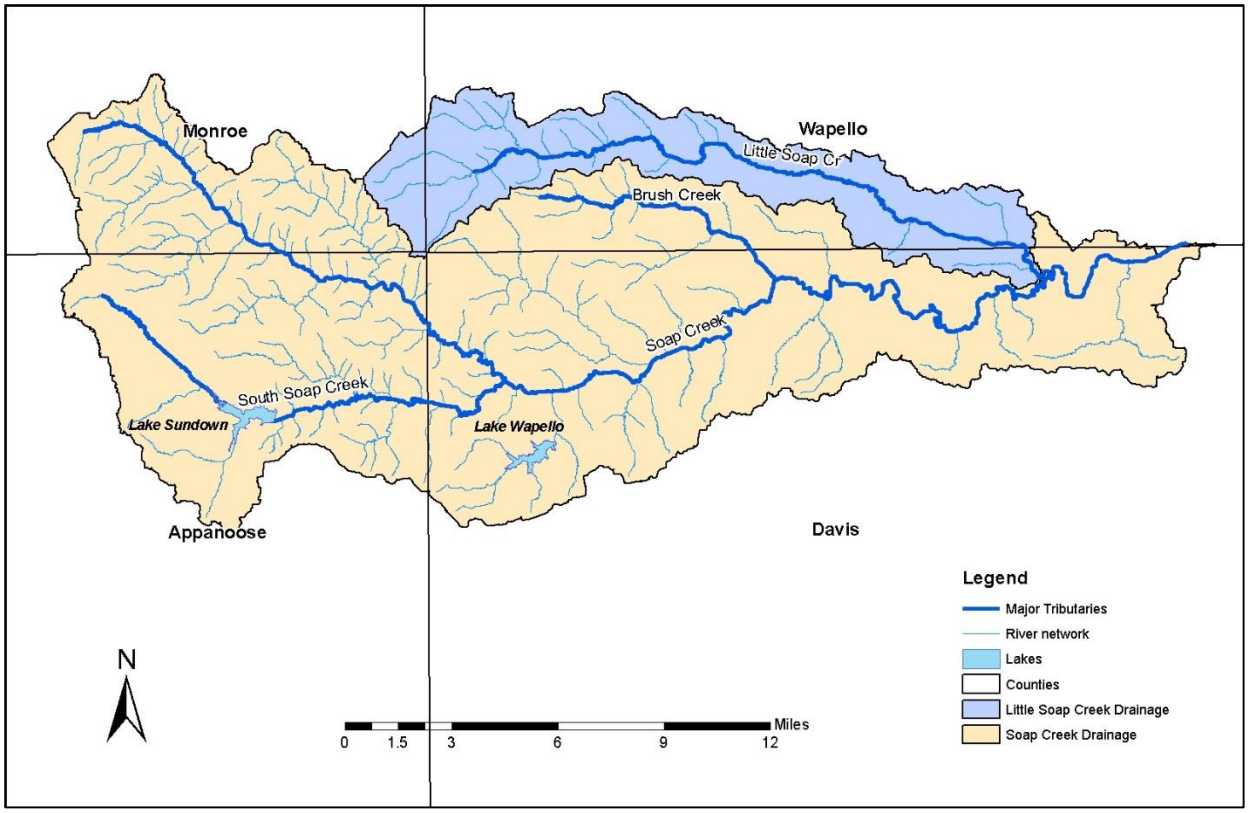

Figure 3.1 The Soap Creek Watershed (HUD10 071000907) drains approximately 258 mi2.

Iowa's climate is marked by a smooth transition of annual precipitation across its landscape from the southeast to the northwest (See Figure 3.2). Of the four Iowa Watershed Project study areas, Soap/Chequest, which is along the southern border, has the largest annual precipitation (38.8 inches), with about 80% of the annual precipitation falling as rain during the months of April – September. During this period, thunderstorms that are capable of producing torrential rains are possible, with the peak frequency of such storms occurring in June.

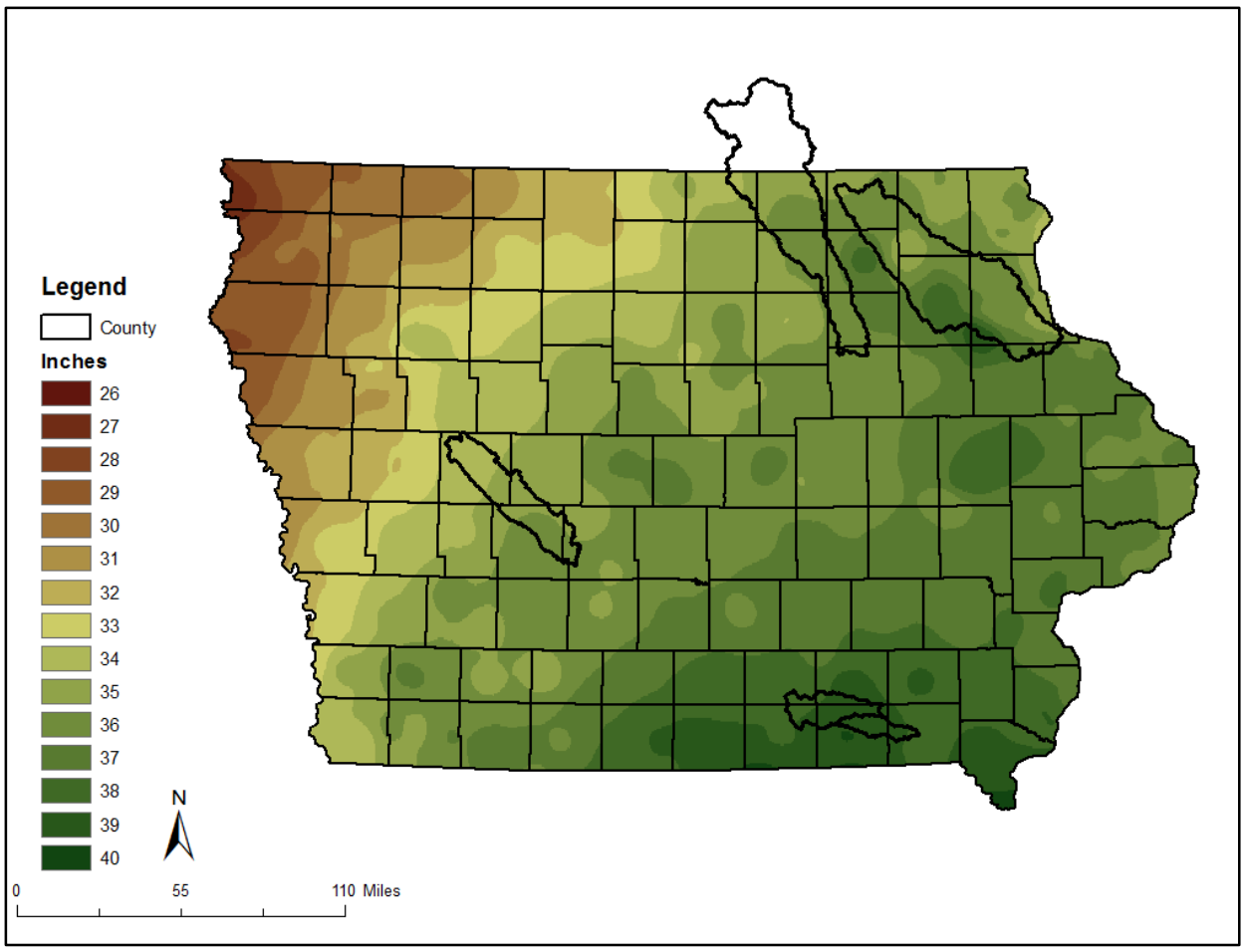

Figure 3.2 Average annual precipitation for Iowa. Precipitation estimates are based on the 30-year annual average (1981-2010) for precipitation gage sites. Interpolation between gage sites to an 800 m grid was conducted by the PRISM (parameter-elevation relationships on independent slopes model) method. Source: http://www.prism.oregonstate.edu/.

3.3. Geology and Soil

The entire Soap Creek Watershed is located within the Southern Iowa Drift Plain (see Figure 3.3.1). This region is dominated by glacial deposits left by ice sheets that extended south into Missouri over 500,000 years ago. The deposits were carved by deepening episodes of stream erosion so that only a horizon line of hill summits mark the once-continuous glacial plain. Numerous rills, creeks, and rivers branch out across the landscape and shape the old glacial deposits into steeply rolling hills and valleys. A mantle of loess drapes the uplands and upper hill

slopes (Iowa Geological &Water Survey, The Iowa Department of Natural Resources, 2014).

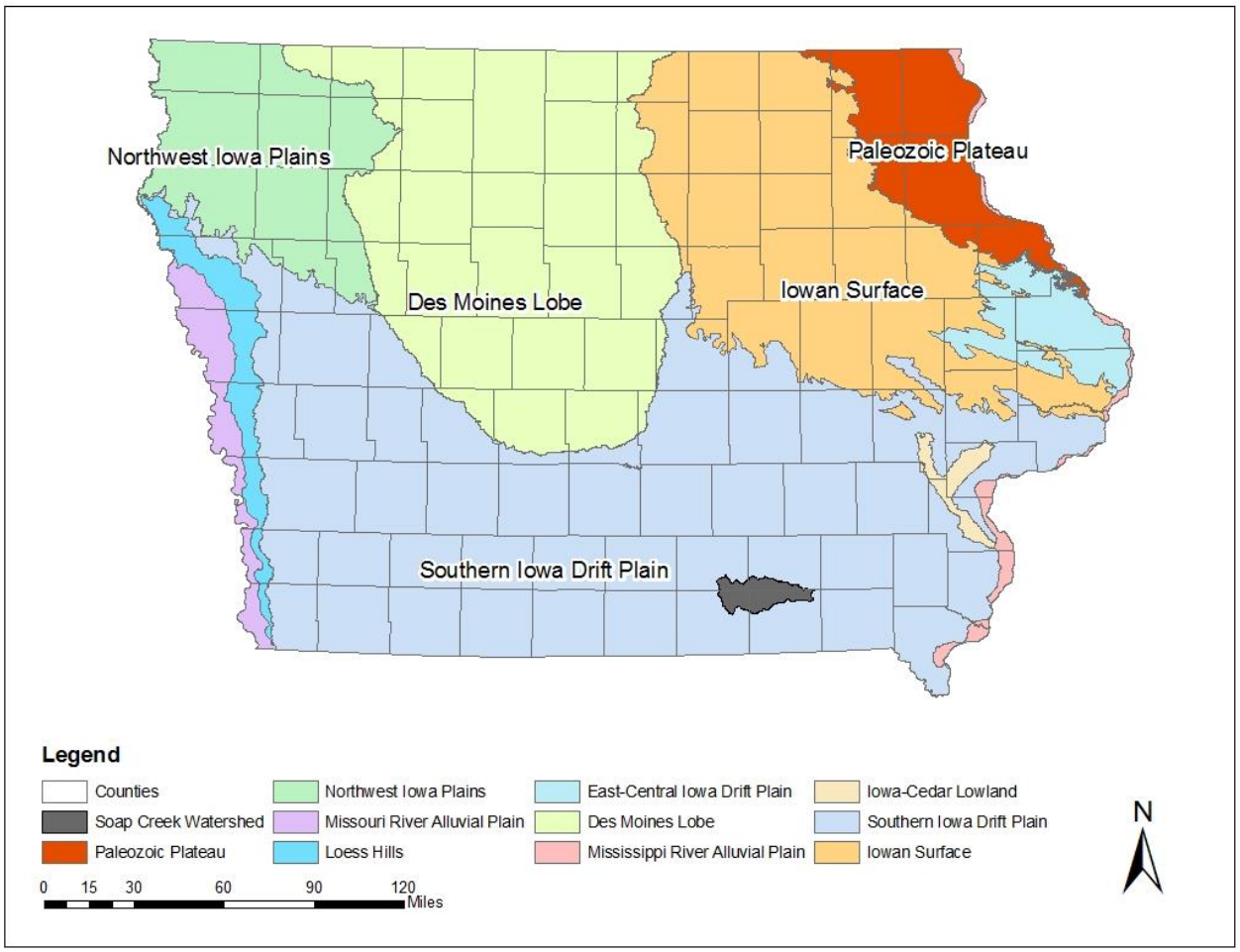

Figure 3.3 Land form regions of Iowa and the location of the Soap Creek Watershed

The Natural Resources Conservation Service (NRCS) classifies soils into four Hydrologic Soil Groups (HSG), A, B, C, and D, based on their runoff potential. A-type soils have the lowest runoff potential, and D-type soils have the highest. In addition, there are dual code soil classes A/D, B/D, and C/D that are assigned to certain wet soils. The first letter applies to the drained condition, and the second applies to the undrained. In the case of these soil groups, even though the soil properties may be favorable to allow infiltration (water passing from the surface into the ground), a shallow groundwater table (within 24 inches of the surface) typically

prevents much from doing so. For example, a B/D soil will have the runoff potential of a B-type soil if the shallow water table were to be drained away, but it will have the higher runoff potential of a D-type soil if it is not. Table 3.1 summarizes some of the properties that are generally true for each HSG A-D. This table is meant to provide a general description of each HSG and is not all inclusive. Complete descriptions of the Hydrologic Soil Groups can be found in the USDA-NRCS National Engineering Handbook, Part 630 – Hydrology, Chapter 7.

Table 3.1 Summary of soil properties and characteristics generally true of Hydrologic Soil Groups A-D.

Hydrologic Soil Types	**Runoff Potential**	**Common Soil Texture(s)**	**Composition**	**Minimum Infiltration Rate[1] (inches/hour)**
A	Low	Sand, gravel	< 10% clay > 90% sand/gravel	> 5.67
B	Moderately low	Loamy sand, sandy loam	10 – 20% clay 50 – 90% sand	1.42 – 5.67
C	Moderately high	Loam containing silt and/or clay	20 – 40% clay < 50% sand	0.14 – 1.42
D	High	Clay	> 40% clay < 50%	< 0.14

[1] For HSG A-C, infiltration rates based on a minimum depth to any water impermeable layer and the ground water table of 20 and 24 inches, respectively.

Figure 3.4 illustrates the soil distribution of the Soap Creek Watershed per digital soils data (SSURGO) that is available from the USDA-NRCS Web Soil Survey (WSS).

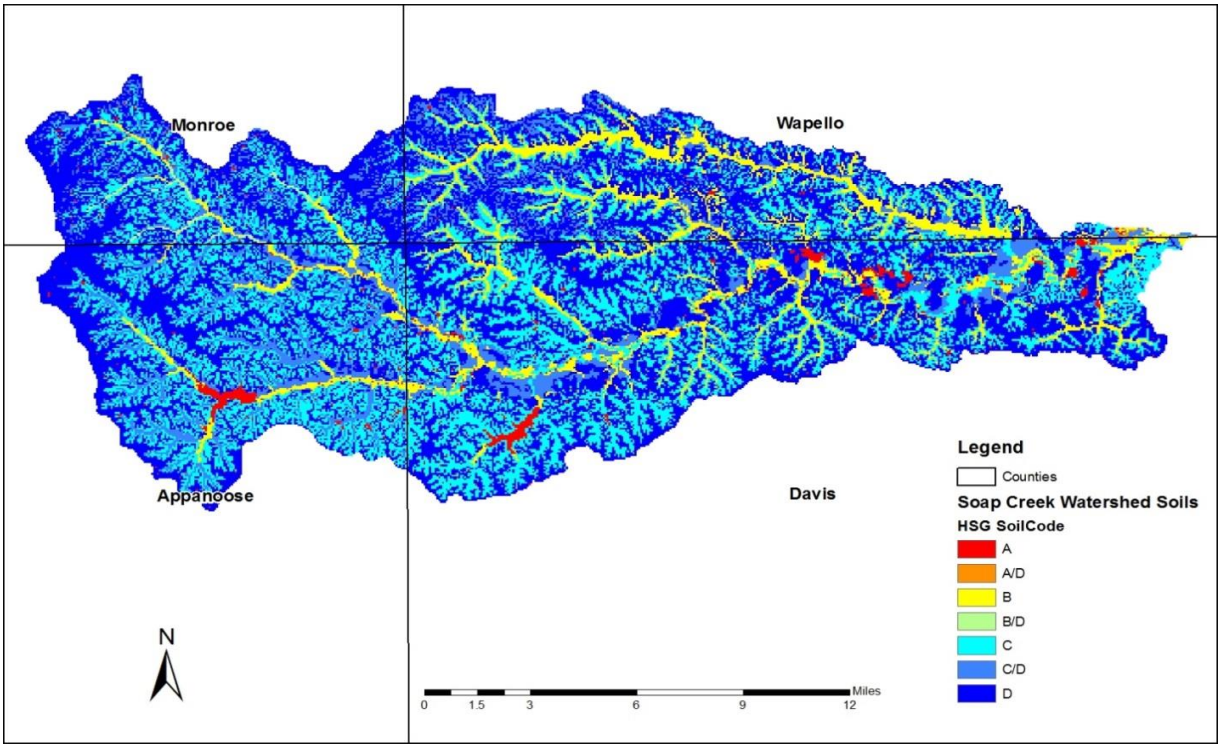

Figure 3.4 Soil Distribution of the Soap Creek Watershed. The Hydrologic Soil Group reflects the degree of runoff potential a particular soil has, with Type A(Red) representing the lowest runoff potential and Type D (Dark Blue) representing the highest runoff potential. The dominant soil type in the basin is HSG D (48%).

The primary soil types are C, C/D, and D (32.7%, 10.0%, and 48.1%, respectively). These soils allow much less water to infiltrate into the ground, resulting in the majority of areas being considered to have high runoff potential. Table 3.2 shows the approximate percentages by area of each soil type for the Soap Creek Watershed.

Table 3.2 Hydrologic Soil Group distribution (by percent area) in the Soap Creek Watershed.

Soil Type (HSG)	Runoff Potential	Approximate Area (%)
A	Lower	~0
A/D		~0
B		8.9
B/D		0.3
C		32.7
C/D		10.0
D	Higher	48.1

3.4. Topography

The topography is characterized by irregular narrow ridges with steep slopes and narrow gullied valleys. Elevation ranges from 1,023 feet to 600 feet at the outlet (see Figure 3.5), and land Slopes are between 0-161% (A flat surface is 0%, a 45 degree surface is 100 percent, and as the surface becomes more vertical, the percent rise becomes increasingly larger). (See Figure 3.6).

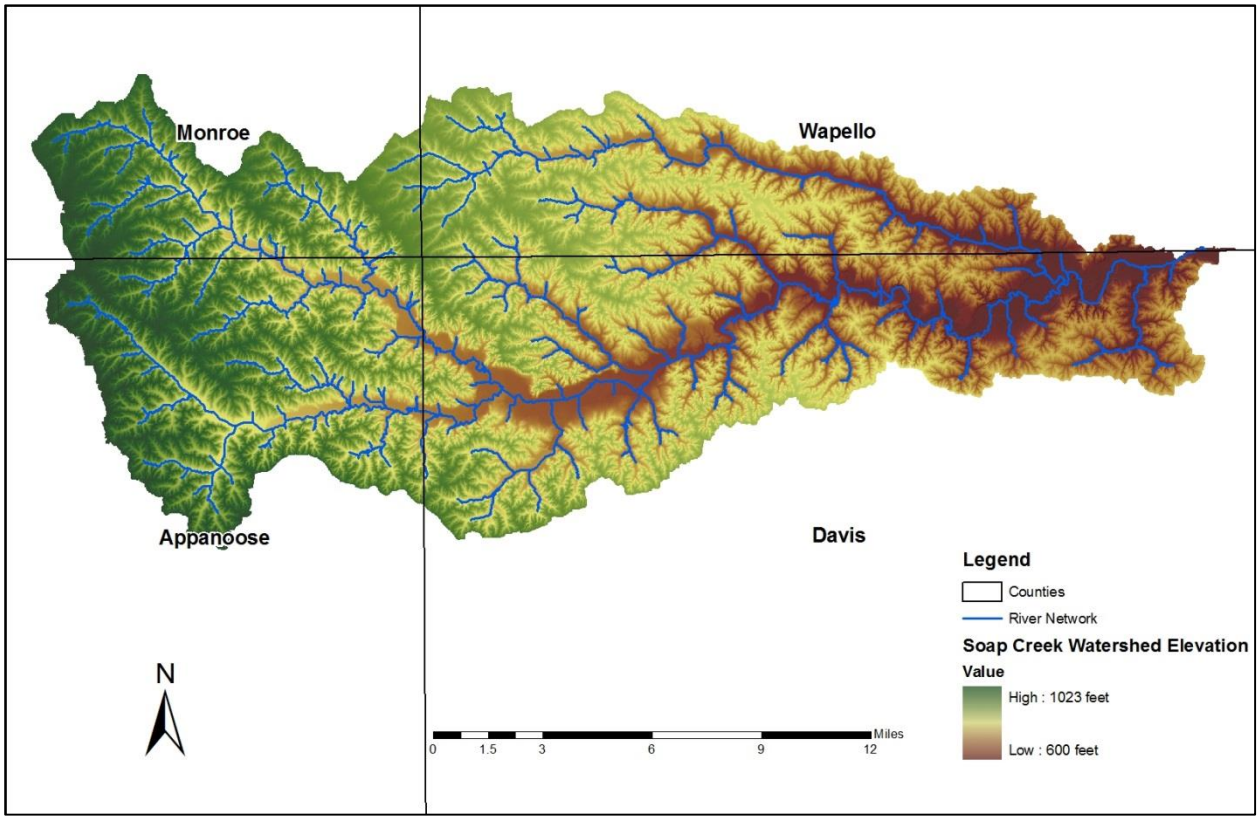

Figure 3.5 Topography of the Soap Creek Watershed. Soap Creek is a relatively steep watershed ranging from 1023 to 600 feet.

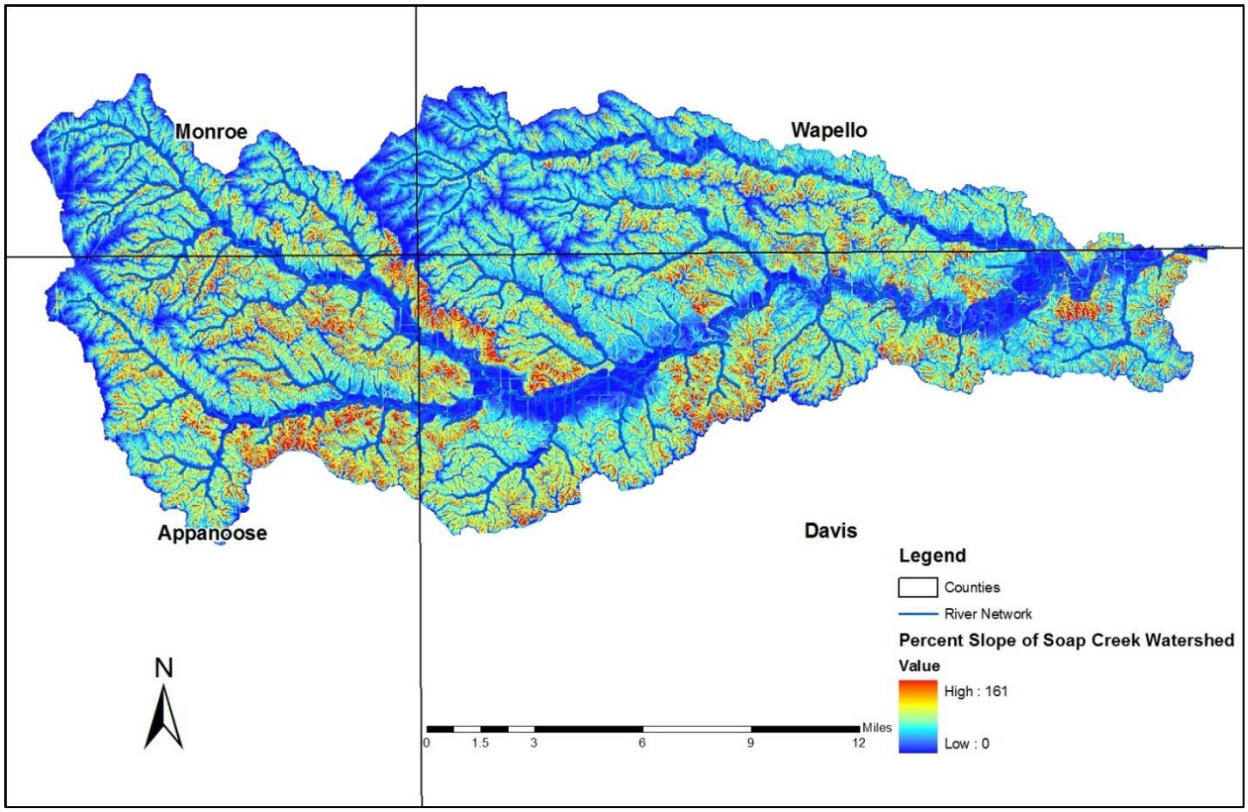

Figure 3.6 Slope of the Soap Creek Watershed, ranges from 0 to 161%.

3.5. Land Use

The Soap Creek Watershed is comprised of approximately 35% pasture/hay and 35% deciduous forest, which are evenly distributed within the watershed (see Figure 3.5.1). Other major land use includes Cultivated Crops, Grassland, and Developed open space consisting of 14%, 5%, and 3%, respectively. There are also several small cities in the watershed: Moravia, Blakesburg, Unionville, Udell, and Floris. Approximately 90% of the land within the watershed is privately owned.

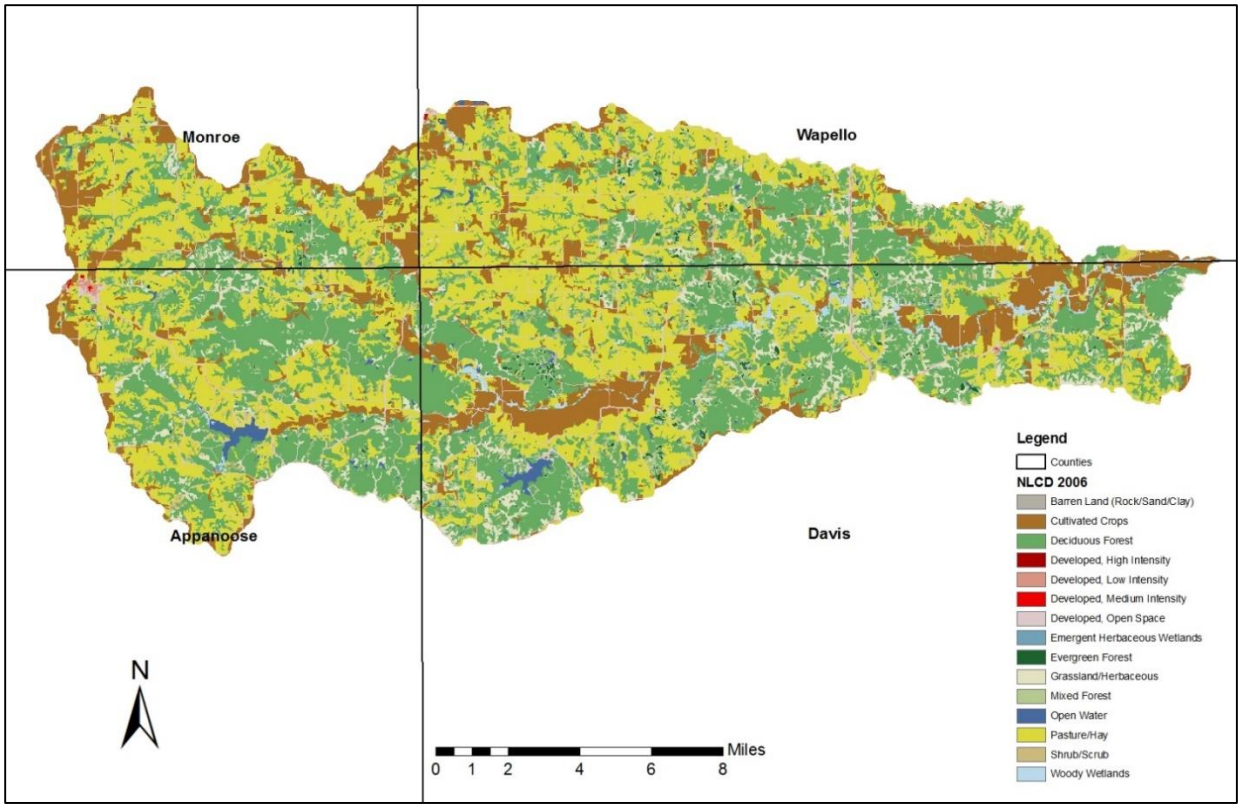

Figure 3.7 Land use composition in the Soap Creek Watershed.

3.6. Instrumentation/data records

The Soap Creek Watershed is gaged with only an IFC stream stage sensor (four in total) for which the water level information is available. The IFC stream stage sensor provides the stage data every 15 minutes. In addition, there are four United States Geological Survey (USGS) operated stage/discharge gages and three National Oceanic and Atmosphere Administration (NOAA) 15 minute/hourly precipitation gages near the watershed. Table 3.3 and Figure 3.8 (below) detail the period of record and the location of the hydrologic and meteorologic instrumentation.

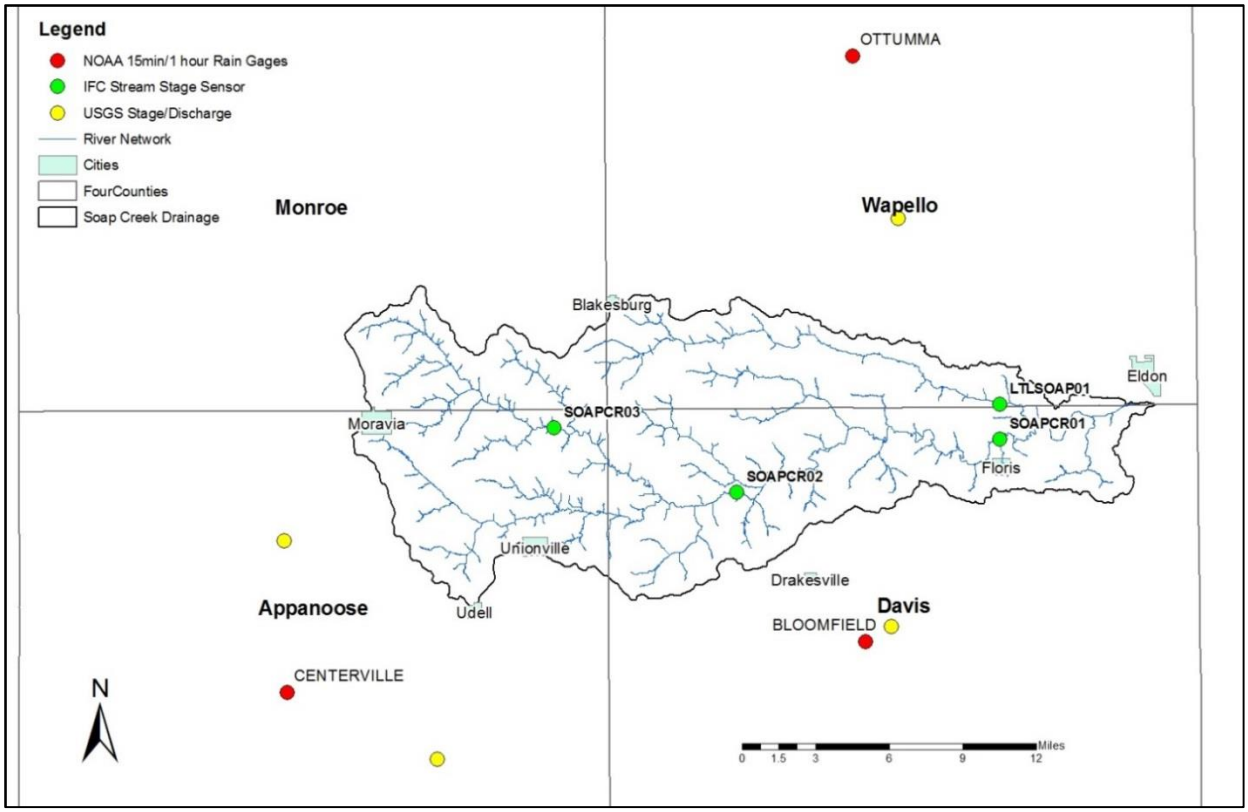

Figure 3.8 Hydrologic and meteorologic instrumentation in and around the Soap Creek Watershed. Eight stage/discharge gages are shown in green or yellow, and three precipitation gages are shown in red.

Table 3.3 Stage/Discharge and Precipitation Gages in and around the Soap Creek Watershed.

Gage Type	**Location**	**Period of Record**
IFC Stream Stage Sensor - LTLSOAP01	Floris, IA	2012 - present
IFC Stream Stage Sensor - SOAPCR01	Floris, IA	2012 - present
IFC Stream Stage Sensor - SOAPCR02	Drakesville, IA	2012 - present
IFC Stream Stage Sensor - SOAPCR03	Unionville, IA	2012 - present
USGS Stage/Discharge - 05494300	Fox River at Bloomfield, IA	1906 - present
USGS Stage/Discharge - 06904010	Chariton River near Moulton, IA	1979 - present
USGS Stage/Discharge - 06903900	Chariton River near Rathbun, IA	1963 - 1969
USGS Stage/Discharge - 05489500	Des Moines River at Ottumwa, IA	1917 – present
NOAA 15 Min/Hourly Precipitation	Ottumwa Industrial Airport, IA	1948 – 2013
NOAA-partnered Daily Precipitation	Bloomfield, IA	1906 – present
NOAA 15 Minute/Hourly Precipitation	Centerville, IA	1948 – 2013

3.7. Floods of Record

Flooding from Soap Creek and its tributaries occurs nearly every year and happens even more frequently in some reaches (United States Department of Agriculture, 1988). The flooding varies by reach with respect to depth and duration. Soap Creek flooded seven times in 1986, with major flooding occurring on April 30. Rainfall of 2.5 to 4.0 inches over the upper end of the watershed causes the flooding (United States Department of Agriculture, 1988). Since there is no streamgage present within the Soap Creek Watershed, established peak discharges have not been determined. However, since the Iowa Flood Center opened, we have installed four IFC stream stage sensors within the Soap Creek watershed (in 2012). Based on the stage result records produced by the stage sensor at Floris, three large water depths (ft) have been recorded since December, 2012: March 10, 2013; April 18, 2013, and May 29, 2013.

3.8. Chapter Summary

This chapter provides the details of the water cycle and the physical characteristics of the Soap Creek Watershed. We used historical precipitation and streamflow records to examine the water cycle of Soap Creek. The average annual precipitation for the Soap Creek Watershed is 38.8 inches. The entire Soap Creek Watershed is located within the Southern Iowa Drift Plain, which is dominated by glacial deposits left by ice sheets that extended south into Missouri over 500,000 years ago. Soils of the watershed have a high runoff potential: the primary soil types are C, C/D, and D (32.7%, 10.0%, and 48.1%, respectively). The topography is characterized by irregular narrow ridges with steep slopes and narrow gullied valleys. Slopes are between 0-161% (A flat surface is 0%, and a 45 degree surface is 100%). The Soap Creek Watershed is comprised of approximately 35% pasture/hay and 35% deciduous forest, which are evenly distributed within the Watershed. Flooding from Soap Creek and its tributaries occurs nearly every year and

more frequently in some reaches (United States Department of Agriculture. 1988).

CHAPTER 4. HYDROLOGIC MODEL DEVELOPMENT OF SOAP CREEK WATERSHED

4.1. Introduction

This chapter summarizes the development of the hydrologic model we used in the Phase I Hydrologic Assessment of the Soap Creek Watershed. We used the United States Army Corps of Engineers' (USACE) Hydrologic Engineering Center's Hydrologic Modeling System (HEC-HMS), Version 3.5 to perform the modeling.

The Hydrologic Modeling System (HMS) is designed to simulate the precipitation-runoff processes of a watershed and to be applicable in a wide range of geographic areas and for watersheds ranging in size from very small (a few acres) to very large (the size of the Soap Creek Watershed or larger).

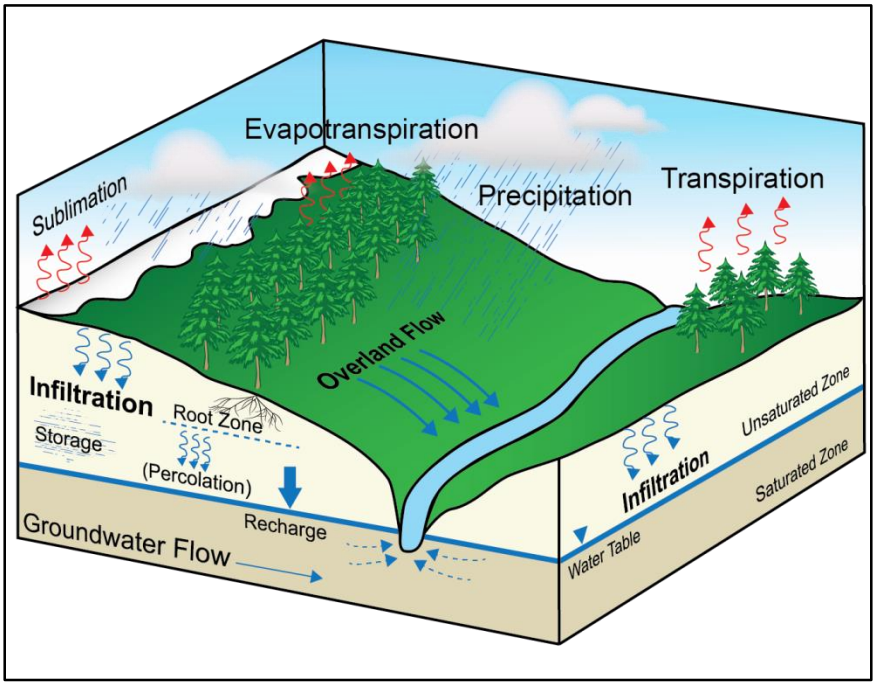

Figure 4.1 Hydrologic processes that occur in a watershed. Phase I modeling only considered the precipitation, infiltration, and overland components of the water cycle.

HMS is a mathematical, lumped parameter, uncoupled, surface water model. This chapter

will briefly discuss each of these terms, as each descriptor plays a role in the models' input demands, required assumptions, and final applicability for using the model's results. The fact that HMS is a mathematical model implies that the different hydrologic processes (shown in Figure 4.1.1 above) are represented by mathematical expressions that were developed to best describe observations or controlled experiments. HMS is a lumped parameter model, meaning that the physical characteristics of the watershed, such as land use and soil type, are "lumped" together and averaged to produce a single representative value for a given land area. Once these averaged values are established within HMS, the value remains constant throughout the simulation instead of varying over time. HMS is an uncoupled model, meaning the different hydrologic processes are solved independently of one another rather than jointly. In reality, surface and subsurface processes are dependent on one another, and their governing equations should be solved simultaneously (Scharffenberg and Fleming, 2010). Finally, HMS is a surface water model, meaning it works best for simulating (large) storm events or wet antecedent conditions where direct runoff and overland flow are expected to dominate the partitioning of rainfall.

The two major components of the hydrologic modeling within HMS are the basin and the meteorological models. The meteorological model stores precipitation data that defines when, where, and how much it rains over the watershed. The basin model defines the hydrologic connectivity of the watershed, how rainfall is converted to runoff, and how water is routed from one location to another.

4.2. Incorporated Structures

In the 1980's, the Soap Creek Watershed Board was formed, and a plan to distribute 154 flood control structures (mainly ponds) was approved. Of 154 structures to be constructed in Soap Creek Watershed, 132 have been constructed as of 2013 (see Figure 4.2.1), all of which were incorporated into the HEC-HMS model. Stage-Storage-Discharge relationships were obtained for each reservoir from the Iowa Department of Natural Resource's Office of Dam Safety in Des Moines, Iowa and from regional NRCS offices. These 132 ponds have been built in several phases over the last 30 years (see Figure 4.2.1). Additionally, two natural reservoirs, Lake Sundown and Lake Wapello, were incorporated into the HMS model. Even though these two natural lakes were not designed or built for flood control, their effects of holding extra water during times of flooding cannot be neglected because of their size.

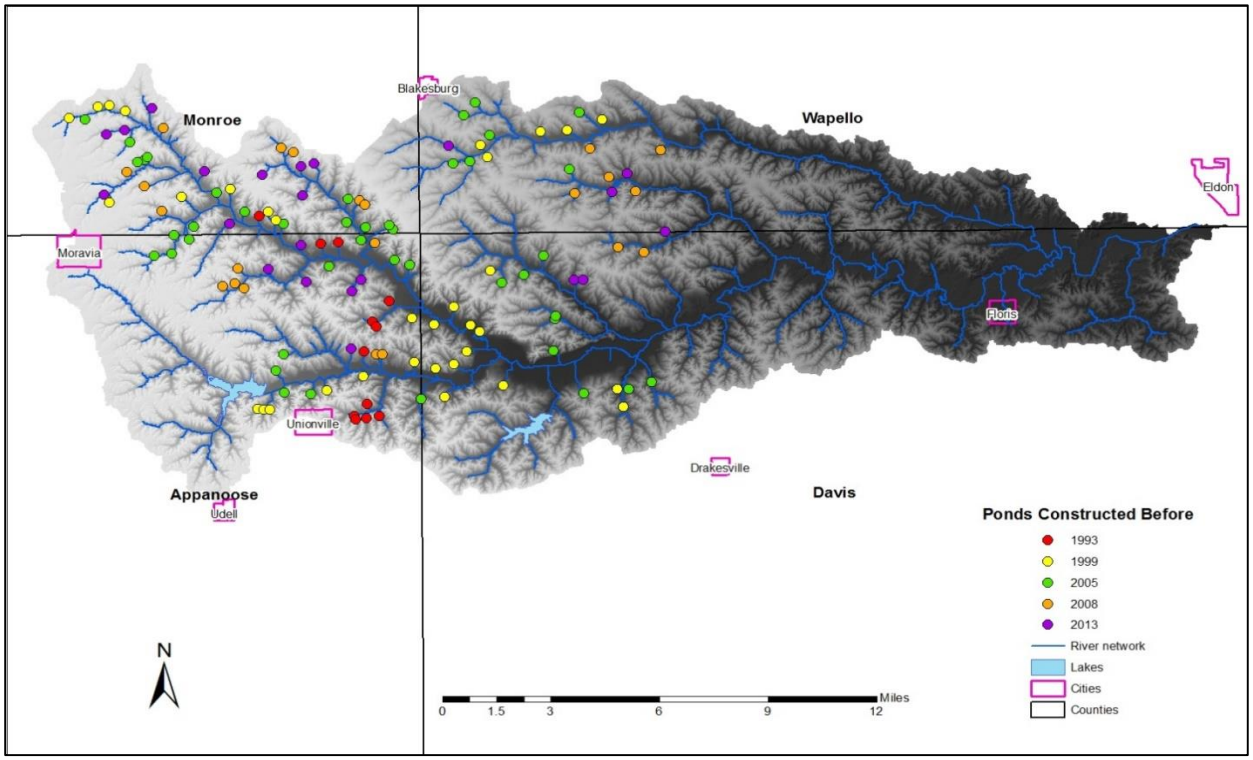

Figure 4.2 Construction progression of the 132 ponds that have been built in the Soap Creek Watershed.

4.3. HEC-HMS Model Development

It is important to note here that two HEC-HMS models have been developed in this study: one for the Soap Creek Watershed, which is the target watershed, and the other for the Fox River Watershed, which is the donor watershed. The Fox River model was developed because there are no USGS stream gages present within the Soap Creek Watershed. Therefore, its HEC-HMS model cannot be calibrated using observed data directly. As stated in the literature review section, model parameters can be transferred to the ungaged watershed model from a gaged watershed model that has similar physical characteristics. The Fox River Watershed was selected as the donor watershed not only because it is adjacent to the Soap Creek Watershed (See Figure 1.1) but also because it has an installed USGS stream gage that can provide sufficient recorded flow data (See Figure A.5). We made a further comparison of the physical characteristics of these two watersheds, and the results illustrated that they are very similar in terms of elevation, slope, soil type, and land use (See Tables B.1and B.2). We provided maps describing the characteristics for the Fox River Watershed in Appendix A (See Figures B.1, B.2, B.3, and B.4). We developed these two HEC-HMS models simultaneously following the same procedures and standards, except that only the Fox River Watershed model was calibrated.

The Soap Creek Watershed is approximately 258 square miles. For modeling purposes, we divided the entire watershed into 642 smaller drainages areas, called subbasins in HMS, with an average area of 0.39 square miles (250 acres), with the largest subbasin being 3.9 square miles (2,500 acres). The Fox River Watershed has a drainage area of around 101 square miles (64,640 acres). It was delineated into 87 subbasins with a maximum area of 1.2 square miles (768 acres). Figures 4.3 and 4.4 show the subbasin delineation for use in the Soap Creek and Fox River Watersheds, respectively.

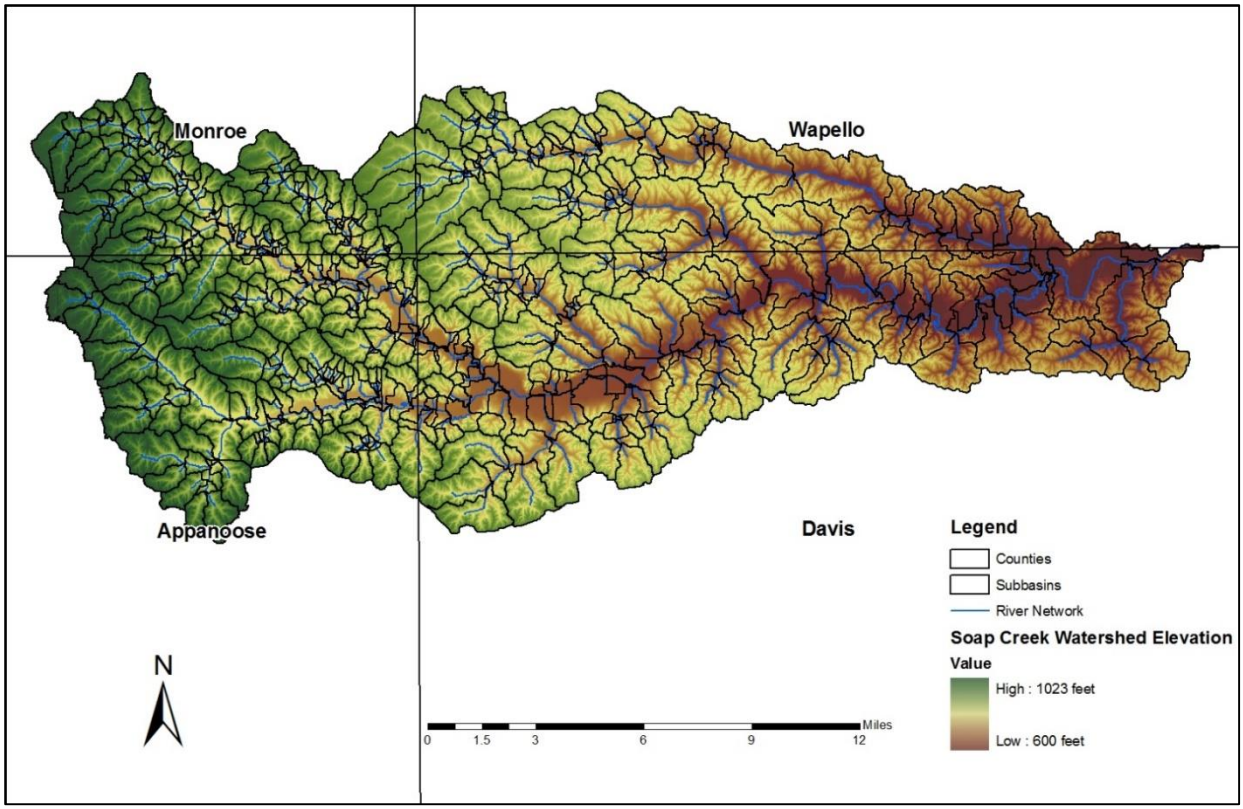

Figure 4.3 Subbasin delineation for use in the Soap Creek Watershed HMS hydrologic model. The watershed was divided into 642 subbasins to better define model parameters based on characteristics such as land use and soil type.

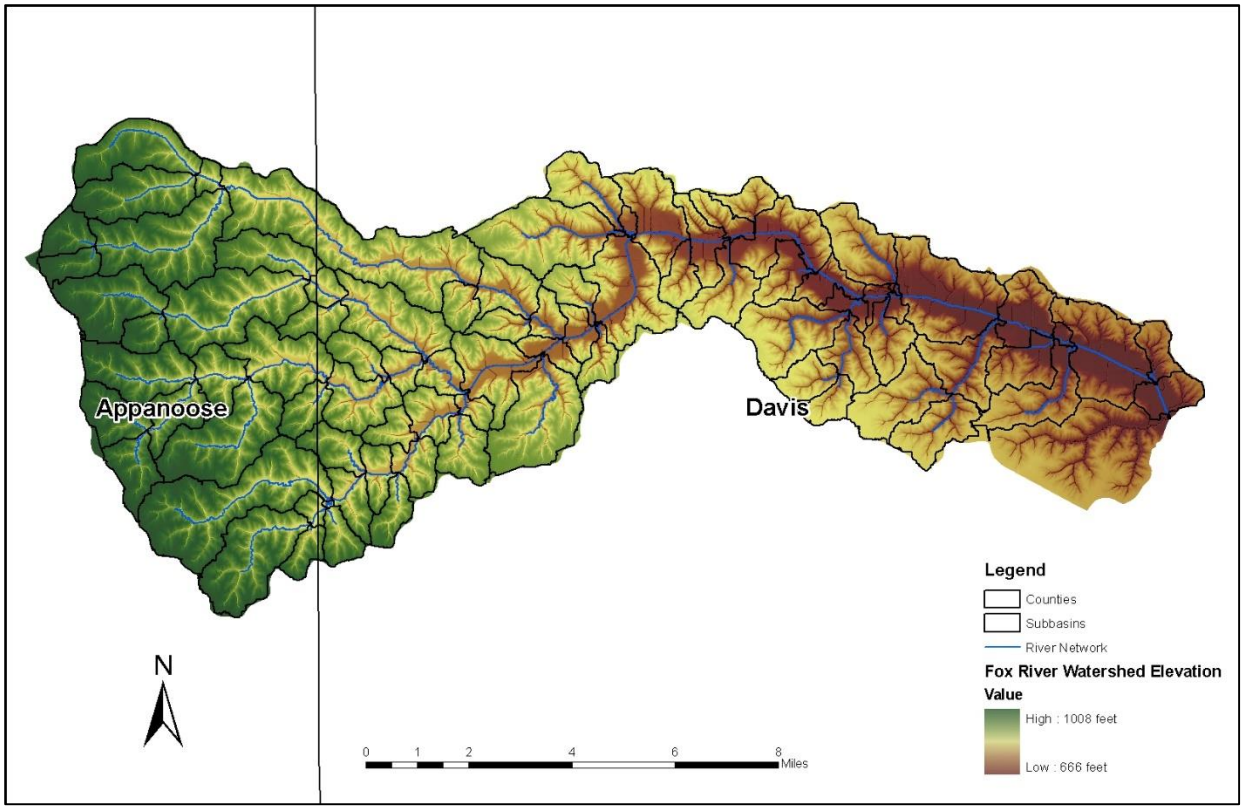

Figure 4.4 Subbasin delineation for use in the Fox River Watershed HMS hydrologic model. The watershed was divided into 87 subbasins to better define model parameters based on characteristics such as land use and soil type.

We used ESRI ArcGIS and Arc Hydro tools for preprocessing terrain, creating flow direction and flow accumulation grids, defining the stream network, and delineating subbasins. For example, we defined the stream network of the Soap Creek Watershed to begin when the upstream drainage area was 0.39 square miles (250 acres), and we delineated subbasins such that a subbasin was defined upstream of all stream confluences. We further manually split GIS-defined subbasins to create an outlet point at each IFC stream stage sensor location as well as at the discharge point of any existing structures within the watershed. In HMS, each subbasin is assigned a single value for the parameter that is being developed.

4.3.1. Meteorologic Models

Meteorologic Models are one of the main components in an HEC-HMS project that is used to specify how much precipitation will be generated for each subbasin.

We used Stage IV radar rainfall estimates (NCEP/EMC 4KM Gridded Data (GRIB) Stage IV Data) as the precipitation input for the simulation of actual rainfall events that are known to have occurred within the watershed. The National Center for Environmental Prediction (NCEP) produces the Stage IV data set by taking Stage III radar rainfall estimates that are produced by the 12 National Weather Service (NWS) River Forecast Centers across the Continental United States and combining them into a nationwide 4 km x 4 km (2.5 mile x 2.5 mile) gridded hourly precipitation estimate data set. These data are available from 2002 to the present. The Stage IV radar rainfall is available for both the Soap Creek and Fox River Watersheds. Figure 4.5 shows an example of the Stage IV radar rainfall estimates of cumulative rainfall during a one-hour period (April 17, 2013 from 3 to 4 a.m.) in the Soap Creek Watershed. This figure demonstrates the gridded nature of the radar rainfall estimate data as well as the distributed nature of rainfall in time and space during large storm events.

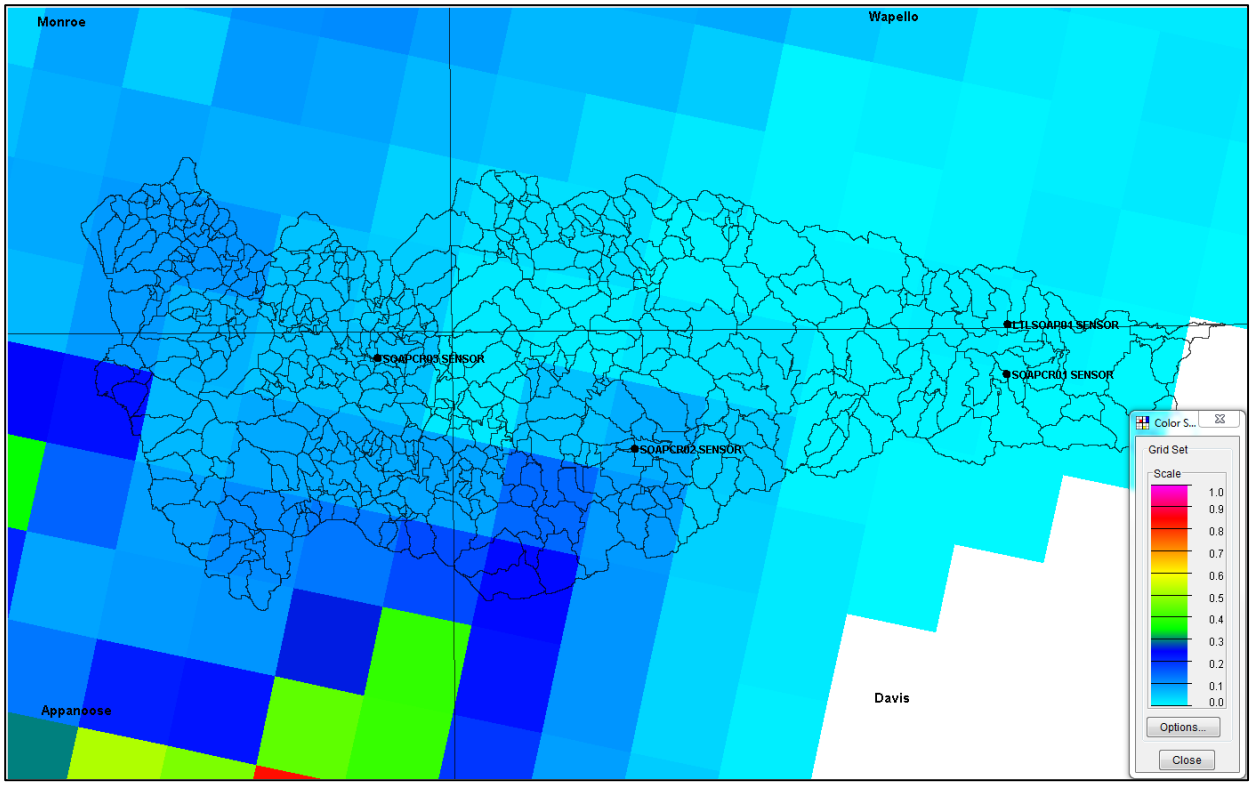

Figure 4.5 Demonstration of the gridded Stage IV radar rainfall product used in the Soap Creek Watershed HMS model. Radar rainfall estimates are available for each hour at a spatial resolution of 2.5 miles× 2.5 miles and were used for calibration and validation of historical storm events.

Use of radar rainfall estimates provides increased accuracy of the spatial and temporal distribution of precipitation over the watershed, and Stage IV estimates provide a level of manual quality control (QC) performed by the NWS that incorporates available rain gage measurements into the rainfall estimates. Actual storms using Stage IV data were the basis for model calibration and validation.

We developed hypothetical storms for comparative analyses such as potential runoff generation, increased infiltration capacity through land use changes or soil improvements, and increased distributed storage within the watershed. In this thesis, we estimated the rainfall intensity of hypothetical storms only for the Soap Creek Watershed model since it is the one used

to run different scenarios.

These hypothetical storms apply a uniform depth of rainfall across the entire watershed with the same timing everywhere. We used Soil Conservation Service (SCS) Type-II distribution, 24-hour storms for all hypothetical storms. Point precipitation values (rainfall depths) for the 2, 5, 10, 25, 50, and 100-year average recurrence interval, 24 hour storms were derived using the online version of the National Oceanic and Atmospheric Administration (NOAA) Atlas 14 – Point Precipitation Frequency Estimates (Perica et al., 2013). We used the basin centroid as the point of reference for the point precipitation frequency estimates that were applied watershed wide for each average recurrence interval storm.

Studies have been performed on the spatial distribution characteristics of heavy rainstorms in the Midwestern United States (Huff and Angel, 1992). Point precipitation frequency estimates are generally only applicable for drainage areas up to 10 square miles before the assumption of spatial uniformity becomes invalid. For drainage areas between 10 and 400 square miles, relations have been established between point precipitation estimates and an areal mean precipitation approximation. Areal reduction factors based on storm duration and drainage area can be found in the *Rainfall Frequency Atlas of the Midwest* (Huff and Angel, 1992). The point rainfall estimates were multiplied by an areal reduction factor of 0.92 (the areal reduction factor for the 258 mi^2 drainage area) for the Soap Creek Watershed.

Table 4.1 Rainfall depths used for hypothetical scenario analysis. The 24 hour duration point rainfall estimates for the 2, 5, 10, 25, 50, and 100 year recurrence intervals were reduced by an areal reduction factor of 0.92.

Hypothetical Storm	*NOAA Point Precipitation*	*Areal Reduced Precipitation*
2 year - 24 hour	3.19”	2.95”
5 year - 24 hour	3.94”	3.64”
10 year - 24 hour	4.65”	4.30”
25 year - 24 hour	5.71”	5.28”
50 year - 24 hour	6.57”	6.08”
100 year - 24 hour	7.52”	6.96”

4.3.2. Basin Models

The basin model defines the hydrologic connectivity of the watershed, how rainfall is converted to runoff, and how water is routed from one location to another.

We used the Soil Conservation Service (SCS) Curve Number methodology to determine the rainfall-runoff partitioning for both of the Soap Creek Watershed and the Fox River Watershed HMS modeling. Curve Number (CN) serves as a runoff index, and values range from 34-100 for the Soap Creek Watershed. The CN of the Fox River Watershed ranges from 58-100. As the CN becomes larger, there is less infiltration of water into the ground, and a higher percentage of runoff occurs. CN values are an estimated, rather than a measured, parameter based primarily on the intersection of a specific land use and the underlying soil type. General guidelines for developing curve numbers based on land use and soil type are available in technical references from the U.S. Department of Agriculture – Natural Resource Conservation Service (USDA-NRCS), previously known as the SCS. The watershed initially had fifteen

different categories, but we reclassified them to ten in order to make the task easier. We defined those land use classes with similar characteristics as one class. Table 4.2 shows the CNs assigned to each land use and the soil type combination for the Soap Creek Watershed HMS model and demonstrates how we reclassify the land use. This classification also applies to the Fox River Watershed HMS model.

Table 4.2 Curve Numbers Assigned to Each Land Use/Soil Type Combination. We used area-weighted averaging to calculate a single Curve Number value for each subbasin. Curve Numbers range from 34-100, with higher values reflecting greater runoff potential.

Original NLCD classification			*Soil Type*			
Number	*Description*	*Reclassification*	*A*	*B*	*C*	*D*
11	Open Water	1 – Wetlands	100	100	100	100
90	Woody Wetlands					
95	Emergent Herbaceous Wetlands					
21	Developed, Open Space	2 – Developed, Open	39	61	74	80
22	Developed, Low Intensity	3 – Developed, Low	61	75	83	87
23	Developed, Medium Intensity	4 – Developed, Medium	77	85	90	92
24	Developed, High Intensity	5 – Developed, High	89	92	94	95
31	Barren Land (Rock/Sand/Clay)	6 – Rock/Sand/Clay	98	98	98	98
41	Deciduous Forest	7 – Forest	44	65	76	82
42	Evergreen Forest					
43	Mixed Forest					
52	Shrub/Scrub	8 – Shrub	34	58	71	78
71	Grassland/Herbaceous	9 – Grassland, Pasture	49	70	80	87
81	Pasture/Hay					
82	Cultivated Crops	10 – Cultivated Crops	68	78	85	88

We generated a CN grid using ESRI ArcGIS with the HEC-GeoHMS extension tools to intersect the 2006 National Land Cover Dataset (NLCD) with digital soils data (SSURGO) available from the NRCS Web Soil Survey (WSS). Upon completing the production of the CN Grid, we used HEC-GeoHMS tools to perform area-weighted averaging within each subbasin in order to assign a composite CN to each subbasin.

Using the NRCS Curve Number methodology for rainfall-runoff partitioning accounts for

precipitation losses due to initial abstraction, which is the initial amount of rainfall that must fall before any runoff begins (losses due to plant interception, soil wetting, and storage in surface depressions), and the amount of precipitation that is estimated to infiltrate into the ground during the simulation. The remaining precipitation is considered excess precipitation and is converted to runoff. We neglected evaporation and transpiration (evapotranspiration) in the modeling since the focus is to simulate short duration, large rain events when evapotranspiration is thought to be a minimal component of the water balance. We did not use CN regeneration, in which the initial abstraction is reset after some time period, since we only considered short duration, event-based storms.

Rainfall-runoff partitioning for an area is also dependent on the antecedent soil moisture conditions (how wet the soil is) at the time rain falls on the land surface. In essence, the wetter the soil is, the less water is able to infiltrate into the ground and the more rain is converted to runoff. Therefore, in order to better predict runoff volumes, we needed a methodology to adjust subbasin CNs to reflect the initial soil moisture conditions at the beginning of a storm simulation.

To account for antecedent moisture conditions at the beginning of a simulation in the HMS model, we used a soil moisture proxy known as the antecedent precipitation index (API) in conjunction with the existing NRCS definitions for the AMC I, II, and III classes. Traditional NRCS methodology attempts to account for different initial soil moisture conditions by classifying CNs into one of three classes: AMC I (dry), AMC II (average or normal), or AMC III (wet), which statistically correspond to the 10%, 50%, and 90% cumulative non-exceedance probabilities of runoff depth, respectively (Hjelmfelt, 1982). To reflect the degree of runoff potential, CNs are either increased (AMC III) or decreased (AMC I) from the average or normal conditions (AMC II) based on the seasonal five-day antecedent rainfall total prior to the time

period being analyzed. The subbasin CNs calculated for the HMS model represent the AMC II condition.

Instead of using the 5-day antecedent rainfall total, which applies equal weight to each of the five days preceding a storm, to describe soil moisture conditions, we used the more flexible API, which may be calculated over a longer time period and which uses a temporal decay constant that allows more weight to be applied to precipitation that fell closer in time to the event of interest in order to determine initial soil moisture conditions (Beck et al., 2009).

The goal of this analysis was to relate CN to API so that we could make appropriate CN adjustments in the HMS model to reflect soil wetness conditions at the beginning of a simulation. This was achieved by assuming that the 10%, 50%, and 90% cumulative non-exceedance probabilities of runoff depth that define the AMC I, II, and III CN classes could be equated to API (so that the AMC I, II, and III CN classes represent the 10%, 50%, and 90% cumulative non-exceedance probabilities of API). Under this assumption, we performed linear interpolation between the three ordered pairs that contained the basin average AMC I, II, and III CNs and the corresponding 10, 50, and 90^{th} API percentiles so that we could determine a CN adjustment for any API percentile. Consequently, we developed a continuous relationship that describes the change in CN that should be applied based on API, as opposed to being based on the traditional NRCS methodology which allows only three discrete possibilities for CN manipulation (the AMC I, II, and III CNs).

Since we calibrated the model for the Fox River Watershed in this project, we conducted an API analysis for the Fox River Watershed. We computed basin average daily API values over a 43 year period (1970 to 2013) using records from NOAA's hourly/daily precipitation stations

in Bloomfield, IA. Like the traditional NRCS method, API analysis in this case has two parts: one for the dormant season and the other for the growing season. In this case, the growing season refers to the months from April 1st to October 31st, while the dormant season includes the months from November 1st to March 31st. Since all of the events used for both calibration and validation happened between April and August, we only analyzed the API for the growing season in this case.

For each storm simulation considered, we calculated the API value for the day before the start of the simulation, computed its probability of non-exceedance using the daily API values from the 43 years record, and used this probability of non-exceedance to determine the percent adjustment in CN to apply to all subbasin CNs in the HMS model. In the present study, we optimized the decay constant based on the minimum mean absolute error (MAE) between the CNs adjustment based on the API analysis and them as needed. Having determined the optimum decay constant, we created the original API Quantile-CN relationship, which is shown as the solid line in Figure 4.6. The four points shown in the figure represent the necessary CN adjustments that were required for the optimal peak discharge correlation in each calibrated storm. As the figure shows, since most CN adjustments for the storms were overestimated, the original API quantile – CN curve was shifted downwards 2.67% based on the calculation. Figure 4.7 shows the existing NRCS definition for antecedent moisture conditions along with the changes that are described here and that were implemented for model calibration and validation.

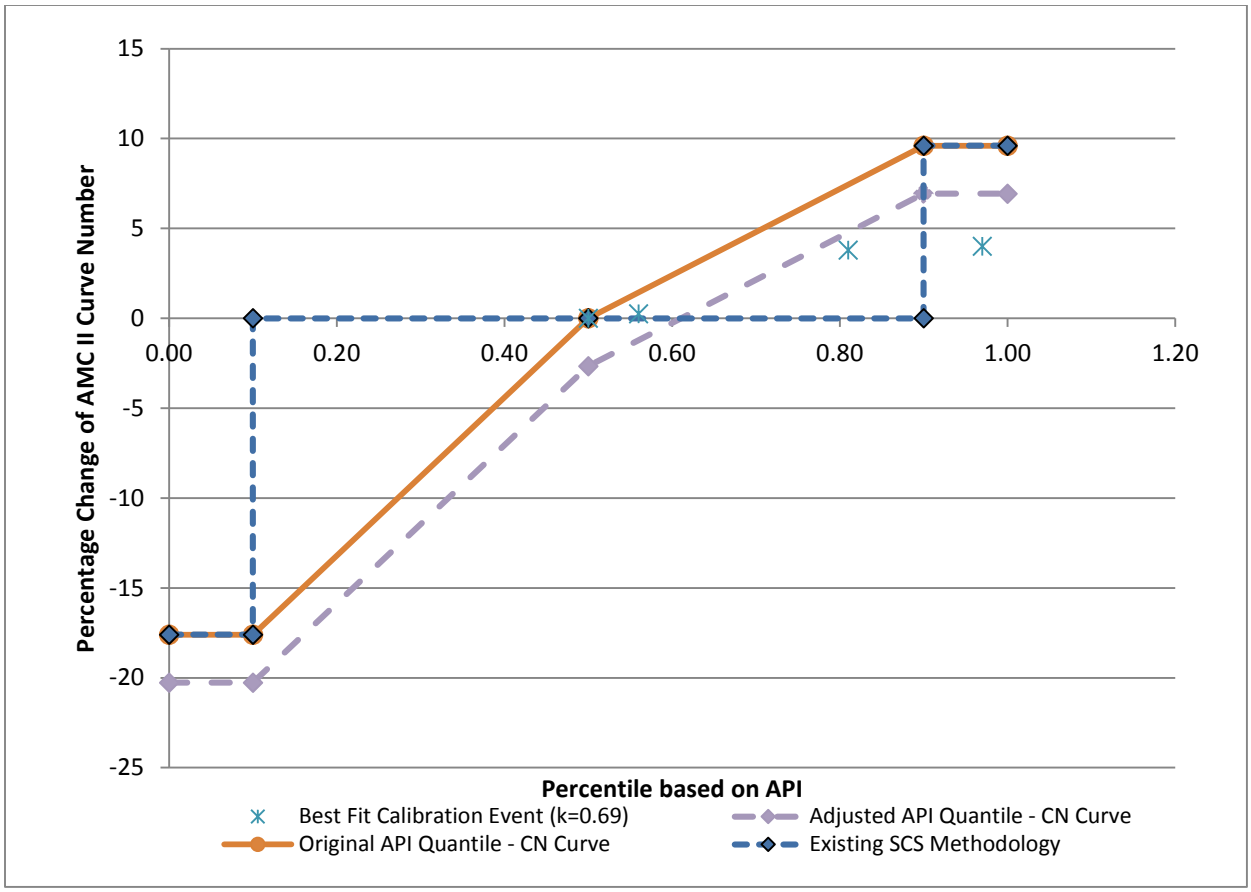

Figure 4.6 Accounting for antecedent moisture conditions in the Fox River Watershed HMS model. We used precipitation gage records to quantify the soil wetness prior to an historical event and applied the corresponding percent change in Curve Number to each subbasin Curve Number to reflect those conditions.

We used the ModClark and Clark Unit Hydrograph to convert precipitation to a direct runoff hydrograph for each subbasin. Both methods account for the translation (delay) and attenuation (reduction) of the peak subbasin hydrograph flow due to the travel time of the excess precipitation to the subbasin outlet and temporary surface, channel, and subsurface storage effects, respectively. The primary difference between the two methods is that the Clark Unit Hydrograph method uses a pre-developed time-area histogram, while the ModClark method uses a grid-based travel time model to derive the translation unit hydrograph. Both methods route the translation unit hydrograph through a linear reservoir to account for temporary storage effects.

The ModClark method requires the same grid used for radar rainfall, so we used this method for simulating the actual (historical) storms used for calibration and validation, whereas we used the Clark method for hypothetical design storm analysis.

Both of these methods required the development of two parameters: the time of concentration and the storage coefficient, both represented in units of time. The time of concentration is defined as the maximum travel time in the subbasin. We used the storage coefficient in the linear reservoir to account for storage effects. The time of concentration can generally be estimated if the lag time, which is the time difference between the center of the mass of the excess precipitation and the peak of the runoff hydrograph. The time of concentration is 1.67 times the lag time, which is a reasonable approximation according to SCS methodology (Mays, 2010). The storage coefficient can be estimated with empirical equations and is some multiple of the time of concentration and the time adjusted through calibration.

Inputs required to determine the basin lag time include the subbasin slope (in percent), the length of the longest flowpath for the subbasin (in feet), and the maximum potential retention (in inches) in the subbasin, which is determined from the subbasin CN. We used ESRI ArcGIS tools for terrain analysis to identify subbasin slopes and the longest flow paths. The following graphic illustrates the SCS methodologies as applied for runoff volume estimation and conversion of the excess precipitation into a runoff hydrograph.

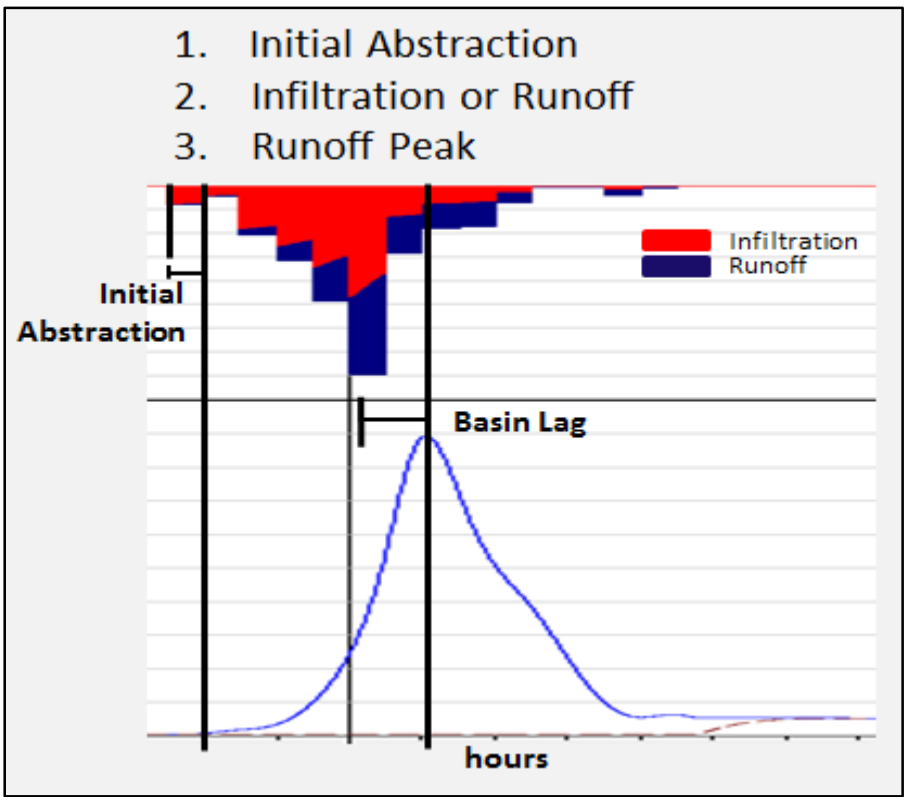

Figure 4.7 Subbasin runoff hydrograph conceptual model. This figure shows how rainfall is partitioned into runoff using the SCS Curve Number methodology and converted to a runoff hydrograph.

ArcGIS to HEC-HMS

Upon completion of GIS processing to prepare the basin topography data, establish the stream network, delineate the subbasins, and develop and assign the necessary parameters to describe the rainfall-runoff partitioning for each subbasin, we used HEC-GeoHMS tools to intersect the subbasins with the appropriate grid system (HRAP) in order to allow use of the Stage IV radar rainfall estimates. Lastly, from ArcGIS, we used HEC-GeoHMS tools to create a new HMS project and export all of the data developed in ArcGIS to the appropriate format so that the model setup was mostly complete upon opening HMS for the first time. Once in the HEC-HMS user's interface, we performed quality checks to ensure that the connectivity of the subbasins and stream network of the watershed were imported correctly.

4.4. Parameters Assigned in HEC-HMS

We used two different methods to compute the baseflow for the Soap Creek and Fox River Watersheds. Since there are no USGS stream gages present within the Soap Creek Watershed, we used Flow Anywhere and Flow Duration Curve Transfer Statistical Methods, which were developed by USGS in cooperation with the Iowa Department of Natural Resources, to compute daily mean streamflow at ungaged locations. The Flow Anywhere statistical method is a variation of the drainage-area-ratio method, which transfers same-day streamflow information from a reference streamgage to another location by using the daily mean streamflow at the reference streamgage and the drainage-area ratio of two locations (Linhart et al., 2012). The Flow Anywhere method modifies the drainage-area-ratio method in order to regionalize the equations for Iowa and determine the best reference streamgage from which to transfer same-day streamflow information to an ungagged location. According to the USGS report, streamgage Fox River at Wayland, Mo (0549500) was determined statistically to be the best reference gage for estimating flows at ungagged locations in the Soap Creek Watershed. Because most floods in Iowa have occurred during the summer, such as the 2007 Midwest and 2008 Iowa Floods, we focus the HEC-HMS simulations on this period. Therefore, we computed and used the daily mean average streamflow of May-October, 2013 for the baseflow separation. After separating the baseflow from streamflow, several typical baseflow were averaged to acquire the initial baseflow for the Soap Creek Watershed, which is 0.0049 cubic meters per second/per square kilometer. We modeled this baseflow for the hypothetical (design) storm of the Soap Creek Watershed.

For the Fox River Watershed, we approximated baseflow by a first order exponential decay relationship for all historical storms. We used the USGS stage/discharge gage for the Fox

River at Bloomfield, IA (05494300) to develop discharge-drainage area (cubic feet per second/per square mile) relationships in order to set initial conditions for streamflow prior to each actual storm event simulation. We applied these unique initial conditions to the appropriate corresponding subbasins within the HMS interface for each actual storm event simulation. We also specified a baseflow recession constant describing the rate of decay of baseflow per day and a threshold indicating when baseflow should be reactivated.

As introduced previously, we executed the flood wave routing in the HEC-HMS model was executed using the Muskingum routing method. Two inputs are required to use the Muskingum routing model in HMS – the flood wave travel time, K, and the weighting factor, X. For the X parameter, we used a value of 0.2 in this model. K can be estimated by dividing the reach length by a reasonable travel velocity (1-5 feet per second, in general) as a starting point, but it is generally best obtained by adjusting the model calibration process using measured discharged records if available. Please refer to section 2.3 for more details.

4.5. Calibration and Validation

Calibration and validation of the models are necessary before using them in research or real-world applications. Successful calibration requires an accurate and reliable historical record of both rainfall and stream data. However, because there is no stream gage present in the Soap Creek Watershed, we calibrated the Fox River Watershed HMS model instead. Once an optimal set of model has been established, it will be entirely or partially transferred to the Soap Creek Watershed HMS model. We introduce each process in the following sections.

We used Stage IV radar rainfall estimates and the USGS gage in the Fox River at Bloomfield, Iowa to calibrate the Fox River model. We selected four storms that occurred between June 2008 and May 2013 for calibration based on their magnitude, time of year, and the

availability of Stage IV radar rainfall and USGS discharge estimates. We selected large, high runoff storms that occurred between May and August to minimize the impacts of snow, rain on frozen grounds, and the freeze-thaw effects that exist during late fall to early spring conditions. Hydrographs for measured and simulated discharge are provided in Figure 4.8.

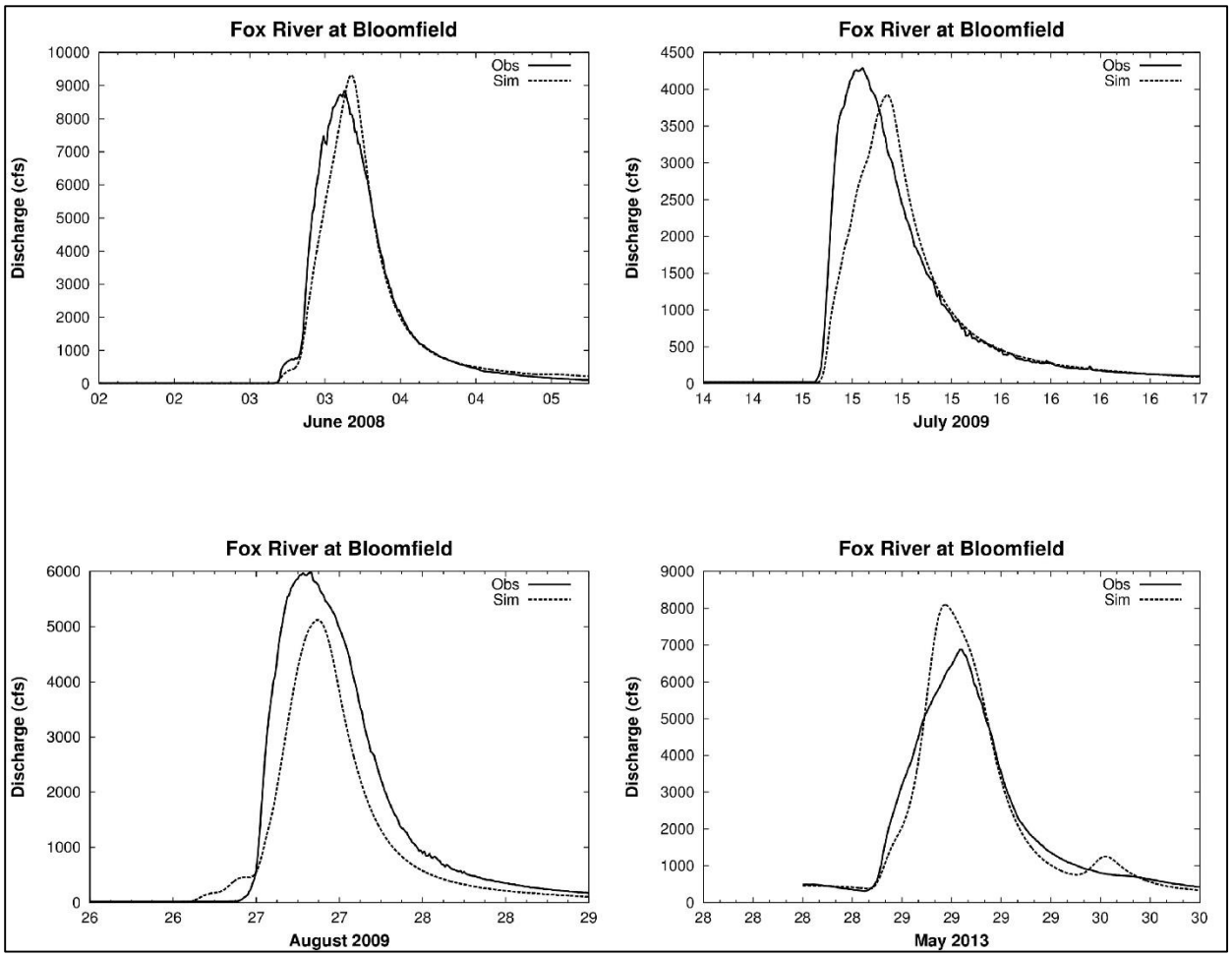

Figure 4.8 Hydrograph comparison for the four different calibration storms.

The June 2008 storm was characterized by a basin wide average rainfall depth of approximately 3.93 inches and a peak discharge of 8871.1 cfs at Bloomfield. Wet conditions were present before the storm, as the API was 0.80 inches, which corresponds to the 0.81 percentile. CNs in the HMS model were increased by 4.8% to reflect these wet conditions, and

the model did a reasonable job simulating this particular storm, as the simulated peak is only 5.6% overestimated, the timing of the peak flow is approximately one hour later, and the runoff volume is underestimated by 6.2%. The average simulated runoff coefficient (cumulated precipitation excess per cumulated precipitation) was 0.61.

The July 2009 storm was characterized by a basin wide average Stage IV radar rainfall depth of 2.00 inches and a peak discharge of 4288.7 cfs at Bloomfield. Wetter conditions were present before the storm since the API was 0.33 inches, which corresponds to the 0.56 quantile. The CNs in the HMS model were decreased by 1.1 % according to the shifted API Quantile-CN curve. The simulated peak flow was 8.6 % underestimated; the timing of the peak flow is approximately 3 hours late; and the runoff volume was underestimated by 12.2%. The simulated runoff coefficient was 0.37.

The August 2009 storm was characterized by a basin wide average Stage IV radar rainfall depth of 2.74 inches and an observed peak discharge of 5978.5 cfs at Bloomfield. Wet conditions were present before the storm, as the API was 0.27 inches, corresponding to the 0.503 percentile. CNs in the HMS were decreased by 2.59 % according to the shifted API Quantile-CN Curve. The simulated peak flow was 14.3% underestimated; the timing of the peak flow is approximately 1 hour late; and the runoff volume is underestimated by 29.6 %. The simulated runoff coefficient was 0.47.

The May 2013 storm was characterized by a basin wide average Stage IV radar rainfall depth of 2.81 inches and a peak discharge of 6879.4 cfs at Bloomfield. Wetter than normal conditions were present before the storm, as the API was 2.14 inches, corresponding to the 0.97 quantile. CNs in the HMS model were increased to reflect wetter conditions by 6.96 %. The

simulated peak flow was overestimated by 15.0 %, while the runoff volumes are nearly identical. The timing of the peak flow was approximately 2 hours early. The simulated runoff coefficient was 0.54.

For model validation, the intent is to use the model parameters developed during calibration to simulate other events and evaluate how well the model is able to replicate observed stream flows. With several of the largest storms already having been selected for calibration or having occurred before the availability of Stage IV radar rainfall estimates (January 2002), we selected the next best available storms. We used the small storm event of April 24-27, 2010 and a large event that occurred April 17-19, 2013 for validation. Figure 4.9 shows the validation results.

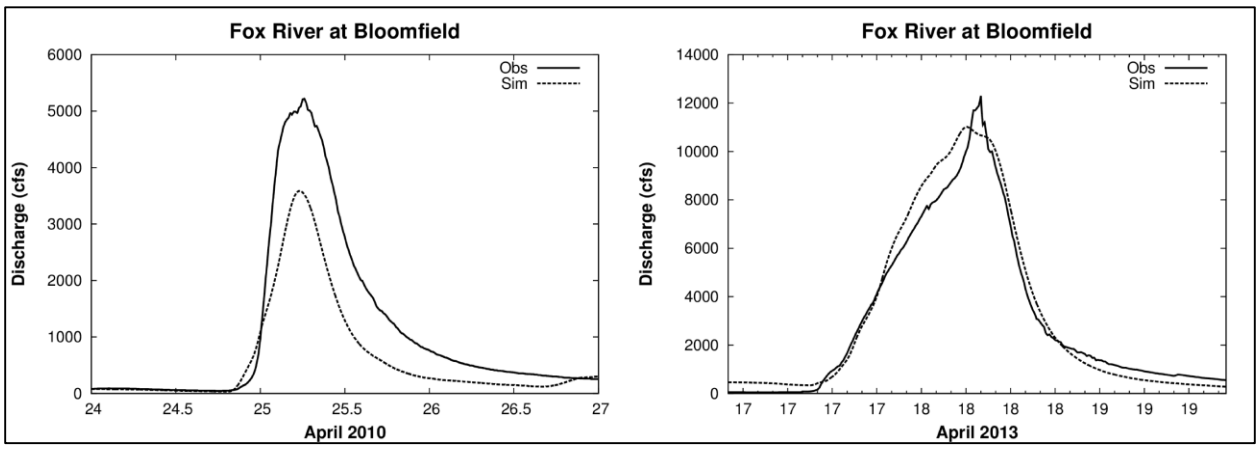

Figure 4.9 Hydrograph comparison for the two different validation storms.

The April 2010 validation storm was characterized by a basin wide average Stage IV radar rainfall depth of 1.69 inches and a peak discharge of 5,219 cfs at Bloomfield. Wetter than normal conditions were present before the storm, as the API was 0.62 inches, corresponding to the 0.75 quantile. The CNs were increased by 3.3% to reflect the wet antecedent moisture condition. Despite more rain being converted to runoff as the wet antecedent moisture conditions

suggested, simulated peak flow and total runoff volume were significantly underestimated in the model (peak flow and runoff volume at Bloomfield were estimated by 31.3 % and 43.5%, respectively). The simulated runoff coefficient was 0.87.

The April 2013 storm was characterized by a basin wide average Stage IV radar rainfall depth of 4.96 inches and a peak discharge of 12,300 cfs at Bloomfield. Wet conditions were present before the storm, as the API was 0.65 inches, corresponding to the 0.76 quantile. Therefore, CNs were increased by 3.5% from the base AMC II condition. As a result, the overall fit of the model is very good, especially for the falling limb. The peak flow was underestimated by 10.5%, while the volume was overestimated by 5.7%. The simulated storm achieved its peak magnitude about 2 hours earlier than the observed one. The simulated runoff coefficient was 0.76.

After finalizing a set of parameters for the Fox River Watershed HMS model, we transferred these parameters to the Soap Creek Watershed model accordingly. The strategy used in this research partially follows the transposition method because we directly used certain optimized parameters, such as the recession constant of baseflow, from the Fox River Watershed. We changed other parameters, such as the velocity of the flow, based on the Soap Creek Watershed's own characteristics. For instance, the Soap Creek Watershed has steeper slopes, so direct runoff flows faster within the Soap Creek Watershed than within the Fox River Watershed. In this case, instead of using the velocity from the Fox River Watershed directly, we computed the ratio of the flow velocities from these two watersheds based on their land slopes and then calculated the flow velocity in the Soap Creek Watershed. The calibration results also indicated that the CN values were overestimated by 2.67%; thus, the CN values for the entire Soap Creek Watershed were decreased by 2.67%. Table 4.3 provides the initial and calibrated parameters for the Fox River Watershed and parameters for the Soap Creek Watershed.

Table 4.3 The initial and calibrated parameters for the Fox River Watershed and Parameters for the Soap Creek Watershed.

Parameters	**Initial Value (Fox River Watershed)**	**Calibrated Value (Fox River Watershed)**	**Transferred Value (Soap Creek Watershed)**
Ratio to peak	0.10	0.06	0.06
Recession Constant	0.90	0.25	0.25
Muskingum K	Based on velocity of 0.7 m/s	Based on velocity of 1.3 m/s	Based on velocity of 1.7 m/s
Curve Number	Initial curve number generated from GIS	Values vary based on antecedent moisture condition	2.67 % decrease overall
Storage Coefficient	2 times the time of concentration	3 times the time of concentration	3 times the time of concentration

4.6. Chapter Summary

This chapter described the process of HEC-HMS model development for the Soap Creek Watershed, including the DEM resource, the Meteorologic Model, and the Basin Model. A significant improvement in our study was the employment of a more flexible method which accounts for the antecedent moisture conditions at the beginning of a simulation. Instead of using the traditional NRCS definitions for the AMC I, II, and III classes, the new method determines the percent adjustment in CN for each storm event according to the API value for the day before the start of the simulation and its probability of non-exceedance that is computed using the daily API values from the 43 year record.

This chapter also described the challenge we faced in the model calibration process. Because of the lack of availability of the measured hydrographs in the Soap Creek Watershed, it cannot be directly calibrated using the historical storms. Consequently, we first calibrated the adjoining Fox River Watershed with one USGS stream gage and then transposed the parameters from Fox River to the Soap Creek Watershed model accordingly. We selected four storms that occurred between June 2008 and May 2013 for calibration, while we used the small event of the

April 2010 and a large event that occurred April 2013 for validation. Model calibration adjusted the initial set of model parameters to make the simulated results more closely match observed hydrographs at gaging stations for historical events with respect to the peak discharges, volumes, time to peak, and the shape of hydrographs.

CHAPTER 5. HYDRAULIC MODEL DEVELOPMENT OF SOAP CREEK WATERSHED

5.1. Introduction

This chapter summarizes the development of the hydraulic model for the Soap Creek river network, for which we used the United States Army Corps of Engineers' (USACE) Hydrologic Engineering Center's River Analysis System (HEC-RAS) Version 4.1. HEC-RAS is an integrated software system that is designed for interactive use in a multi-tasking, multi-user network environment. It is capable of performing one-dimensional hydraulic calculations for a full network of natural and constructed channels. The current version of HEC-RAS is able to support steady and unsteady flow water surface profile computations, sediment transport/movable boundary computation, and water quality analysis. In this thesis, we focus exclusively on the unsteady flow simulation.

Like the steady flow simulation, the unsteady flow simulation incorporates the hydraulic calculations for cross-sections, bridges, culverts, and other hydraulic structures. Additionally, it has the ability to model storage areas and hydraulic connections between storage areas as well as between stream reaches. The main function of the HEC-RAS model is to compute the water elevations for all locations of interest along the channels. The data needed to perform unsteady flow simulation are the geometric data and unsteady flow data. We will explain each form of data in detail in the following sections. Note that this thesis is not intended to calibrate or validate the Soap Creek HEC-RAS model. The simulation results presented in Chapter 6 are meant to demonstrate how the different routing methods will affect the hydrograph predictions.

5.2. HEC-RAS Model Development

5.2.1. Creating the RAS GIS Import File

The first step in developing a HEC-RAS model is to create the geometric data, which can be accomplished using ArcGIS 9.3 as well as the ArcView GIS extension, HEC-GeoRAS, which was specially designed to process geospatial data for use with HEC-RAS. The geometric file includes information about the river centerlines, junctions, flow path lines, stream banks, cross sections, and other physical attributes of river channels. The essential datasets used for HEC-GeoRAS are the terrain data (LiDAR DEM) with 3 meter resolution and the river network for the Soap Creek Watershed. The river network defines the extent of the Soap Creek and all of the tributaries that collect the runoff from contributing areas. It would be ideal to include all tributaries in the model, but too much detail often makes simulations overly expensive or causes numerical instabilities. Thus, in our study, the HEC-RAS model only includes three major tributaries of the Soap Creek: South Soap Creek, Brush Creek, and Little Soap Creek. Soap Creek flows eastward to its outlet, which is approximately 55 miles away, into the Des Moines River. Soap Creek is below Little Soap Creek and has a length of 24 miles. Figure 5.1 displays the modeled stream network.

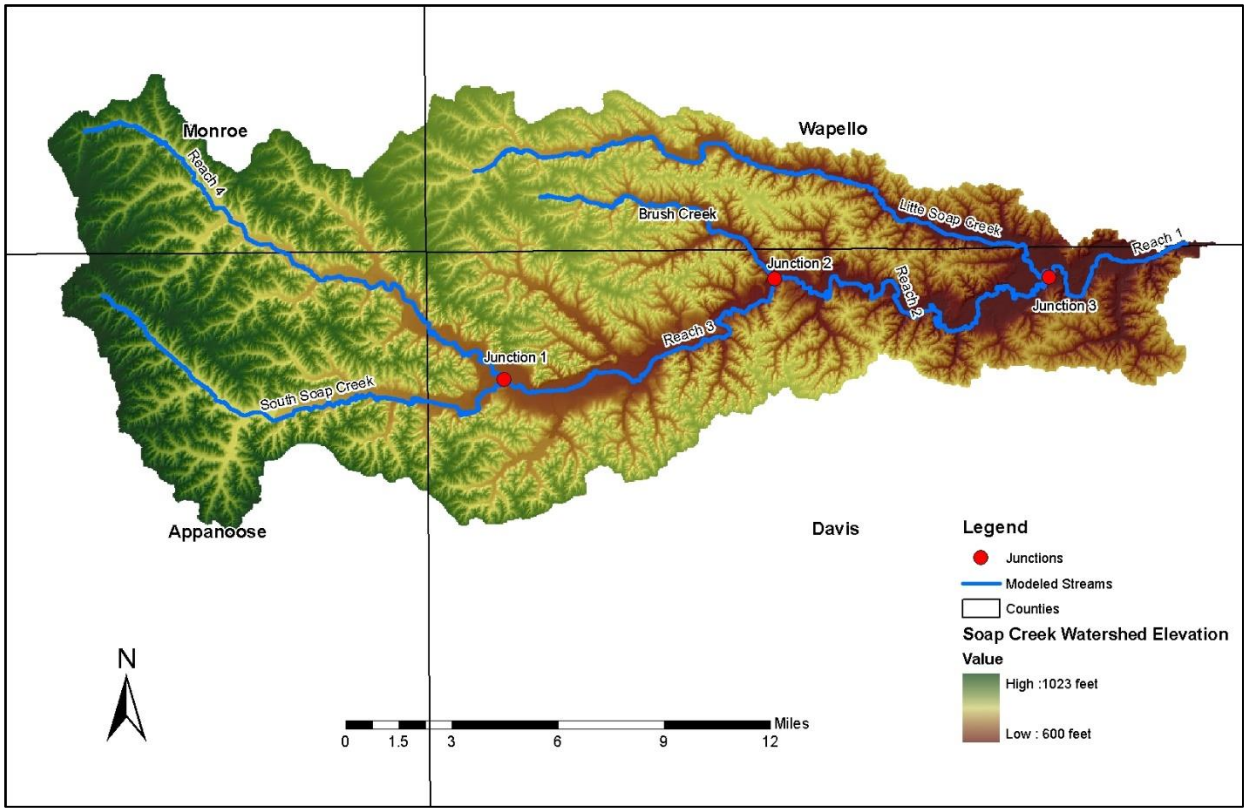

Figure 5.1 Soap Creek Hydraulically Modeled Streams

We extracted the river centerline used to establish the river network for HEC-RAS from the river network that was created before. It is comprised of the Soap Creek and its three major tributaries, with a total length of 107 miles. Junctions are necessary in the HEC-RAS model to account for the places in which tributaries combine or distributaries split. In order to model the entire network of the Soap Creek simultaneously, we created three junctions (see Figure 5.1). There are two methods of modeling the hydraulics at a junction for unsteady flow. One is the Force Equal WS Elevations (momentum), which forces the upstream water surface equal to the downstream water surface. This method requires fairly closed cross sections to be placed around a junction so that stability problems will not arise. The other method is the Energy Balance (Energy) method, which uses the energy equation across the junction to solve for water surface elevation. The Energy Balance method assumes that the energy loss due to the angle of tributary

flow is negligible and is a very useful option for the medium to steep streams or where the junction reach lengths are fairly long. We chose the Energy Balance Method in our study based on the model's performance. The stream lengths across the junction between the two bounding cross sections must also be entered into the HEC-RAS model. In the following figure, we used an aerial photograph to draw and identify the flow path lines, stream banks, and cross sections on top of the LiDAR DEM.

Cross sections are the key inputs into the HEC-RAS model. They contain much information, including data on the elevation of the main channel and over banks, bank stations (locations that separate the main channel from the floodplain), and the downstream reach lengths (distance between cross sections). An adequate number of cross sections is required to sufficiently represent the geometry of the Soap Creek river network. In our study, we placed more than 500 cross sections with spacing that ranged from 20 to 1000 m (see Figure 5.2). We allowed less distance between areas in which abrupt changes in channel geometry occur. In addition, we placed two cross sections upstream and downstream of any hydraulic structures (e.g., bridge/culvert) in order to compute the energy loss from contraction and expansion. We imported the geometric data described above directly into the HEC-RAS model.

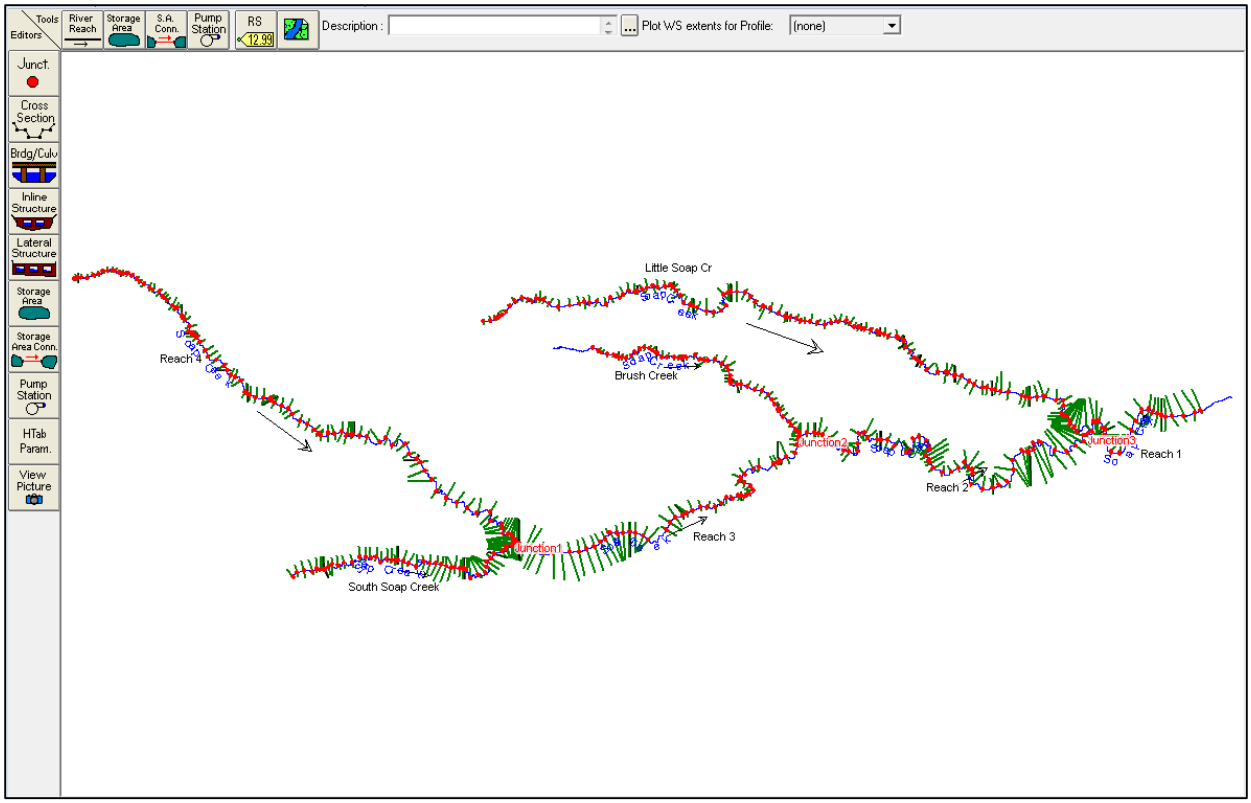

Figure 5.2 Cross sections for the unsteady state model in the Soap Creek river network.

5.2.2. Manning's roughness coefficient

Manning's roughness coefficient represents the resistance to flow in the channels and floodplains. The Manning's n-value depends on a number of factors, which include surface roughness, vegetation, channel irregularities, degree of meander, obstructions, and size and shape of the channel (Intuition & Logic, Inc., 2009). Manning's n values need to be assigned to both the channel and overbank flow areas in order to compute the energy losses due to friction. In our study, we created statewide Iowa Manning's roughness coefficient shapefiles by using a land use feature class (National Land Cover Database 2011) with Manning's n defined for different land use types. Table 5.1 lists the land use descriptions and their corresponding Manning's n values, which were recommended by the IDNR. They also suggested that for the channel whose

contributing drainage area is less than 10 mi^2, a Manning's roughness coefficient of 0.045 can be used, while for the channel whose drainage area is greater than 10 mi^2, 0.035 can be used. We manually altered the Manning's n values for the channel in the HEC-RAS in order to conform to these recommendations. A typical cross section with roughness coefficients is shown in Figure 5.3.

Table 5.1 Range of Manning's n values utilized for the overbank

NCLD 2001 Classification	Manning's roughness coefficient
11 - Open water	0.02
21 - Developed, Open Space	0.03
22 - Developed, Low Intensity	0.05
23 - Developed, Medium Intensity	0.1
24 - Developed, High Intensity	0.15
31 - Barren Land	0.05
41 - Deciduous Forest	0.12
42 - Evergreen Forest	0.12
43 - Mixed Forest	0.12
52 - Scrub/Shrub	0.08
71 - Grassland/Herbaceous	0.035
81 - Pasture/Hay	0.035
82 - Cultivated Crops	0.07
90 - Woody Wetlands	0.1
95 - Emergent Herbaceous Wetland	0.045

Table 5.2 Range of Manning's n values utilized for the main channel

Contributing Drainage Area	Manning's roughness coefficient
Less than 10 square miles	0.045
Greater than 10 square miles	0.035

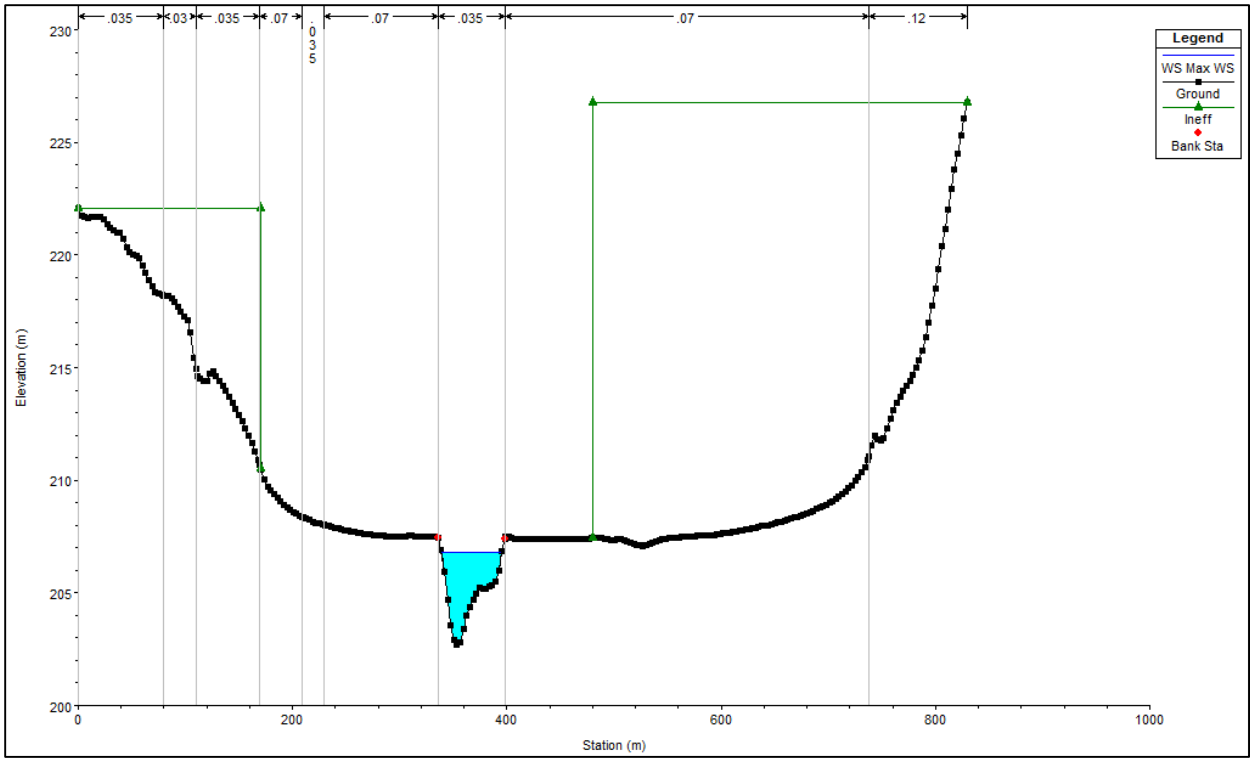

Figure 5.3 Typical cross section in the Soap Creek HEC-RAS model.

5.2.3. Hydraulic Structure Data Input

Since hydraulic structures such as bridges and culverts can cause energy loss and attenuate hydrographs, it is important to include their effects in the HEC-RAS model. We incorporated 42 bridges and 2 inline structures into the Soap Creek HEC-RAS model and created four cross sections to model each hydraulic structure in the HEC-RAS. The four cross sections include a downstream cross section where the flow has fully expanded, two cross sections that are located just downstream and upstream of the bridge/culvert, and an upstream cross section before flow starts to contract. The HEC-RAS v4.1 User's Manual Chapter 6 provides more details on this methodology. Generally, the flow lengths between the bridge cross sections and the upstream and downstream cross sections should be determined by field investigation during high flows. However, it is not feasible to do so for each hydraulic structure. Traditionally, the

Corps of Engineers recommends locating the upstream cross section at a distance that is equal to one times the average length of the side constriction caused by the structure abutments. The HEC-RAS User's Manual also recommends that the expansion length can be estimated by multiplying the expansion ratio by the average obstruction length. Table 5.3 provides guidance for determining the expansion ratio based on the average bed slope (S), the ratio of the bridge opening width to the total floodplain width (b/B), and the Manning n value ratio of the overbanks to the main channel (nob/nc).

Table 5.3 Ranges of Expansion Ratios (HEC-RAS v4.1 User's Manual, January 2010).

		nob / nc = 1	nob / nc = 2	nob / nc = 4
b/B = 0.10	S = 1 ft/mile	1.4 – 3.6	1.3 – 3.0	1.2 – 2.1
	5 ft/mile	1.0 – 2.5	0.8 – 2.0	0.8 – 2.0
	10 ft/mile	1.0 – 2.2	0.8 – 2.0	0.8 – 2.0
b/B = 0.25	S = 1 ft/mile	1.6 – 3.0	1.4 – 2.5	1.2 – 2.0
	5 ft/mile	1.5 – 2.5	1.3 – 2.0	1.3 – 2.0
	10 ft/mile	1.5 – 2.0	1.3 – 2.0	1.3 – 2.0
b/B = 0.50	S = 1 ft/mile	1.4 – 2.6	1.3 – 1.9	1.2 – 1.4
	5 ft/mile	1.3 – 2.1	1.2 – 1.6	1.0 – 1.4
	10 ft/mile	1.3 – 2.0	1.2 – 1.5	1.0 – 1.4

The geometry data, including the deck/roadway, piers, and embankment slope, of each bridge also needs to be entered into the HEC-RAS model. Ideally, these data should be collected by field work. In order to save time and simplify the model, we made some assumptions in our study. For instance, we assumed the bridge decks to be 1-2 meters thick based upon recommendations by the engineers who had visited several of the sites. We measured the width of each bridge from the 2013 aerial photograph. The bridge deck profile and the station and

elevation points were extracted from Lidar DEM (Last Return) with 1 meter resolution. Theoretically, the last return represents the bare earth terrain, but this is not always the case. The laser pulses emitted from the terrestrial Lidar systems can be reflected from man-made structures, vegetation, or the earthen surface (USGS, 2014). Figure 5.4 represents the typical bridge geometry in the HEC-RAS model.

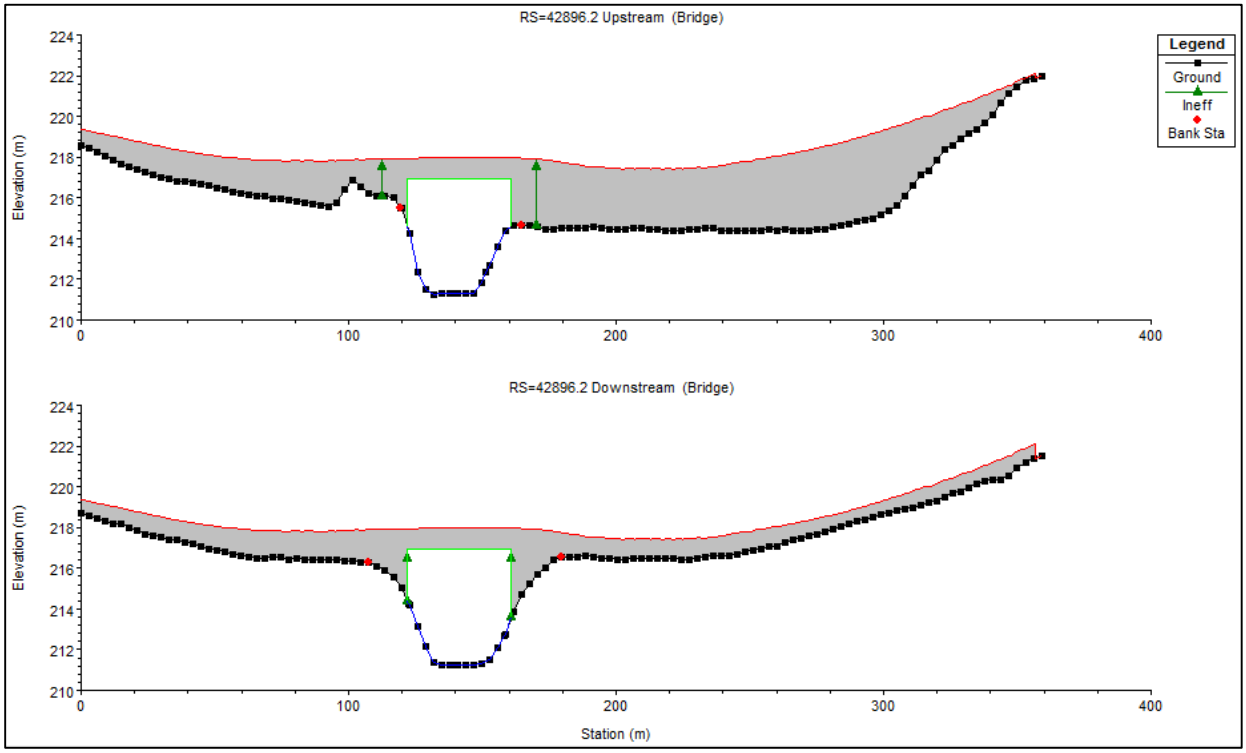

Figure 5.4 Typical bridge geometry in the HEC-RAS model.

5.2.4. Ineffective Flow Areas

The ineffective flow area refers to the area containing water that is not actively being conveyed. Ineffective flow areas often form upstream and downstream of bridges and where other man-made or natural barriers disrupt flow. To determine the initial estimate for the stationing of the ineffective areas upstream and downstream of the bridges, we used a ratio of 1:1 for the ineffective flow area contraction, and we used a ratio from 2:1 to 4:1 for the ineffective

area for the ineffective flow expansion. Setting an ineffective area requires at least one station and one elevation, which is usually called the trigger elevation. When the water surface becomes greater than the trigger elevation, the ineffective flow area will convey flow (for non-permanent ineffective flow areas). The trigger elevations are different for the upstream and downstream cross sections of one bridge. The trigger elevations at upstream sections were set to be slightly lower than the lowest high chord of the bridge. At the downstream cross sections, the trigger elevations were defined as lower than the lowest low chord of the bridge. Figure 5.4 also represents the trigger elevations at both the upstream and downstream of a bridge.

5.2.5. Unsteady Flow Data

Unsteady data are required to perform an unsteady flow simulation. Unsteady flow data is comprised of boundary conditions and initial conditions. Boundary conditions must be specified for each modeled constituent at all locations where flow enters the system, including the upstream boundaries of the main channel and its tributaries and lateral inflows (HEC-RAS 4.1 User's Manual, January 2010 p. 19-6). Several different types of boundary conditions are available: flow hydrograph, stage hydrograph, stage and flow hydrograph, rating curve, and normal depth. We chose flow hydrographs for the boundary conditions since they can be directly exported from the HEC-HMS model. We used the Normal Depth assumption as the downstream boundary condition in the Soap Creek HEC-RAS model. Because the energy slope is unknown, we approximated it by using the slope of the channel bottom. The average bed slope of Soap Creek is 0.0009. However, this is not the slope ultimately used in this model since we increased the slope to 0.0012 to eliminate model instabilities.

Additionally, we established the boundary conditions at internal locations within the river

system in the form of later inflow hydrographs in order to capture the runoff generated from the drainage area along the channel or the small tributaries that are not included in the hydraulic model. The lateral inflow hydrographs also can be read from the DSS file generated from the HEC-HMS model. Figure 5.5 shows how to bring in the hydrograph generated from subbasin W8830 between cross sections RS: 3767.715 and RS: 2284.864.

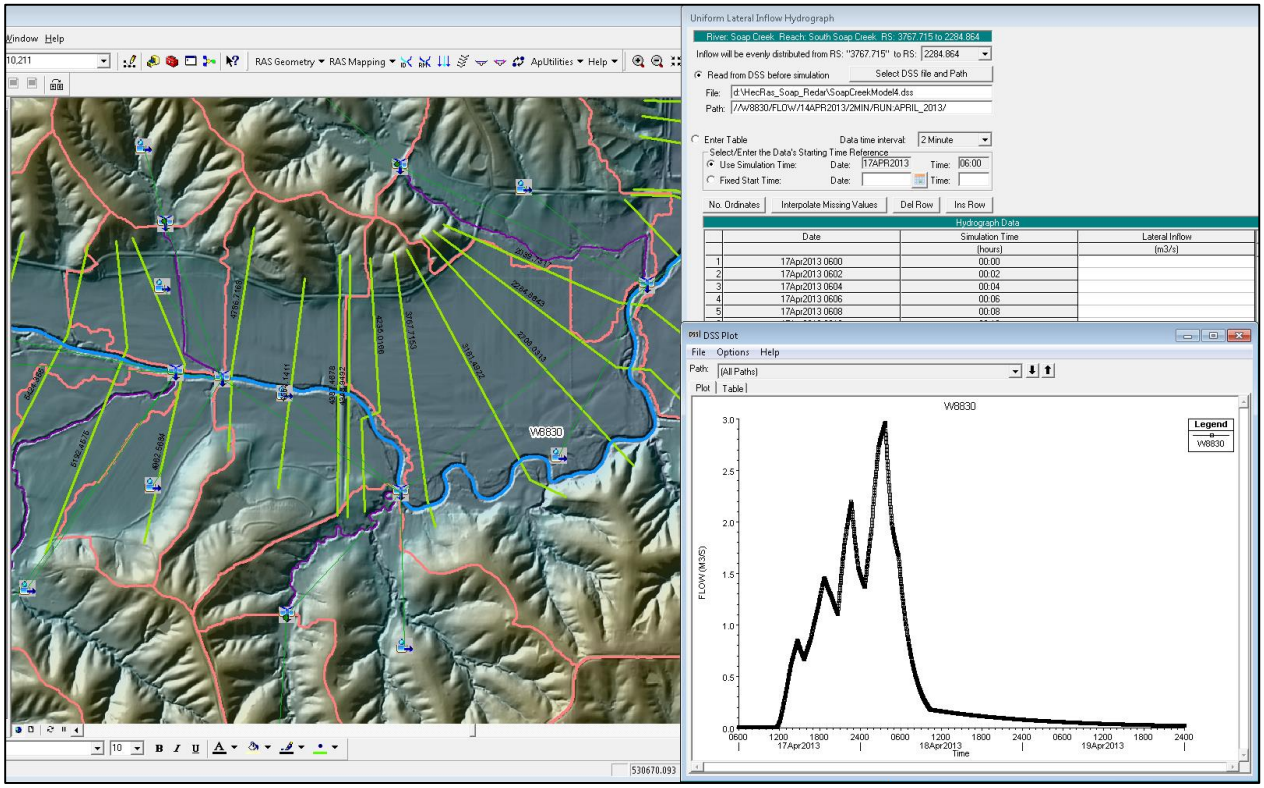

Figure 5.5 Example of assigning a uniform lateral inflow hydrograph between two cross sections.

Initial conditions are also necessary and consist of flow and stage information at each of the cross sections as well as elevations for any storage areas defined in the system (HEC-RAS v4.1 User Manual, 2010 p. 8-12). The most common method of establishing initial conditions is to enter the flow data for each reach and have the program perform a steady flow backwater run to compute the corresponding stages at each cross section. We estimated the base flow of the

Soap Creek Watershed as 0.0049 $m^3/s/km^2$ by using the method introduced by USGS. Therefore, we approximated the initial flow for each reach by multiplying 0.0049 times the drainage areas. The estimated initial flow data are shown in Table 5.3. When we ran the model with this set of initial flow data, it was unable to reach completion since several cross sections went dry. Therefore, the initial flows were increased incrementally to ensure that the river bed never goes dry during the entire simulation process. Table 5.3 also shows the final set of initial conditions of two different simulations.

Table 5.4 Boundary conditions set up for the Soap Creek HEC-RAS model for two different storms.

Reach Name	*Initial Estimate (m^3/s)*	*100-year 24-hour Storm (m^3/s)*	*April 17-20, 2013 Storm (m^3/s)*
Little Soap Creek	0.53	4.5	3
Reach 4	0.69	7	3
Reach 3	1.88	9	5
Reach 2	2.48	12	5
Reach 1	3.19	16	5
Brush Creek	0.23	5	3
South Soap Creek	0.53	2	3

5.3. Challenges

DSS files enable the transition between the HEC-HMS and HEC-RAS models, but there is currently no simplified one-step process to accomplish this. It is a time-consuming process because, operationally, one must browse the desired DSS file and reference the pathname for every two specified cross sections between which to insert the lateral inflow. In the Soap Creek HEC-RAS model, there are over several hundred pairs of cross sections which means it is necessary to repeat this action several hundred times. During this process, it is very easy to add or omit lateral inflows. One way to avoid this mistake is to compare the water volume under the hydrographs at the same location between the two models and make sure the water volume is

conservative. Sometimes you have to add multiple lateral inflows between the two cross sections, but HEC-RAS Version 4.1 lacks this capacity. Instead of adding these lateral inflows manually in an excel file and then copying and pasting them into the HEC-RAS model, creating a junction to combine them in the HEC-HMS mode beforehand would be much easier. Consequently, it is only necessary to reference that junction and save a lot of time in the future, especially when it is necessary to run other storm simulations.

Another challenge is determining the two cross sections between which to insert the lateral inflows in the HEC-RAS model. It is a subjective process because there is more than one reasonable way to insert the lateral inflows, and different people may take different approaches. However, different insert positions could result in quite different final hydrographs. Therefore, it is wise to make use of the stream network as well as the hillshade shapefile when adding the lateral inflows. This information could more effectively ascertain the flow directions. Meanwhile, it is important to avoid adding too many lateral inflows between two cross sections during a short distance because a sudden increase in flow could yield instability.

Furthermore, stability issues may arise again after updating DSS files because the flows inserted between cross sections are changed. Therefore, it is necessary to restabilize the model. During this model stabilization process, it is not recommended to make any changes to the model geometry. However, adjustment of the initial flows and computation time steps could be a good starting point.

5.4. Calibration and Validation

We used observed stage hydrographs at four IFC stage sensor locations during the period of April 17 – 19, 2013 to calibrate the HEC-RAS model. The IFC Stage Sensor only provides the stream heights at 15-minute interval. The IFC Stage Sensors are attached to the downstream faces of the bridges and emit a sonar signal to measure the distance to the water surface. We used the distance from each sensor to the stream bottom minus the measured distance between the water surfaces to calculate the stream depths. This calculation process assumed the distance between the sensor and the stream bed to be unchanged since the sensor was installed. In order to calibrate the HEC-RAS model, the observed stream depths must first be converted into stage hydrographs by adding the stream bed elevations at the IFC Stage Sensor locations. There are two sets of stream bed elevations available. One set was provided by IFC Water Resources Engineer Tony Loser and was measured on May 6, 2014. Another set of elevations was extracted from the 3 meter resolution Lidar DEM, which is used in the HEC-RAS model. All of them are referenced in the North American Vertical Datum of 1988 (NAVD 88). Both elevation sets are listed in Table 5.4.

Table 5.5 Measured and modeled stream bed elevations at four IFC Stage Sensor locations.

Location	Measured Stream Bed Elevation (ft)	Modeled Stream Bed Elevation (ft)	Difference (ft)
LTLSOAP01	644.17	643.86	-0.31
SOAPCR03	768.73	769.88	1.15
SOAPCR02	707.04	708.28	1.24
SOAPCR01	630.34	636.45	6.11

As Table 5.4 shows, measured stream bed elevations are almost the same at LTLSOAP01 as at the modeled elevations, while they are lower at the other three locations. This may result, in part, from the temporal changes in the stream bed. Additionally, we extracted the modeled stream bed elevations from the Lidar DEM, which cannot penetrate the surface of the water to

detect the stream bed. Therefore, the modeled stream bed elevations might reflect the water surface elevations rather than the stream bed elevations unless the stream was dry when they were measured. We used both sets of stream bed elevations to generate two sets of stage hydrographs. Figure 5.6 illustrates the comparison of simulated and observed stages based on measured and modeled stream bed elevations at four IFC Stage Sensor locations.

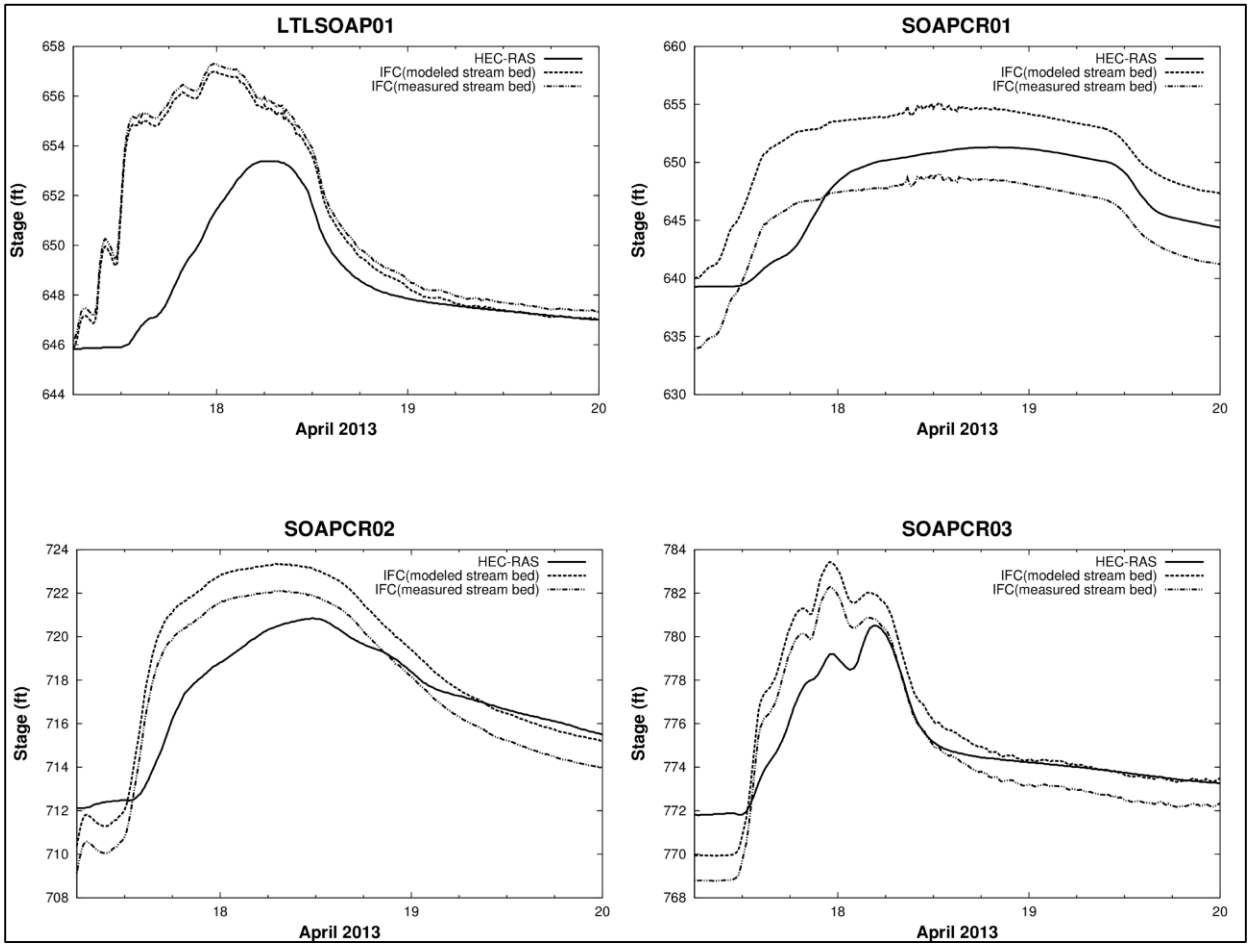

Figure 5.6 HEC-RAS simulated stage hydrographs and IFC observed stage hydrographs with different stream bed elevations at four IFC Stage Sensor locations for the April 17-20, 2013 storm.

As Figure 5.6 shows, after switching the stream bed elevations from measured to modeled, the stage hydrographs were shifted up except at the LTLSOAP01 location. The simulated stage hydrographs fit the shifted ones fairly well at the receding limb, except at the

SOAPCR01 location. We calculated the correlation coefficients between the simulated and observed stage hydrographs at these four locations as follows: 0.703, 0.848, 0.950, and 0.892 for LTLSOAP01, SOAPCR01, SOAPCR02, and SOAPCR03, respectively. These values are significantly high, which means there is good correlation with respect to time between the simulated and observed stage hydrographs. However, a small offset in time still exists between the simulated and observed stage hydrographs. In order to identify how much shift the simulated stage hydrograph should make to achieve the best fit between the simulated and observed stage hydrographs, we conducted a correlation coefficient study. This analysis calculates the correlation coefficient between the simulated and observed hydrographs every time after shifting the simulated stage hydrographs 15 minutes forward. Figure 5.7 represents the correlation coefficient versus shift time at the four locations.

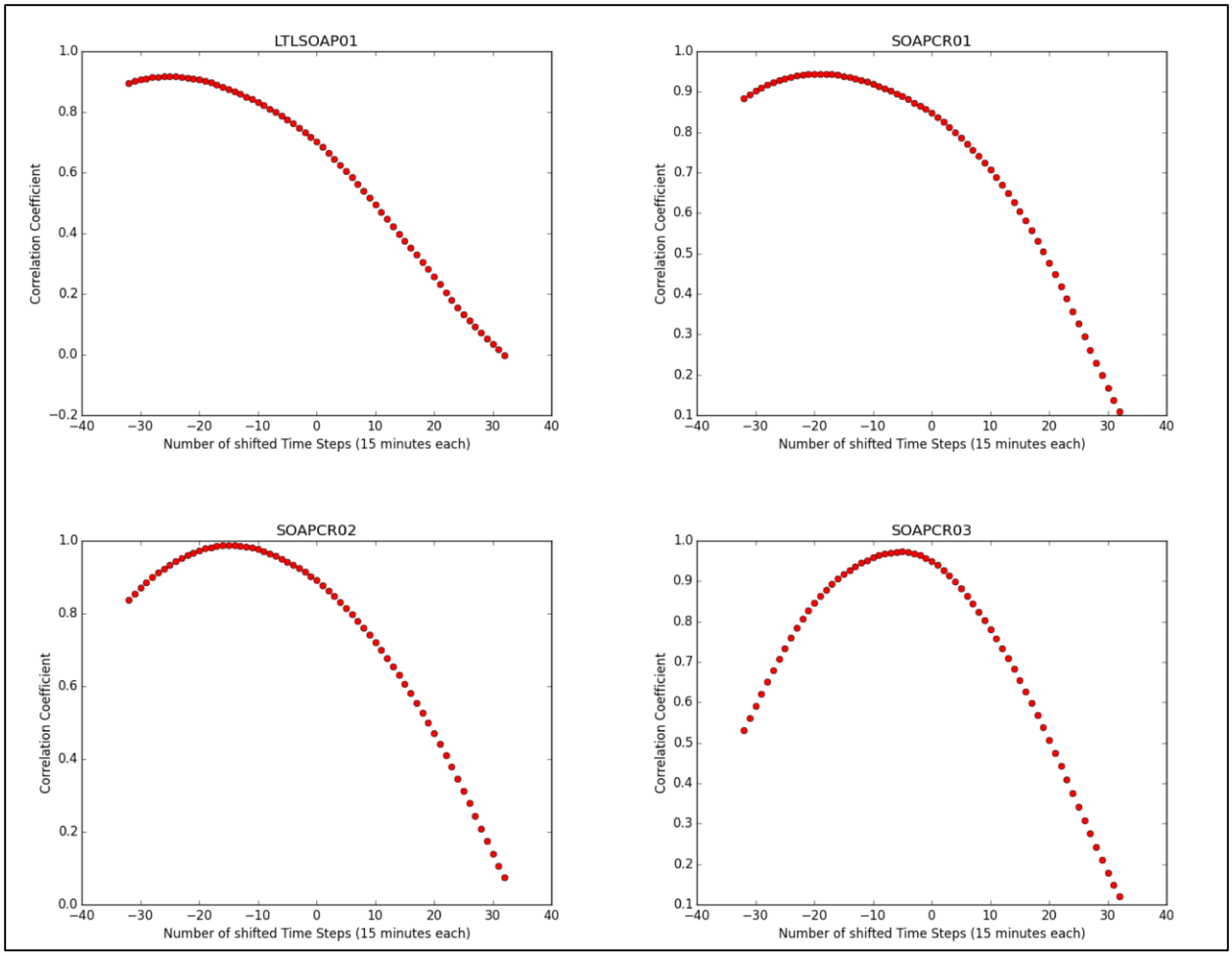

Figure 5.7 Correlation coefficient versus number of shifted time steps at four IFC Stage Sensor locations.

At the LTLSOAP01 location, the correlation coefficient achieves its maximum value of 0.918 after shifting the simulated stage hydrograph by 375 minutes to the left. The simulated stage hydrograph needs to be shifted to the left by 285 minutes to achieve the best coefficient of 0.944 at SOAPCR01. The best coefficient is achieved when the stage hydrograph is shifted by 225 minutes to the left at SOAPCR02 and the correlation coefficient is 0.988. At the SOAPCR03 location, the correlation coefficient achieves its maximum value of 0.973 when the simulated stage hydrograph is shifted towards to the left by only 75 minutes. In addition, according to Figure 5.6, there is a significant discrepancy in water volume between the simulated and

observed stage hydrographs. There are two possible reasons: 1) The HEC-HMS model of the Soap Creek Watershed underestimated the direct runoff volume or 2) the IFC stage sensors overestimated the direct runoff volume.

Manning's roughness coefficient is one of the main variables used in calibrating a hydraulic model (HEC-RAS User's Manual Version 4.1, 2010, P 8-45). Before calibrating the HEC-RAS model, we conducted a sensitivity study of Manning's roughness coefficient by multiplying the roughness coefficients of the main channel by constants 0.8, 0.9, and 1.1. The main purpose of the sensitivity study is to understand the effects that the varying values of the roughness coefficient can have on the peak stage, time to peak, and general hydrograph shape. The sensitivity analysis kept all other model parameters the same. Figures 5.8 – 5.11 plotted the stage hydrographs with various roughness coefficients. Generally, the stage will become higher with increased roughness coefficients, and vice versa, because higher roughness coefficients cause lower velocity and subsequently result in lower conveyance. Table 5.5 summarizes the maximum stages and peak of time for various roughness coefficients at LTLSOAP01, SOAPCR01, SOAPCR02, and SOAPCR03. The results indicate that the increase in Manning's roughness coefficients did not significantly affect the time of peak.

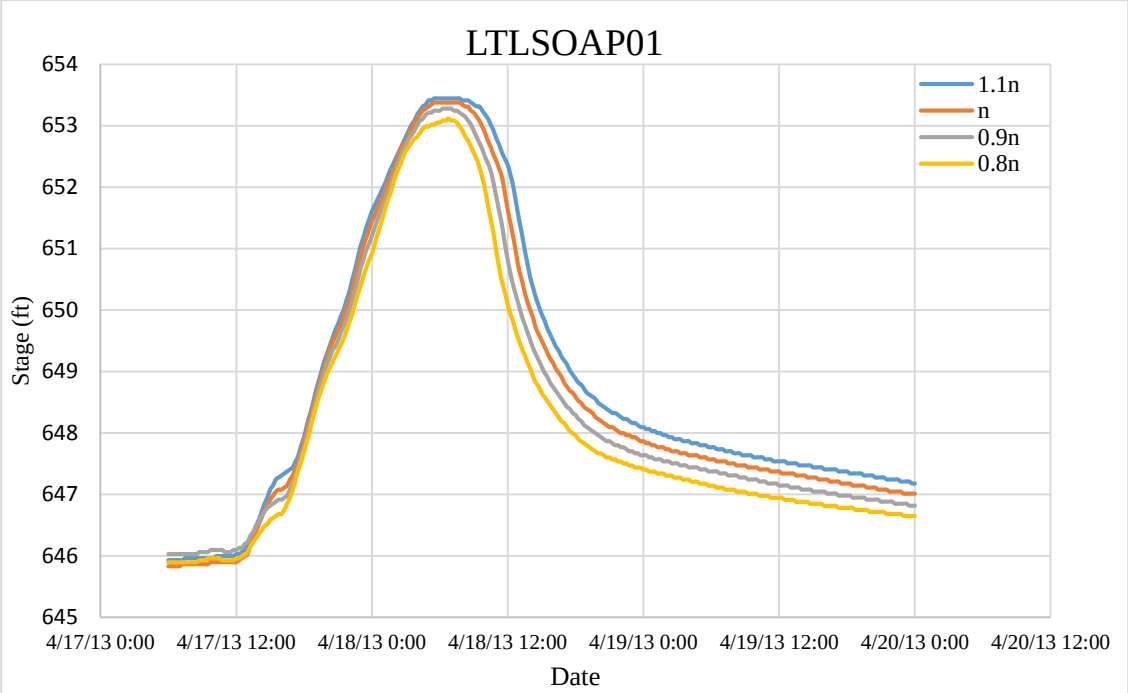

Figure 5.8 Stage hydrographs with changes of Manning's roughness coefficients in main channels at LTLSOAP01.

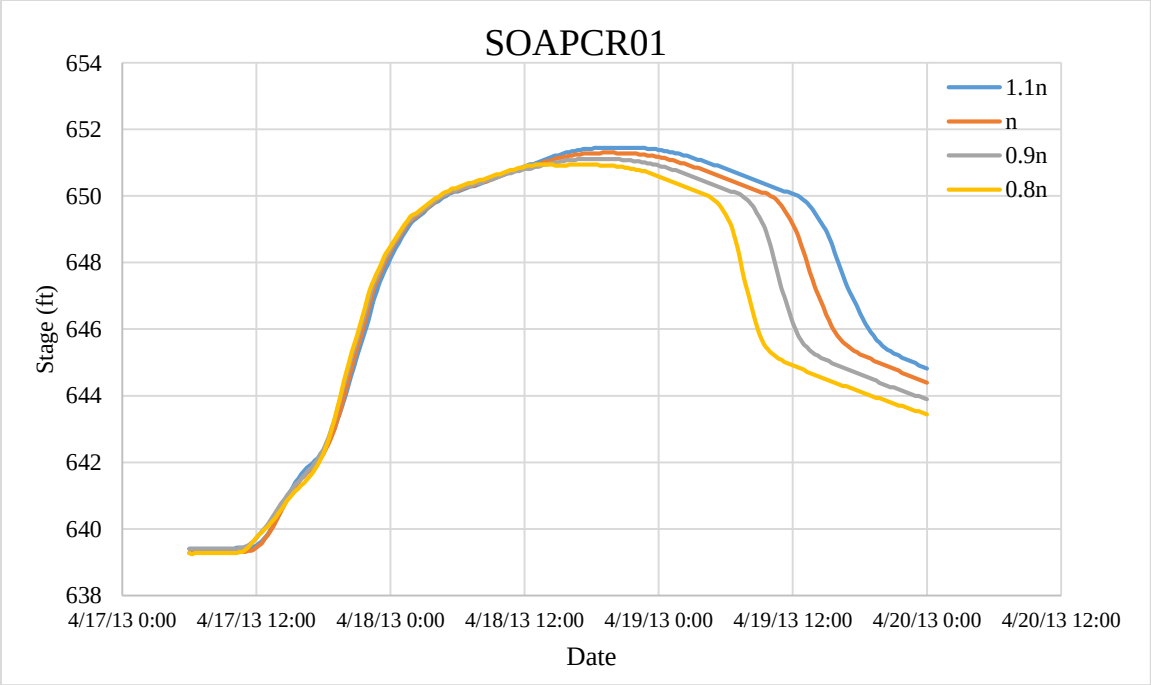

Figure 5.9 Stage hydrographs with changes of Manning's roughness coefficients in main channels at SOAPCRO1.

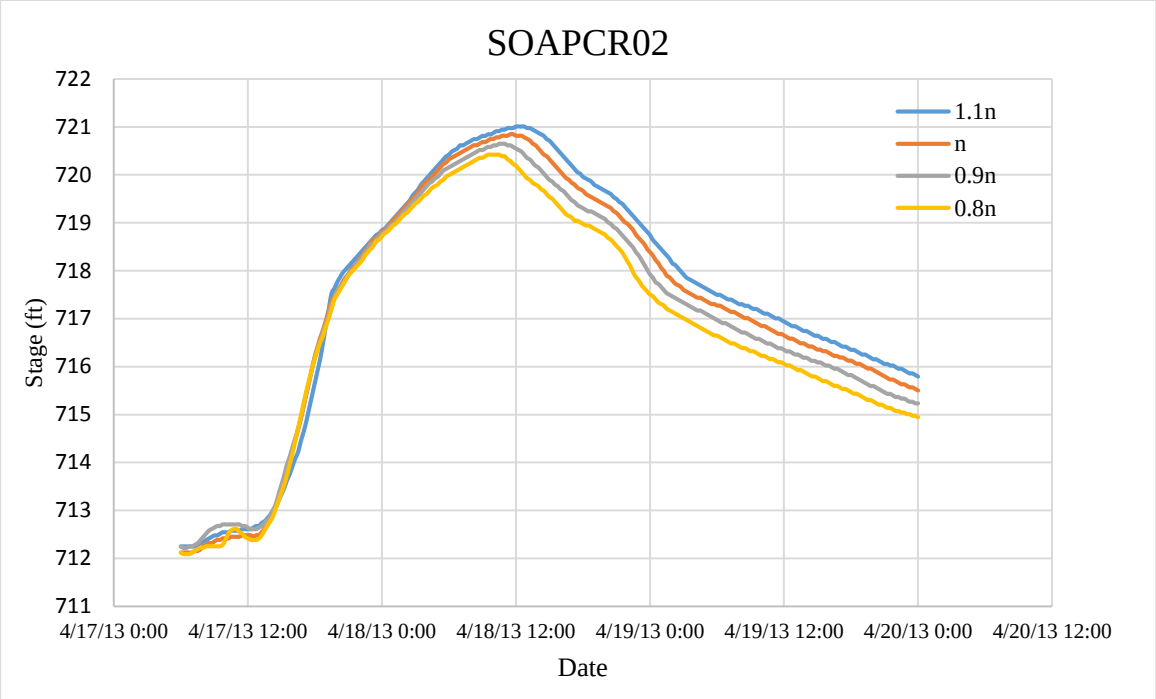

Figure 5.10 Stage hydrographs with changes of Manning's roughness coefficients in main channels at SOAPCR02.

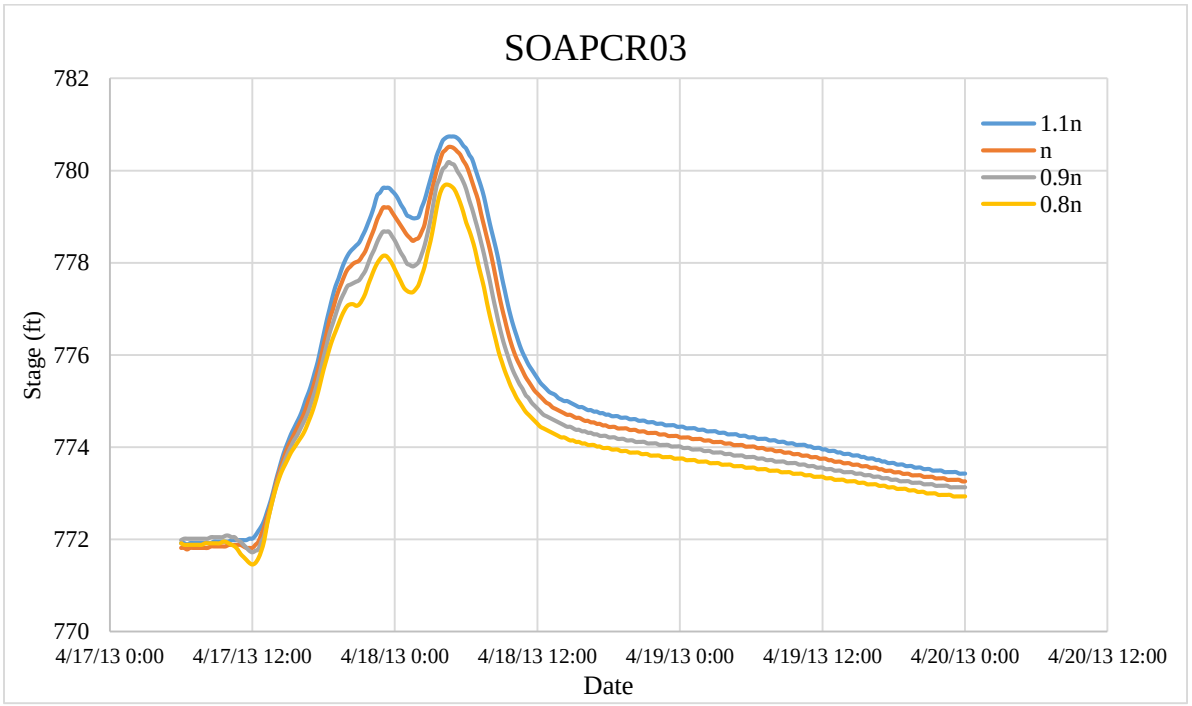

Figure 5.11 Stage hydrographs with changes of Manning's roughness coefficients in main channels at SOAPCR03.

Table 5.6 Summary of maximum stages and time of peak for various roughness coefficients in main channels at four IFC sensor locations.

Manning's Roughness Coefficients	LTLSOAP01		SOAPCR01		SOAPCR02		SOAPCR03	
	Peak Time	Stage (ft)	Peak Time	Stage (ft)	Peak Time	Stage (ft)	Peak Time	Stage (ft)
1.1n	4/18/2013 6:30	653.44	4/18/2013 20:00	651.44	4/18/2013 12:30	721.01	4/18/2013 4:30	780.74
n	4/18/2013 6:30	653.38	4/18/2013 19:30	651.31	4/18/2013 11:30	720.85	4/18/2013 4:30	780.51
0.9n	4/18/2013 7:00	653.28	4/18/2013 18:30	651.11	4/18/2013 10:30	720.65	4/18/2013 4:30	780.18
0.8n	4/18/2013 6:45	653.11	4/18/2013 13:45	650.95	4/18/2013 10:00	720.42	4/18/2013 4:30	779.69

In our study, we use the HEC-RAS model to simulate large storms during which the flow rises from the main channel to the flood plain. In this situation, the overbank roughness has to be considered because the composite *n* used for the model calculation is computed based on both main channels and overbank roughness. Therefore, we conducted a similar sensitivity analysis of Manning's roughness coefficients by multiplying the overall roughness coefficients, which include both the main channel and overbanks, by constants 1.1, 1.2, and 1.3. We did not decrease the roughness coefficients this time, as the HEC-RAS model would crash for coefficients that are too low. We plotted the stage hydrographs for increased as well as original roughness coefficients in Figures 5.12 – 5.15. Basically, we obtained similar results by changing the overall roughness coefficients as we did from changing only the main channels' roughness coefficients. We also provide a summary table (See Table 5.6) here. From Table 5.5 and Table 5.6, it is clear that the stage increases more when increasing the overall roughness coefficients. In addition, these two tables show that the time of peak stage at LTLSOAP01 and SOAPCR03, which are located at the upstream of the Soap Creek, did not change significantly when changing the roughness coefficients. However, the time delay of the peak stage becomes more apparent at SOAPCR02 and SOAPCR03, which are located at the downstream because more attenuation

will occur as water moves downstream.

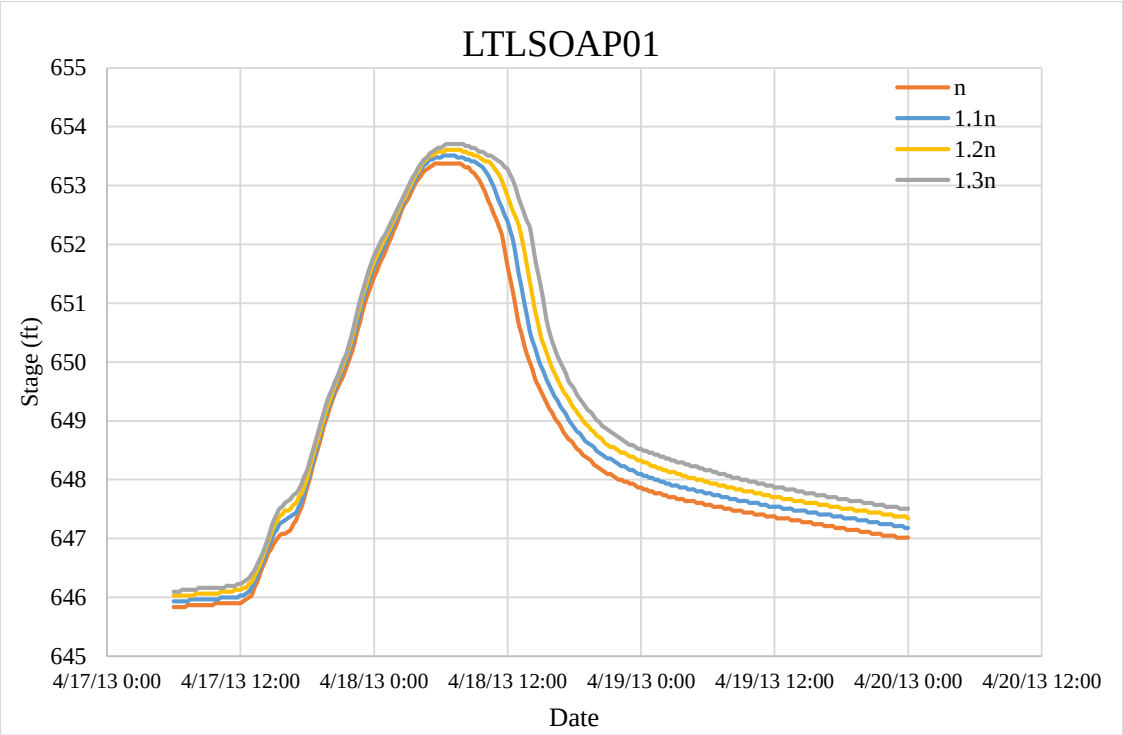

Figure 5.12 Stage hydrographs with changes in overall roughness coefficients at LTLSOAP01.

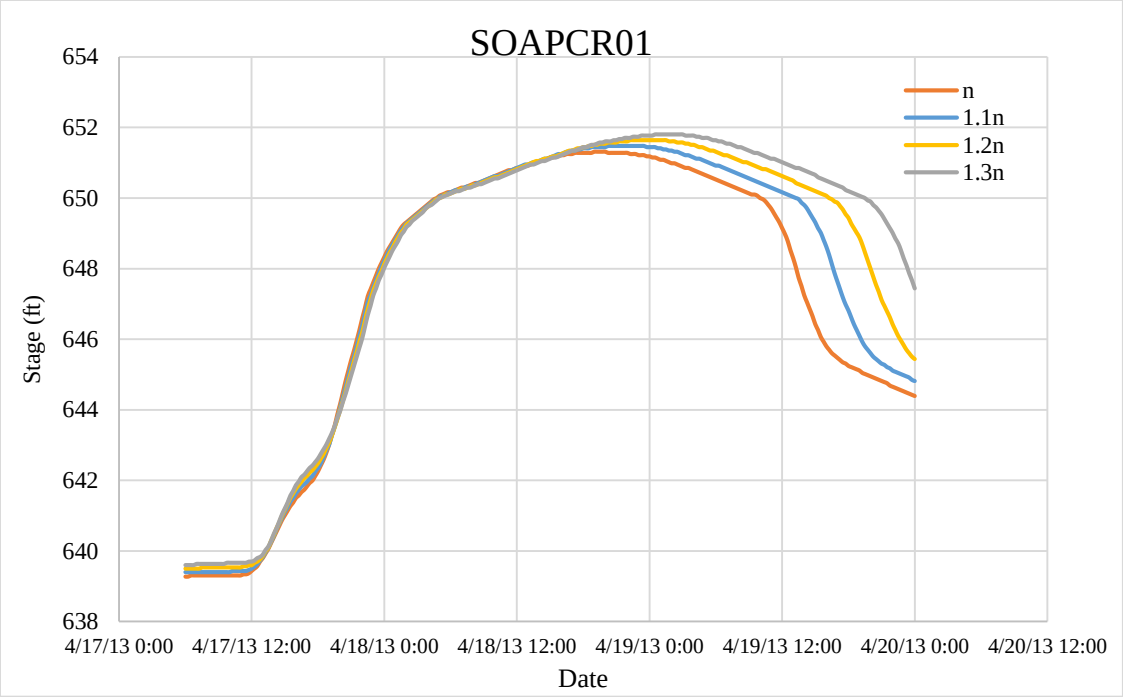

Figure 5.13 Stage hydrographs with changes in overall roughness coefficients at SOAPCR01.

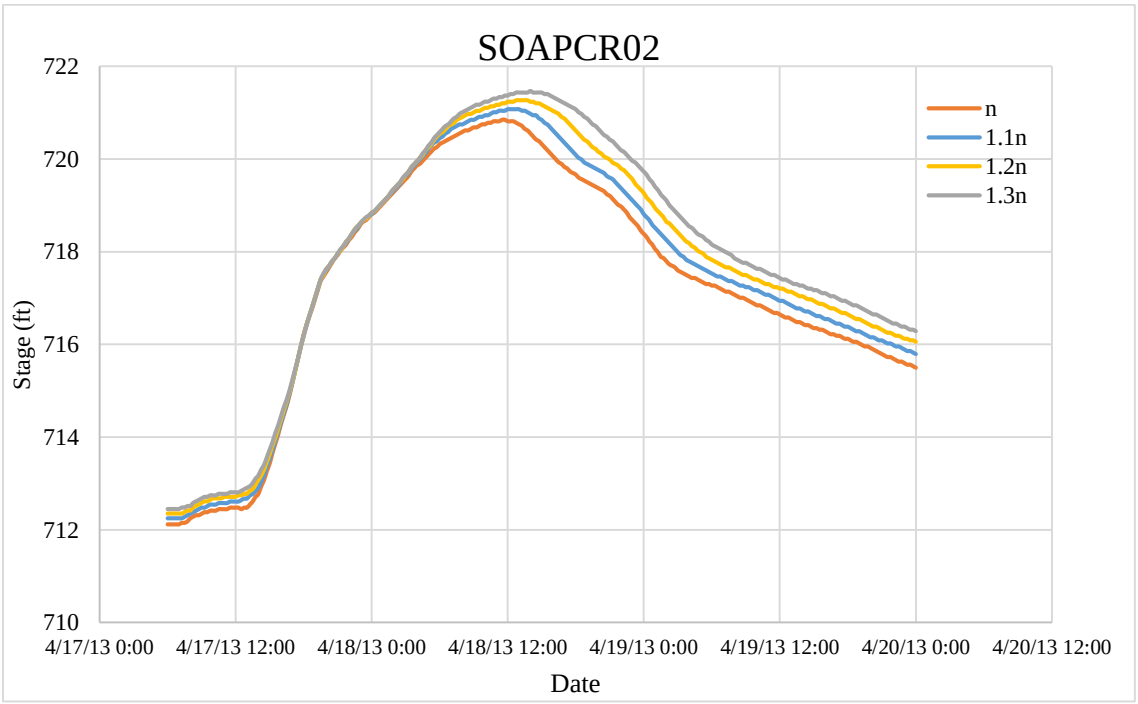

Figure 5.14 Stage hydrographs with changes in overall roughness coefficients at SOAPCR02.

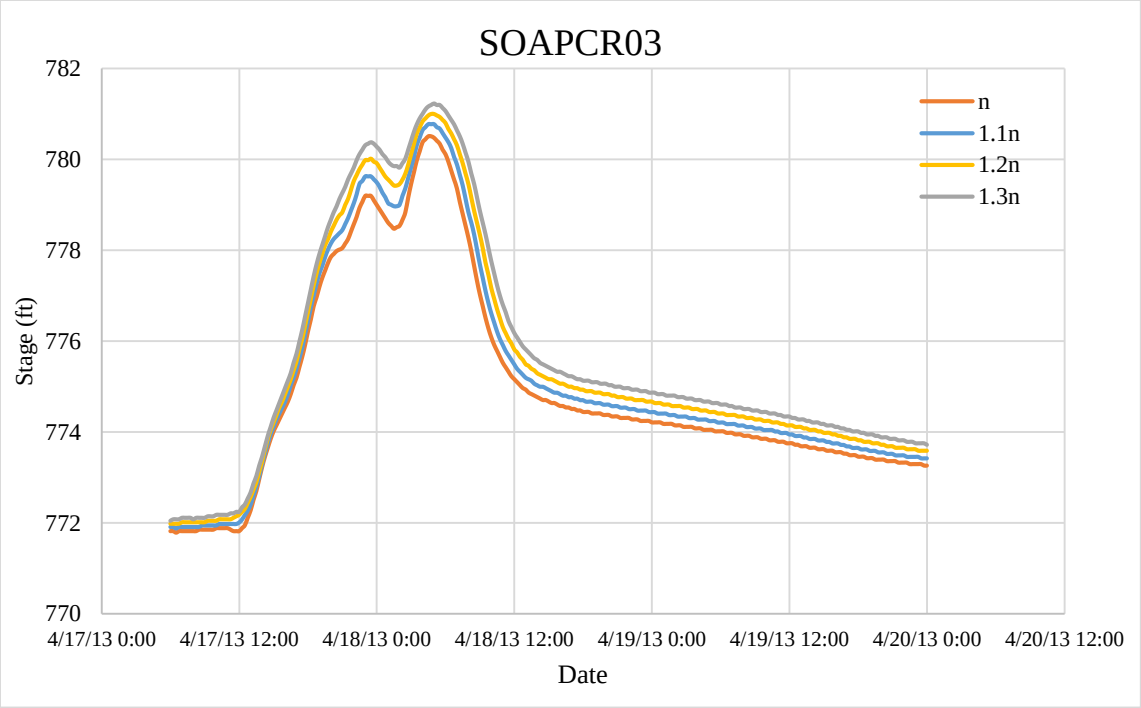

Figure 5.15 Stage hydrographs with changes in overall roughness coefficients at SOAPCR03.

Table 5.7 Summary of maximum stages and time of peak for various overall roughness coefficients at four IFC stage sensor locations.

Manning's Roughness Coefficients	LTLSOAP01		SOAPCR01		SOAPCR02		SOAPCR03	
	Peak Time	Stage (ft)	Peak Time	Stage (ft)	Peak Time	Stage (ft)	Peak Time	Stage (ft)
n	4/18/2013 6:30	653.38	4/18/2013 19:30	651.31	4/18/2013 11:30	720.85	4/18/2013 4:30	780.51
1.1n	4/18/2013 6:30	653.51	4/18/2013 22:00	651.47	4/18/2013 12:30	721.08	4/18/2013 4:30	780.77
1.2n	4/18/2013 7:00	653.61	4/19/2013 0:00	651.64	4/18/2013 13:00	721.27	4/18/2013 5:00	781.00
1.3n	4/18/2013 7:30	653.71	4/19/2013 1:30	651.80	4/18/2013 14:00	721.47	4/18/2013 5:00	781.23

Based on the Manning's roughness coefficient sensitivity analysis, adjusting the Manning's roughness coefficients is not an effective way to reduce the time difference between simulated and observed hydrographs. Also, the stage hydrograph comparison indicates that the most significant difference between simulated and observed hydrographs is the direct runoff volume rather than the timing. To increase the simulated direct runoff volume, we increased the

overall CNs used in the HEC-HMS model by 9.6% from the original values to reflect the wet antecedent moisture condition in which almost all of the rainfall is converted into direct runoff. After corrections, the average CN was increased from 79.7 to 89.7. We then compared the observed and simulated stage hydrographs with corrected CNs (See Figure 5.16).

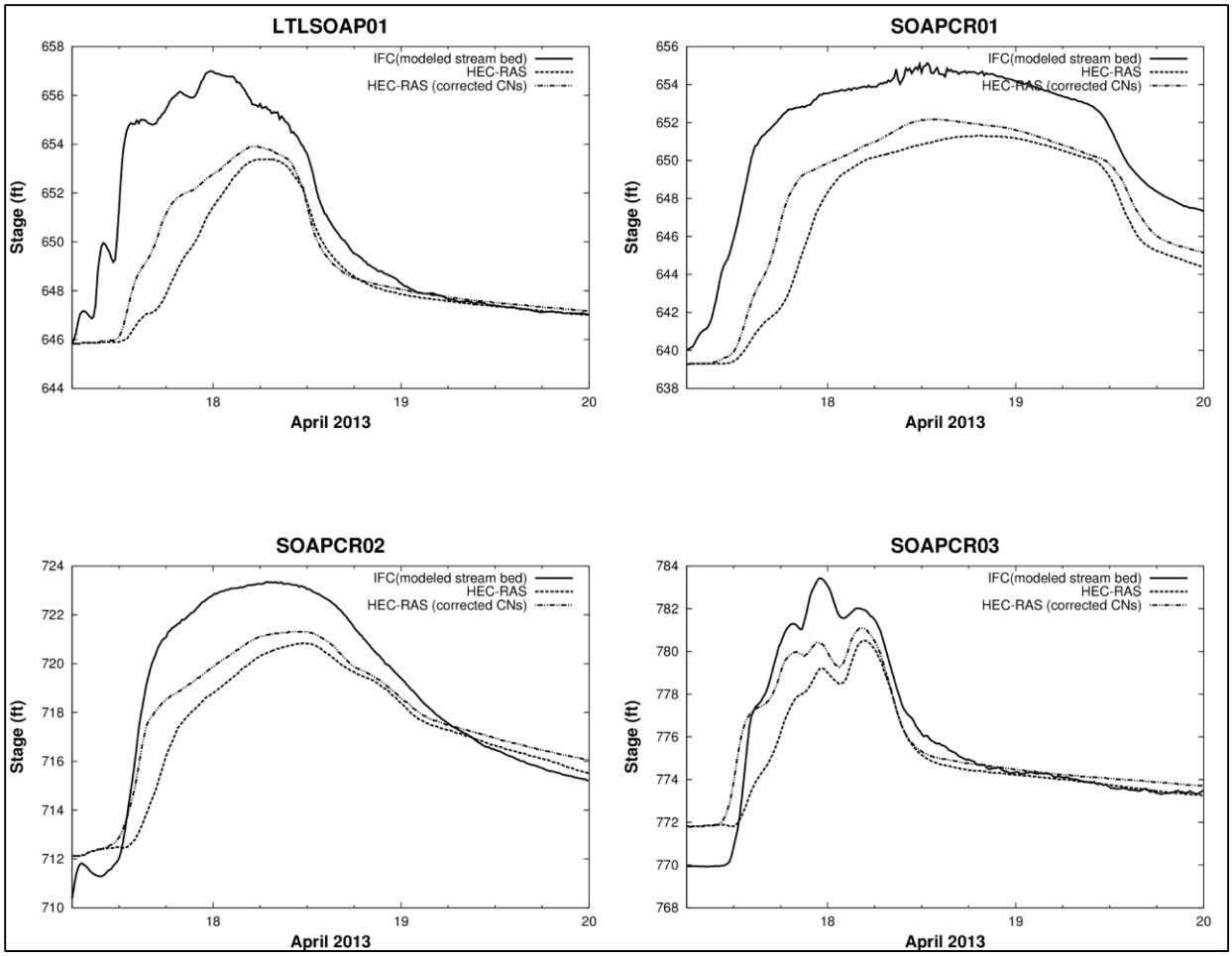

Figure 5.16 Comparison between observed stage hydrographs and simulated stage hydrographs with corrected CNs at four IFC Stage Sensor locations for the April 17-20, 2013 storm.

As Figure 5.16 shows, the simulated direct runoff volumes increased slightly after increasing the CNs because, as the CNs increase, a greater amount of rainfall is converted to direct runoff. However, the simulated direct runoff volumes at these four locations still cannot

meet the observed ones. When calibrating the HEC-RAS model, it is necessary to make sure the model parameters, no matter what the Manning's roughness coefficient or the CNs are, are within the realistic range. Therefore, we believe that this discrepancy may result from the uncertainties and errors associated with the radar rainfall data or with the IFC stage sensor measurements. As introduced earlier in Chapter 5, we calculated the observed water depths using the distance from each sensor to the stream bottom minus the measured distance between the water surfaces. This calculation process assumed the distance between the sensor and the stream bed is unchanged. This assumption introduces some uncertainties to the data because the steam bed may have changed due to scour or deposition of sediments. Therefore, the HEC-RAS model cannot be calibrated in our case due to the lack of reliable observed stage hydrographs.

5.5. Chapter Summary

This chapter summarized the process of HEC-RAS model development for the Soap Creek river network. The Soap Creek HEC-RAS model consists of seven reaches, with a total length of 107 miles. We extracted more than 500 cross sections from a 3 meter resolution Lidar DEM, which we used to represent the Soap Creek river network. We incorporated 42 bridges and 2 inline structures into this model in order to compute the energy losses dues to contraction and expansion. We simulated two storms using the Soap Creek HEC-RAS model: one is the 100-year 24-hour design storm, and the other is a historical storm that occurred during the period of April 17-20 in 2013. We ran the HEC-HMS model first with each storm and then re-imported the hydrographs into the HEC-RAS model as boundary conditions and lateral inflows between cross sections. In order to reduce instabilities, we set the initial flows were set to values that were higher than those used for the HEC-HMS model.

At the beginning, we selected the storm event that occurred during the period of April 17-20, 2013 for calibration purposes. The correlation coefficient analysis implies that there is a strong correlation between simulated and observed stage hydrographs. Furthermore, the sensitivity study of Manning's roughness coefficient indicates that changing the roughness coefficient is not an effective way to calibrate the model since the main discrepancy between the simulated and observed stage hydrographs is the direct runoff volume. This may result from the uncertainties and errors associated with the rainfall radar data or the stage hydrographs observed by the IFC stage sensors. Therefore, we did not calibrate the Soap Creek HEC-RAS model in our study due to the lack of available reliable data.

CHAPTER 6. ANALYSIS OF SCENARIOS/MODEL RESULTS

This thesis focuses on the HEC-HMS and HEC-RAS models that we developed for the Soap Creek Watershed. We used the HEC-HMS model to understand the effects of existing ponds, identify areas in the watershed with high runoff, and run simulations to help understand the potential impact of alternative flood mitigation strategies in the watershed. We used the HEC-RAS model to estimate water surface elevations and flowrates at the cross sections of interest. Additionally, we compared the hydrographs generated from the HEC-HMS and HEC-RAS models in order to identify the effects of the routing method on study results.

6.1. Effects of Existing Ponds

One strategy to lessen the effects of runoff is to construct a system of storage locations throughout the watershed (distributed storage). The most common type of flood storage is a pond. In agricultural areas, ponds usually hold some water all the time. However, ponds also have the ability to store extra water during runoff periods. This so-called flood storage can be used to reduce flood peak discharge.

Unlike approaches for reducing runoff, storage ponds do not change the volume of water that runs off the landscape. Instead, storage ponds (Figure 6.1) hold floodwater temporarily and release it at a slower rate. Therefore, the peak flood discharge downstream of the storage pond is lowered. The effectiveness of any one storage pond depends on its size (storage volume) and how quickly water is released. By adjusting the size and the pond outlets, storage ponds can be engineered to efficiently utilize the available storage for large floods and lessen downstream flood damage.

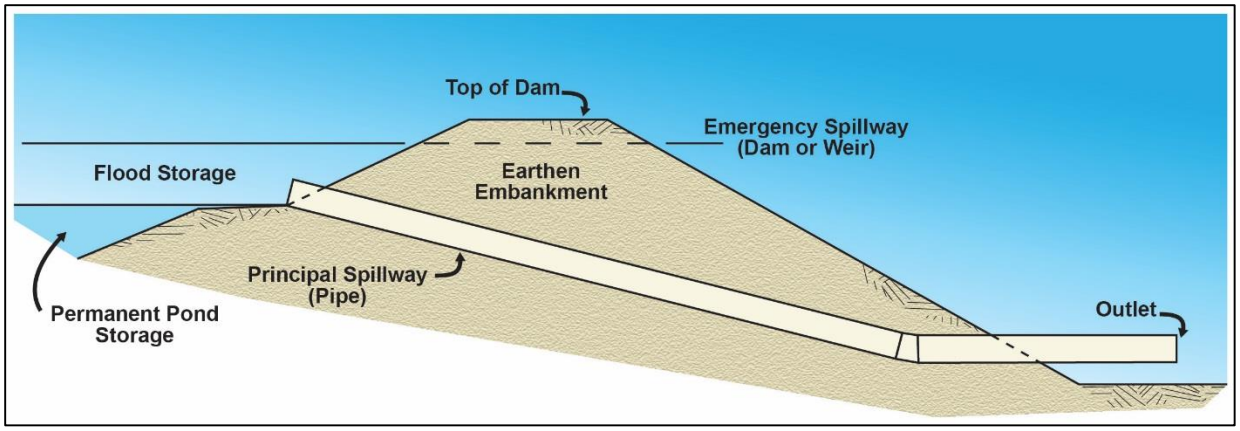

Figure 6.1 Schematic of a pond constructed to provide flood storage.

Generally, these ponds have a permanent pond storage area, which means that the pond holds water all the time. This is accomplished by constructing an earthen embankment across a stream and setting an outlet (usually a pipe) called the principal spillway at some elevation above the pond floor. When there is a storm event, runoff enters the pond. Once the elevation of the water surface is greater than the pipe outlet, water will pass through the pipe and leave the pond at a controlled rate. Additionally, the earthen dam is built higher than the pipe, which allows for greater storage capacity within the pond. An emergency spillway that can discharge water at a much faster rate than the pipe is set some elevation higher than the pipe. The emergency spillway is constructed as a means to rapidly release rising waters in the pond so that they do not damage the earthen embankment. The volume of water stored between the principal and emergency spillways is called the flood storage.

A system of ponds located throughout a watershed is an effective strategy for reducing flood peaks at many stream locations. In the 1980s, landowners in southern Iowa came together to form the Soap Creek Watershed Board. Their motivation was to reduce flood damage and soil loss within the Soap Creek Watershed. They adopted a plan that included locations for 154

distributed storage structures (mainly ponds) that could be built within the watershed. As of 2014, 132 of these structures have been built. Appendix A provides the general information for each pond.

We gathered the design data for each pond that had built from the state NRCS office in Des Moines, which included location, area, and the stage-storage-discharge relationship. When modeling ponds in the HEC-HMS, the model needs a stage-storage-discharge relationship for each structure. Table 6.1 shows an example relationship input to HEC-HMS for one of the ponds (Project 26-32). Project 26-32 is located near the intersection of Alfalfa Avenue and Arbor Blvd. in Davis County and controls a drainage area of 93.4 acres.

Table 6.1 Stage-Storage-Discharge Table for Project 26-32.

Stage (ft)	*Storage (ac-ft)*	*Discharge (ft^2/s)*
796.0	0.00	0.00
797.0	0.10	2.73
798.0	1.32	4.67
799.0	3.31	4.81
800.0	5.48	4.96
801.0	7.90	5.09
802.0	10.67	5.23
803.0	13.78	5.36
803.5	15.51	5.43
804.0	17.23	15.82
804.5	19.12	48.30
805.0	21.01	110.82
805.5	23.07	190.22
806.0	25.12	293.34
806.5	27.34	427.02
807.0	29.55	598.14
807.5	31.93	813.66
808.0	34.30	1080.62
809.0	39.40	1581.43
810.0	44.87	2239.52
811.0	50.70	3077.97

We ran the HMS model with ponds to simulate the effects of flood storage on peak discharges. We made separate model runs using the following pond scenarios: no ponds, ponds built before 1993, ponds built before 1999, ponds built before 2005, ponds built before 2008, and ponds built before 2013. We chose the four index points shown in Figure 6.2 as locations for evaluating the flood peak reduction effects of the ponds. Tables 6.2 – 6.5 show the area upstream of each index point, the area controlled by ponds for each index point, and the percentage of the area that is controlled. The tables also show the peak flow reduction at index points for different pond scenarios for the 25-year 24-hour storm (5.28 inches). We also provide the nearest cross

streets to the index points in the table for reference.

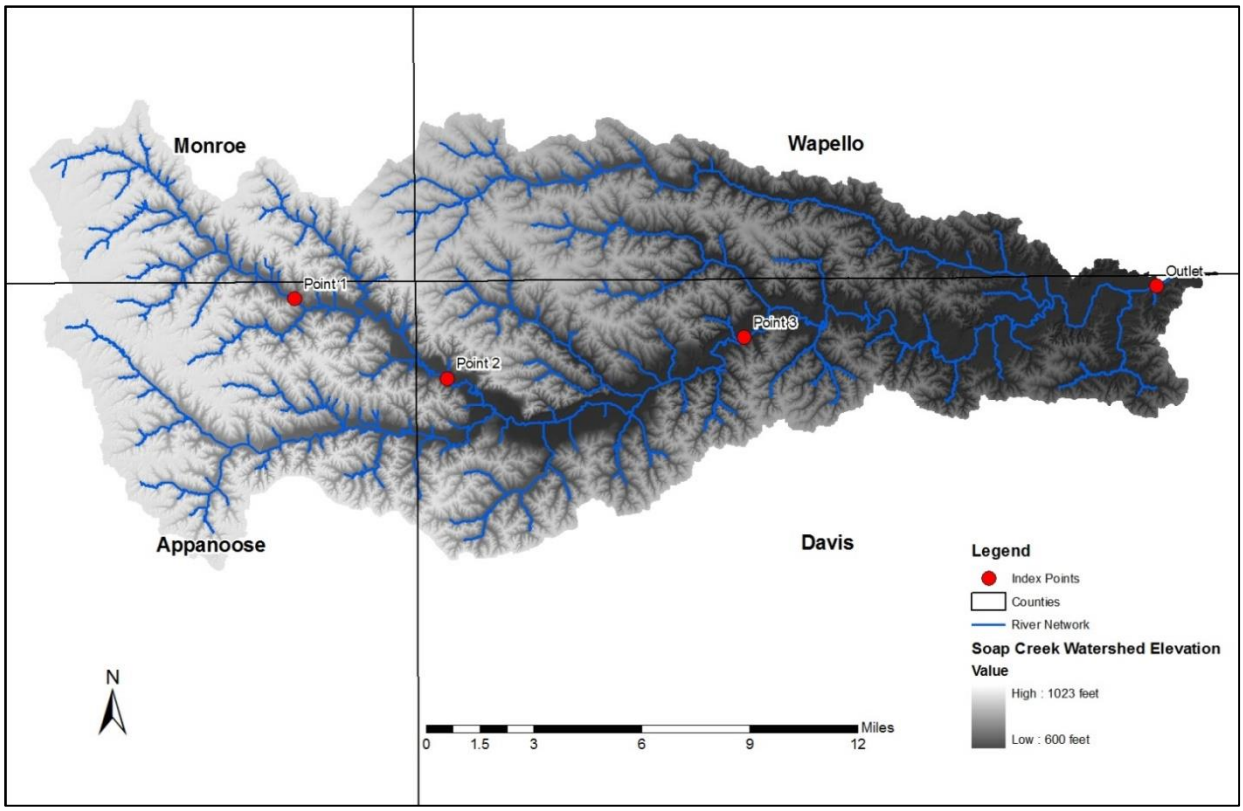

Figure 6.2 Four index locations used for comparing watershed improvement scenarios to current conditions. Nearest road intersections to each Index Point are provided in the tables below.

Table 6.2 Upstream area for Index Point 1 and peak flow reduction for the 25-year 24 hour storm (5.28 inches in 24 hours).

Index Point 1 402nd St/310th Ave – S4 T70N R16W	Upstream Area - 17,738 acres			
	Protected Area (acres)	*Protected Area*	*Peak Flow (cfs)*	*Peak Flow Reduction*
No ponds	0	0%	9,122	0.0%
Before 1993	131	0.7%	9,072	0.5%
Before 1999	2,103	11.9%	8,437	7.5%
Before 2005	5,178	29.2%	6,925	24.1%
Before 2008	5,951	33.5%	6,441	29.4%
Current	9,363	52.8%	5,446	40.3%

Table 6.3 Upstream area for Index Point 2 and peak flow reduction for the 25-year – 24 hour storm (5.28 inches in 24 hours).

Index Point 2 Asteria Blvd/ 134th – S18 T70N R15W		Upstream Area - 33,821 acres		
	Protected Area (acres)	*Protected Area*	*Peak Flow (cfs)*	*Peak Flow Reduction*
No ponds	0	0%	15,323	0.0%
Before 1993	1,242	3.7%	15,139	1.2%
Before 1999	4,116	12.2%	14,454	5.7%
Before 2005	8,461	25.0%	12,682	17.2%
Before 2008	11,108	32.8%	11,290	26.3%
Current	15,994	47.3%	9,832	35.8%

Table 6.4 Upstream area for Index Point 3 and peak flow reduction for the 25-year – 24 hour storm (5.28 inches in 24 hours).

Index Point 3 Jewel Avenue – S10 T70N R14W		Upstream Area - 94,705 acres		
	Protected Area (acres)	*Protected Area*	*Peak Flow (cfs)*	*Peak Flow Reduction*
No ponds	0	0%	27,263	0.0%
Before 1993	2,892	3.1%	25,967	4.8%
Before 1999	9,538	10.1%	24,879	8.7%
Before 2005	19,520	20.6%	22,036	19.2%
Before 2008	22,264	23.5%	20,709	24.0%
Current	27,577	29.1%	19,247	29.4%

Table 6.5 Upstream area for the Soap Creek Outlet and peak flow reduction for the 25-year 24-hour storm (5.28 inches).

Outlet		Upstream Area (acre) - 161,143		
	Protected Area (acres)	*Protected Area*	*Peak Flow (cfs)*	*Peak Flow Reduction*
No ponds	0	0.0%	37,674	0.0%
Before 1993	2,892	1.8%	36,198	3.9%
Before 1999	10,268	6.4%	34,612	8.1%
Before 2005	25,235	15.7%	30,674	18.6%
Before 2008	30,781	19.1%	29,078	22.8%
Current	39,208	24.3%	27,228	27.7%

Figure 6.3 shows the how peak flow reduction changes for the 25-year 24-hour storm with pond construction. When ponds are built, a greater percentage of the upstream area must drain through them (see Table 6.2 - 6.5). A similar trend is seen at all four index locations since

as the percentage of protected area increases, there tends to be a proportional increase in the peak flow reduction.

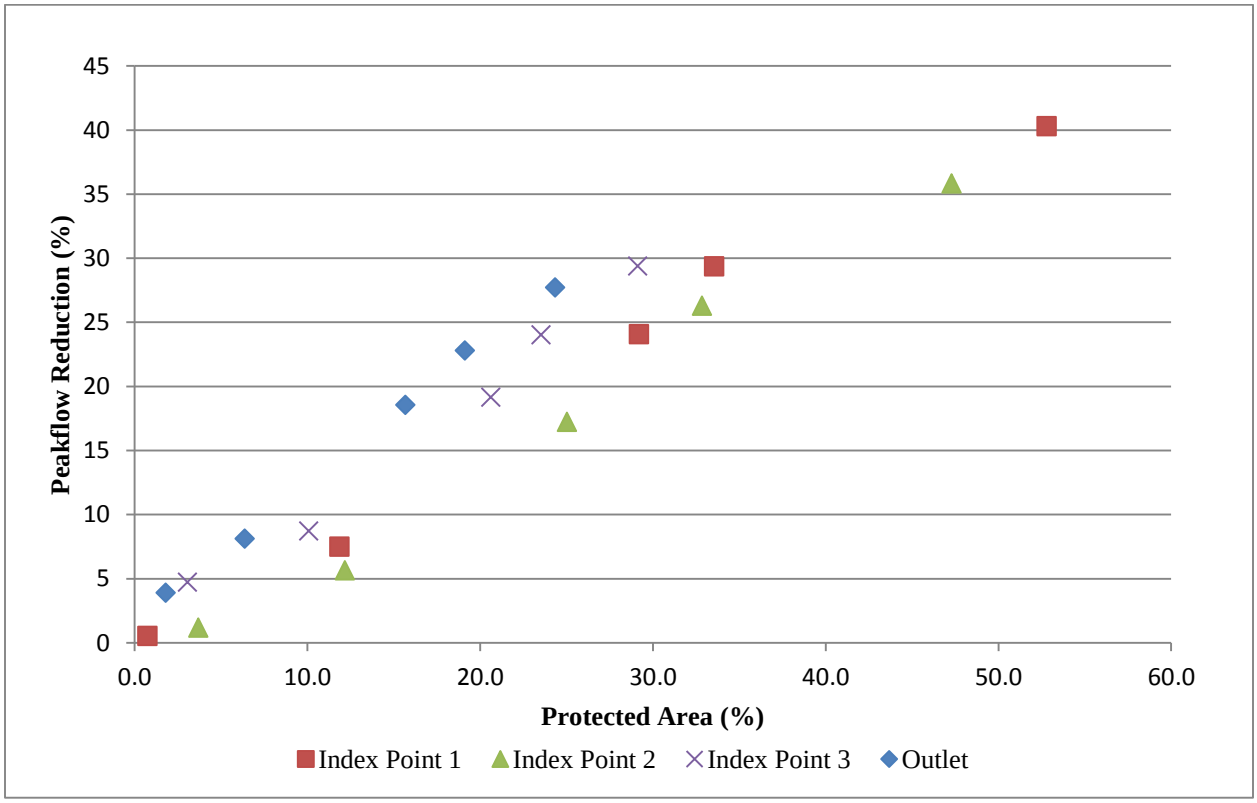

Figure 6.3 Peak flow reduction versus percentage of the area that is controlled by the ponds at different index points for 25-year 24-hour design storm (5.28 inches).

Figure 6.4 compares simulated flood hydrographs for the no ponds condition (Without Ponds) to those with 132 built ponds (With Ponds) for the 25-year 24-hour design storm (5.28 inches of rain in 24 hours). For the hydrographs shown, peak flow reduction ranges from 28-40%. The percent reduction is greatest for index point 1, which is located in the upper half of the watershed and decreases towards the outlet.

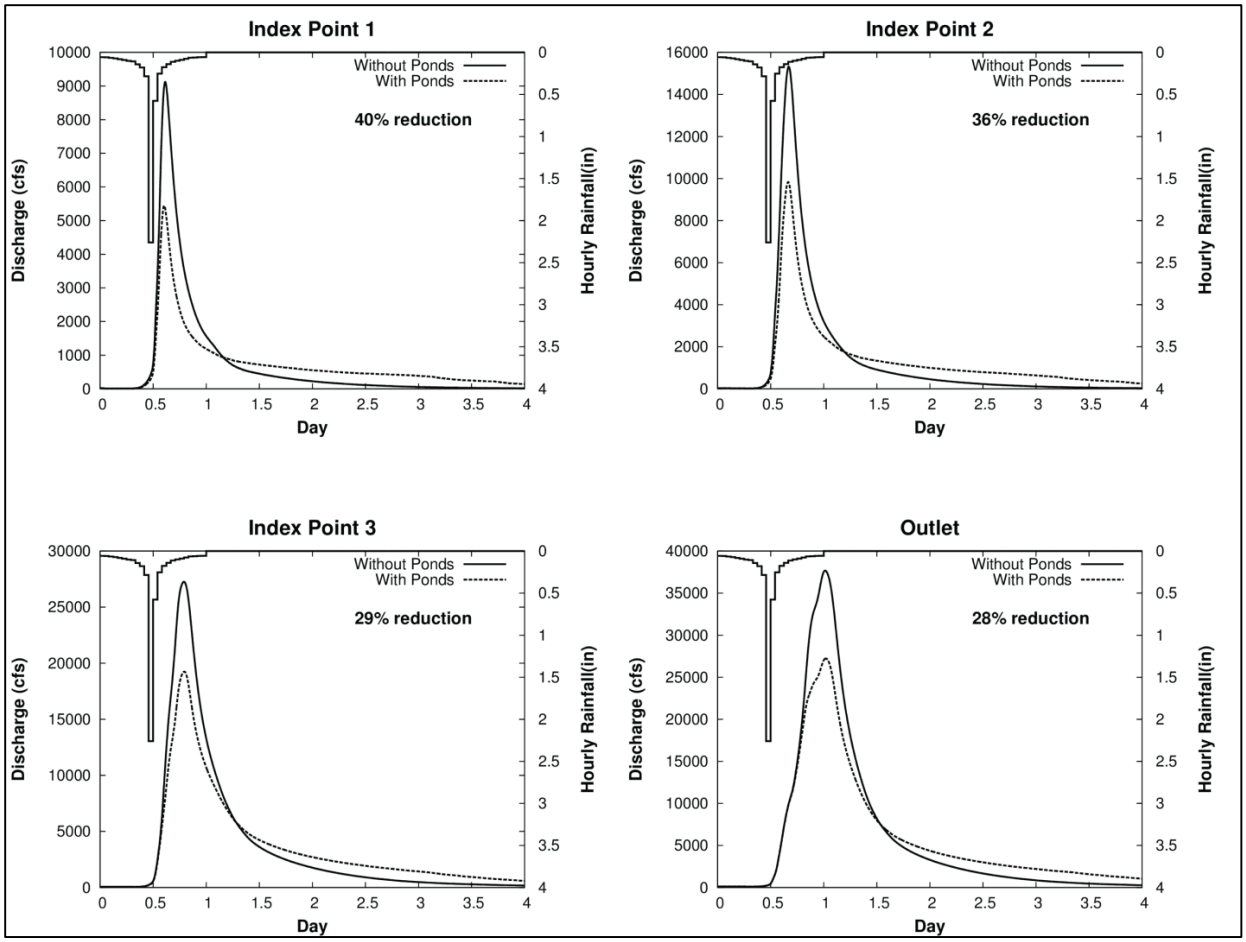

Figure 6.4 Comparison of hydrographs with 132 ponds and without ponds for the 25-year 24-hour design storm (5.28 inches).

We then used the no ponds condition as a baseline to make other comparisons for the 10-, 25-, 50-, and 100-year return period 24-hour SCS design storms. Figure 6.5 shows the peak discharge reductions at the four index points for the four different 24-hour design storms (10-year, 25-year, 50-year, and 100-year) and the comparison of the no pond and 132 built pond (current) conditions. As noted above, the peak flow reduction effect varies with drainage area. It is typically larger for small drainage areas, where the location is closer to the headwater ponds, and decreases in the downstream direction. The figure shows that the percent of peak flow reduction at each index point is nearly identical for all the simulated flood events. At index point 1, the peak flow reductions are around 40% for the four design storms, whereas they are near

27% at the outlet.

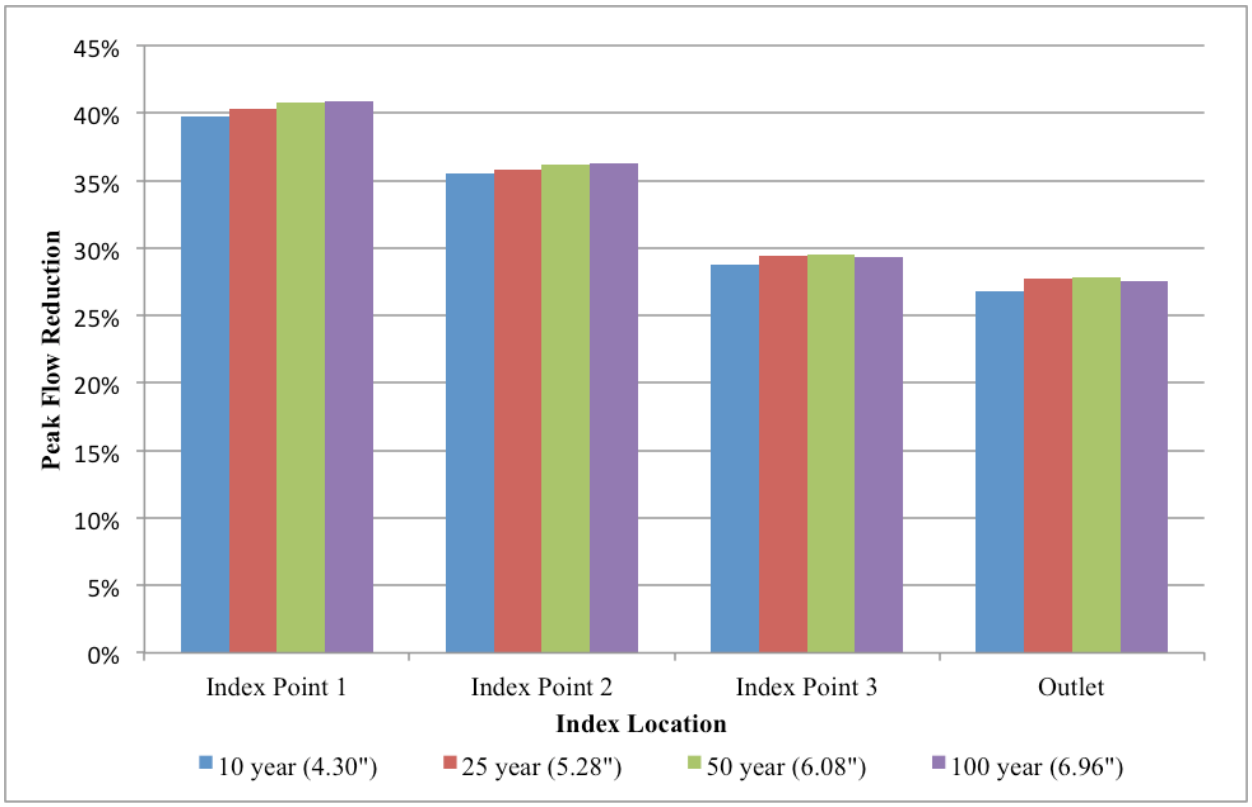

Figure 6.5 Peak discharge reductions for the model with ponds built before 2013. Results are shown at four index locations moving from upstrem (left) to downstream (right) for four different 24-hour design storms.

To illustrate how effectively the ponds utilize their storage in the simulated flood events, we created pond storage and pond usage maps for each design storm (Figures 6.6 to 6.13). Results are shown for the 10-, 25-, 50, and 100-year return period 24-hour SCS design storms.

The pond storage maps show the maximum volume of water stored divided by the upstream drainage area. Reporting the pond storage as a depth makes it easier to determine what fraction of the precipitation is stored in the pond. A red circle indicates that the pond usage is more than 100%, which means that the water level has reached or exceeded the emergency

spillway elevation.

Figure 6.6 shows the pond storage map for the 10-year storm (4.30 inches in 24 hours). Many of the ponds hold at least 1 inch of the total accumulation at their peak, which corresponds to about 23% of the total precipitation for the storm. Figure 6.7 shows the pond usage map for the 10-year design storm, in which only 4 of the 132 ponds reach their maximum designed storage. This indicates that the ponds have the potential to hold much more water.

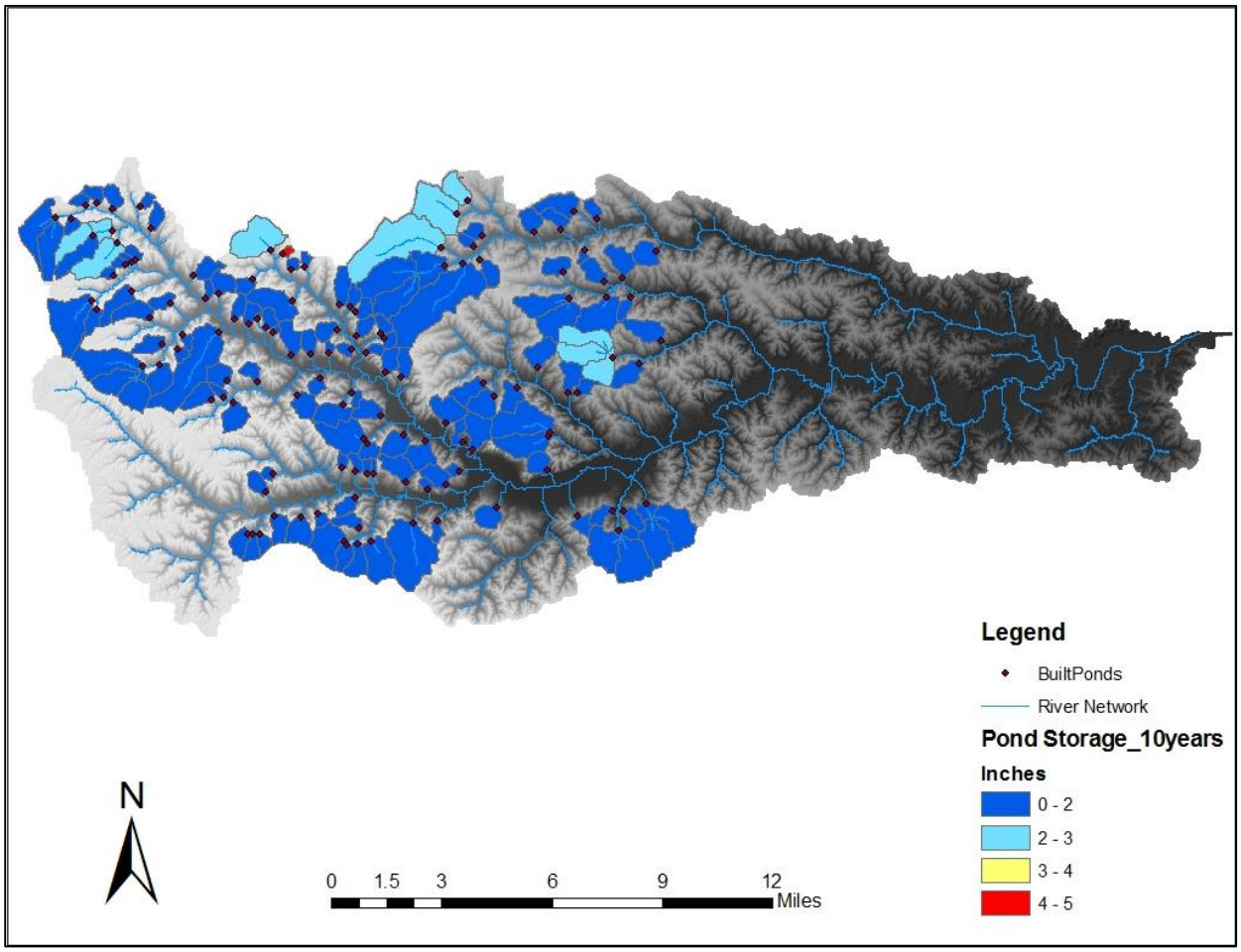

Figure 6.6 Peak Storage for the ponds built before 2013 (132 total)
for the 10-year 24-hour design storm (4.30 inches).

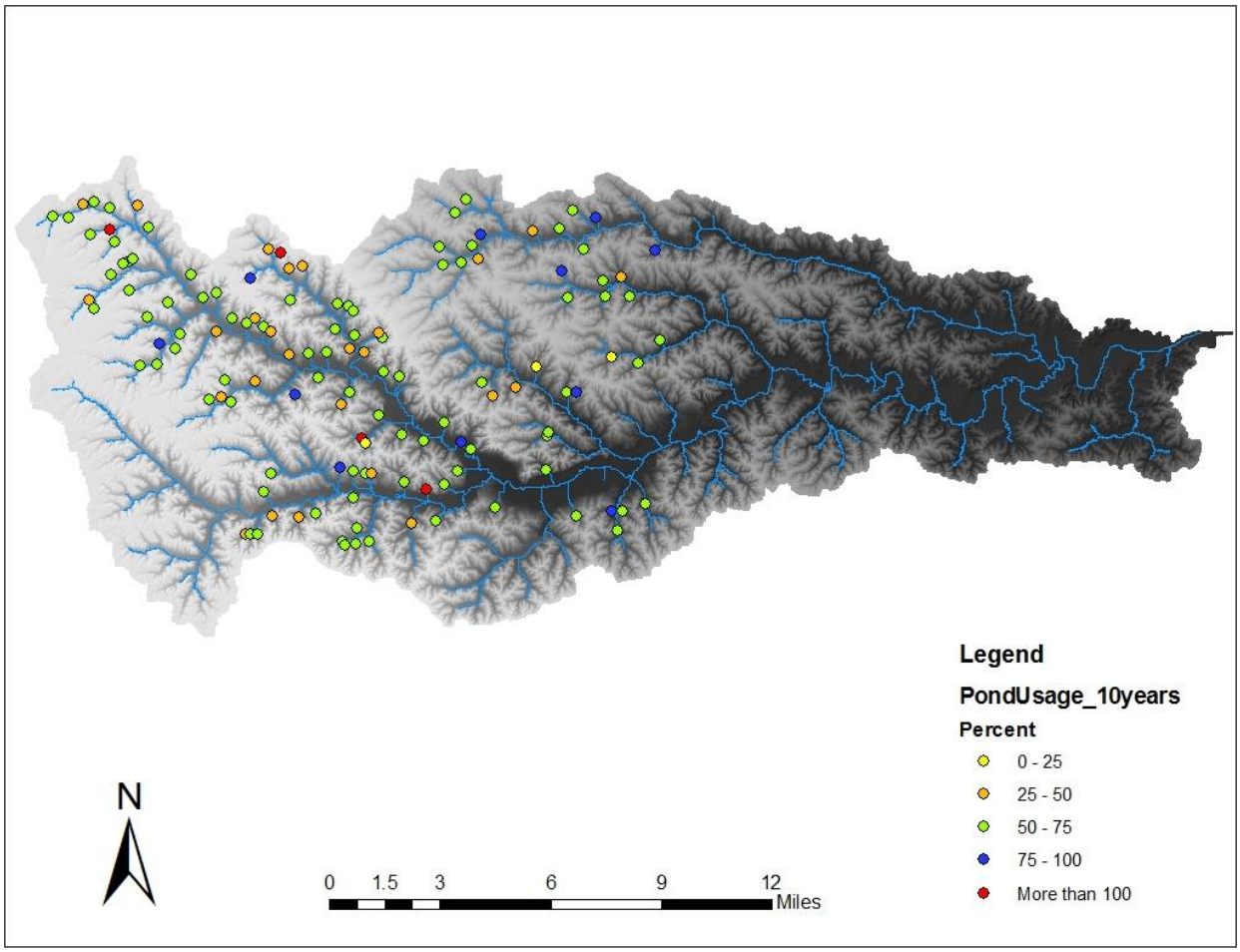

Figure 6.7 Percentage of storage for each pond used for the 10-year 24-hour designs storm (4.30 inches).

The results for the 25-year design storm (5.28 inches in 24 hours) are shown in Figures 6.8 and 6.9. Figure 6.8 shows that a larger percentage of the storm precipitation is stored by the ponds for this larger event, and several of the ponds store as much as 2-3 inches of the rain (or about 40 - 55% of the total rainfall). Figure 6.9 shows that 25 of the 132 ponds have reached maximum flood storage.

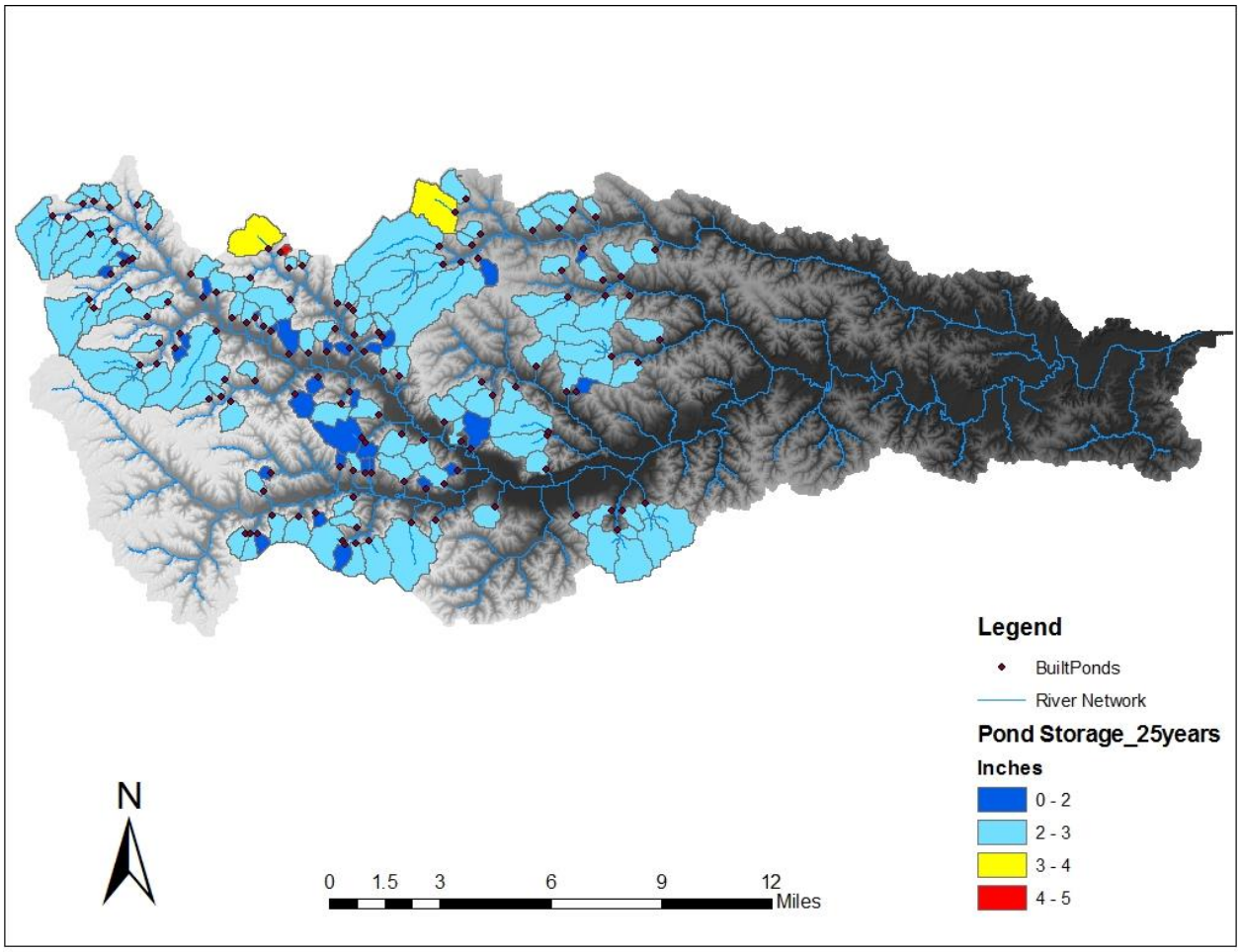

Figure 6.8 Peak Storage for the ponds built before 2013 (132 total)
for the 25-year 24-hour design storm (5.28 inches).

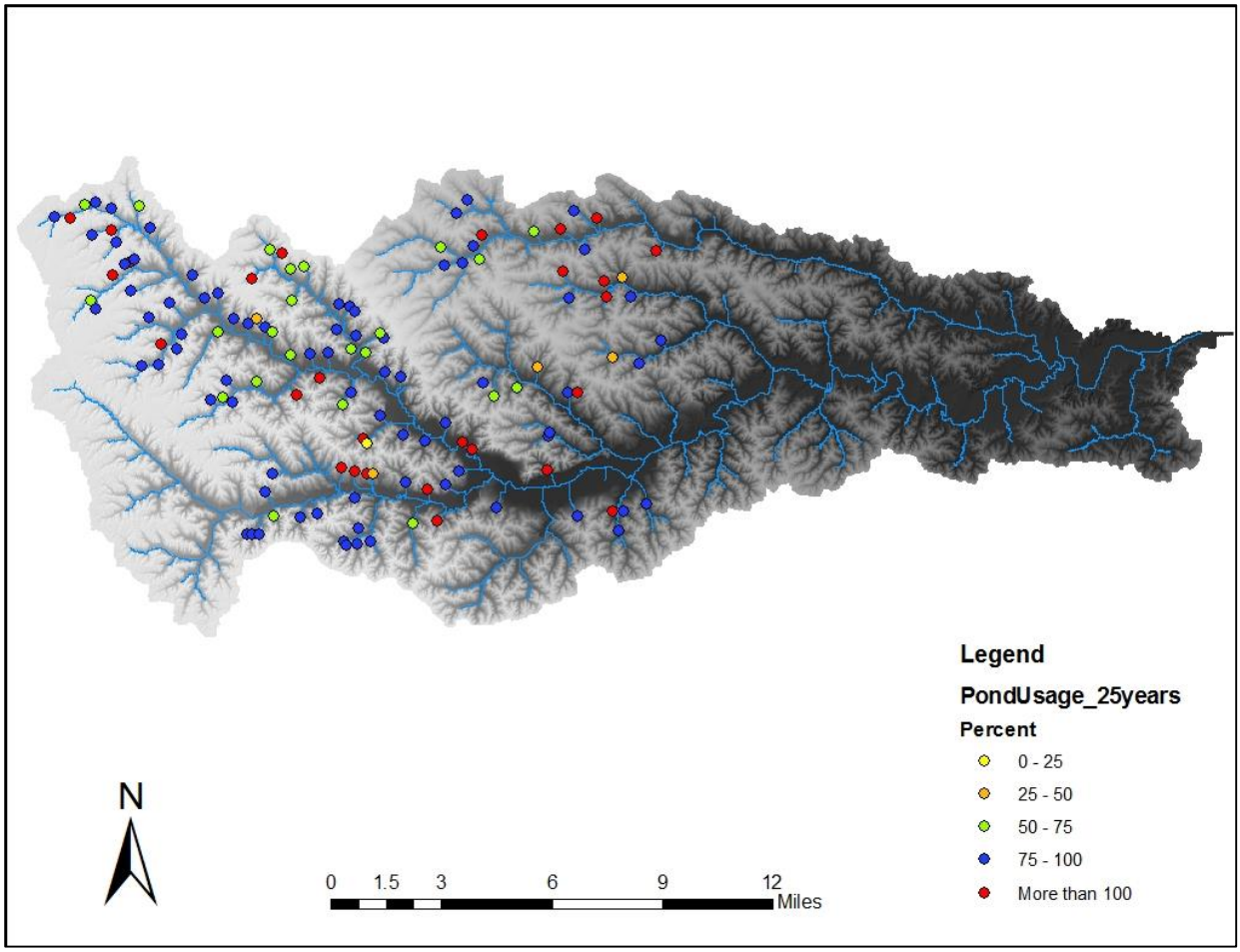

Figure 6.9 Percentage of storage each pond used for the 25-year 24-hour designs storm (5.28 inches).

For the 50-year design storm (6.08 inches in 24 hours), Figure 6.10 shows that many of the ponds are holding at least 3 inches of the total accumulation during the peak, or about half of the total precipitation. Figure 6.11 shows that 88 of the 132 ponds (67%) have reached their maximum flood storage by the 50-year design event.

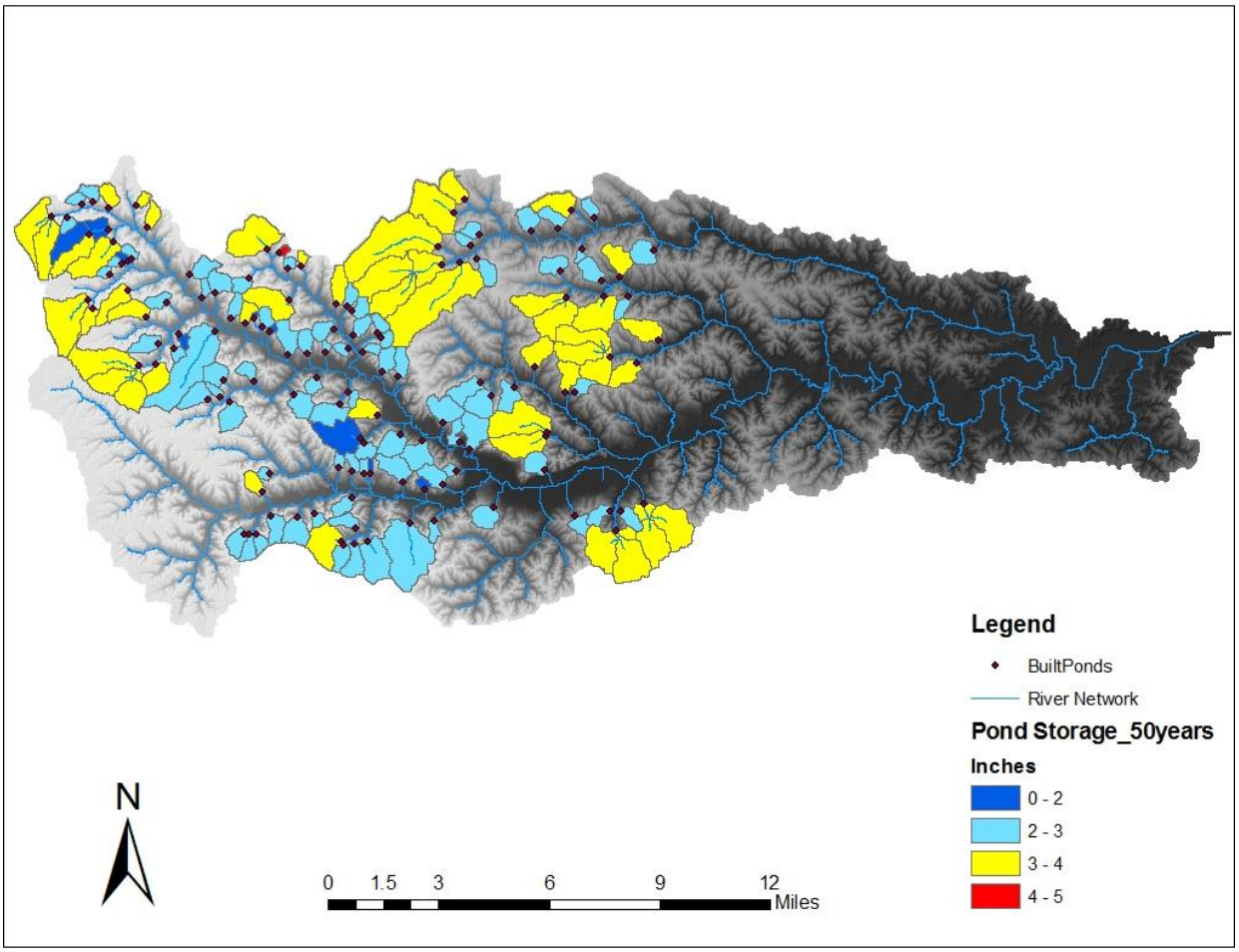

Figure 6.10 Peak Storage for the ponds built before 2013 (132 total) for the 50-year 24-hour design storm (6.08 inches).

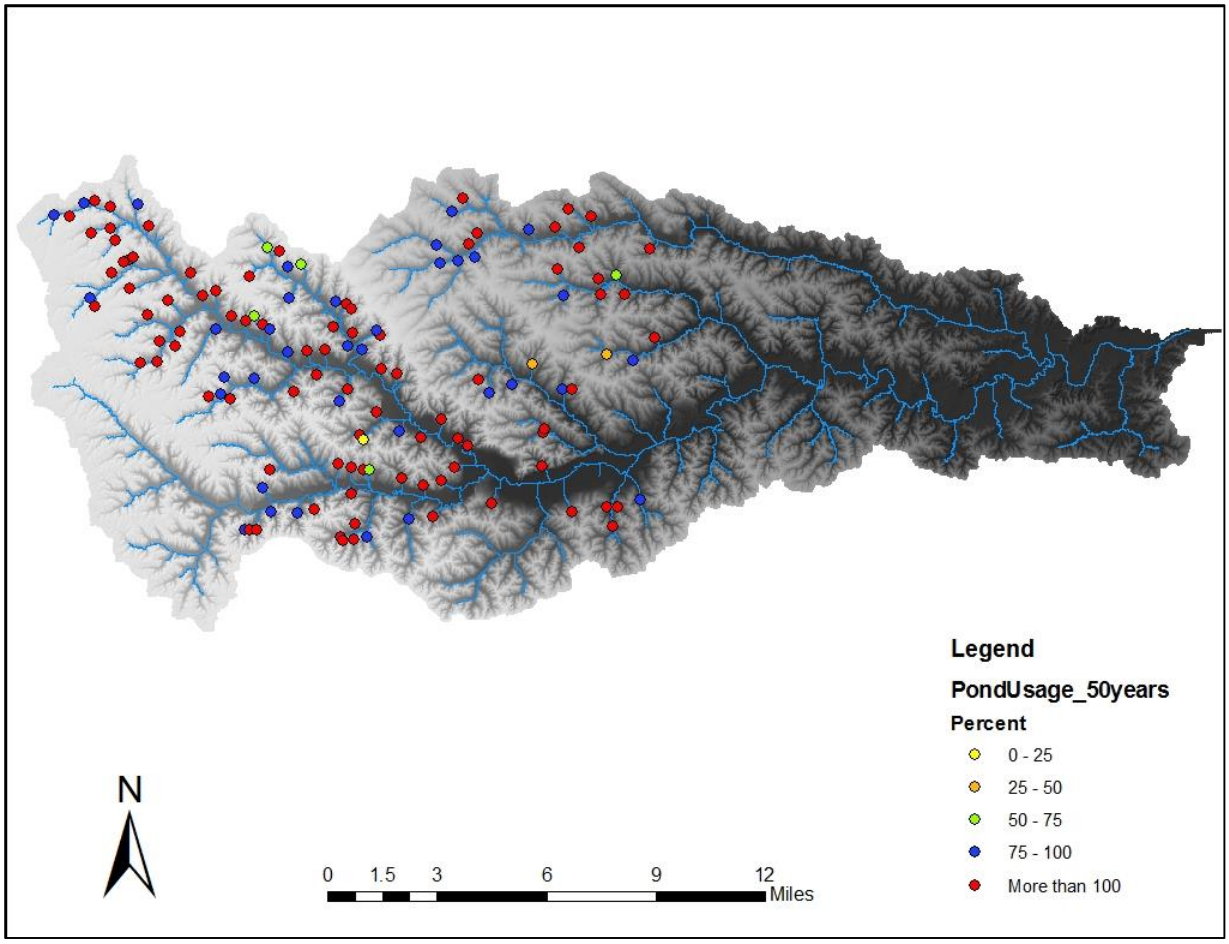

Figure 6.11 Percentage of storage each pond used for the 50-year 24-hour designs storm (6.1 inches).

The 100-year storm (6.96 inches in 24 hours) was the largest design storm simulated and shows the effects that the distribution of ponds has on a major flood. Figure 6.12 shows that many of the ponds are holding at least 3.0 inches of rain at their peak, and some can even hold 4-5 inches. Figure 6.13 indicates that almost all ponds have reached their maximum flood storage (121 out of 132 ponds), which shows that the system is nearing its total capacity and, in heavier rains, the ponds would not likely be able to hold back much more precipitation as effectively.

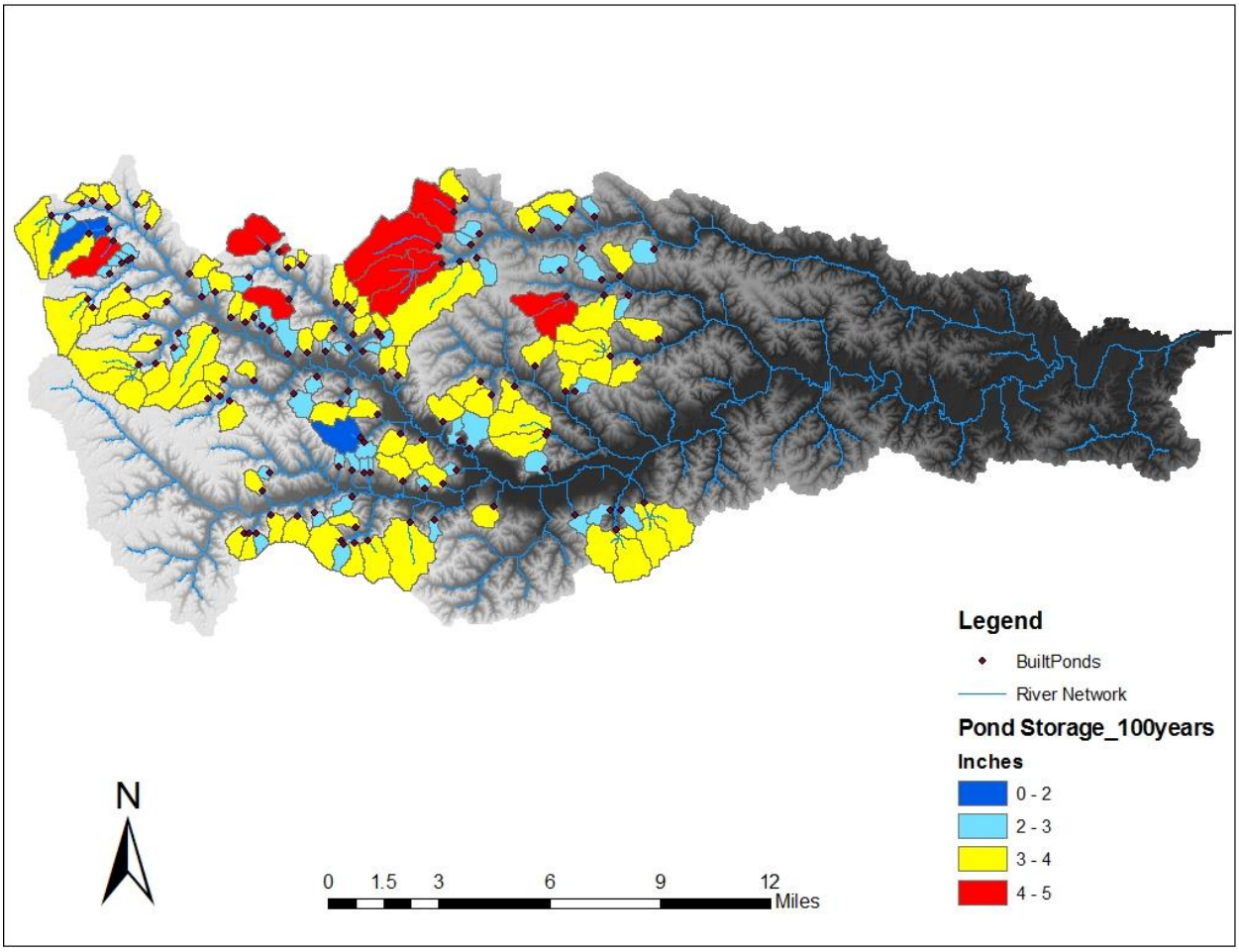

Figure 6.12 Peak Storage for the ponds built before 2013 (132 total)
for the 100-year 24-hour design storm (6.96 inches).

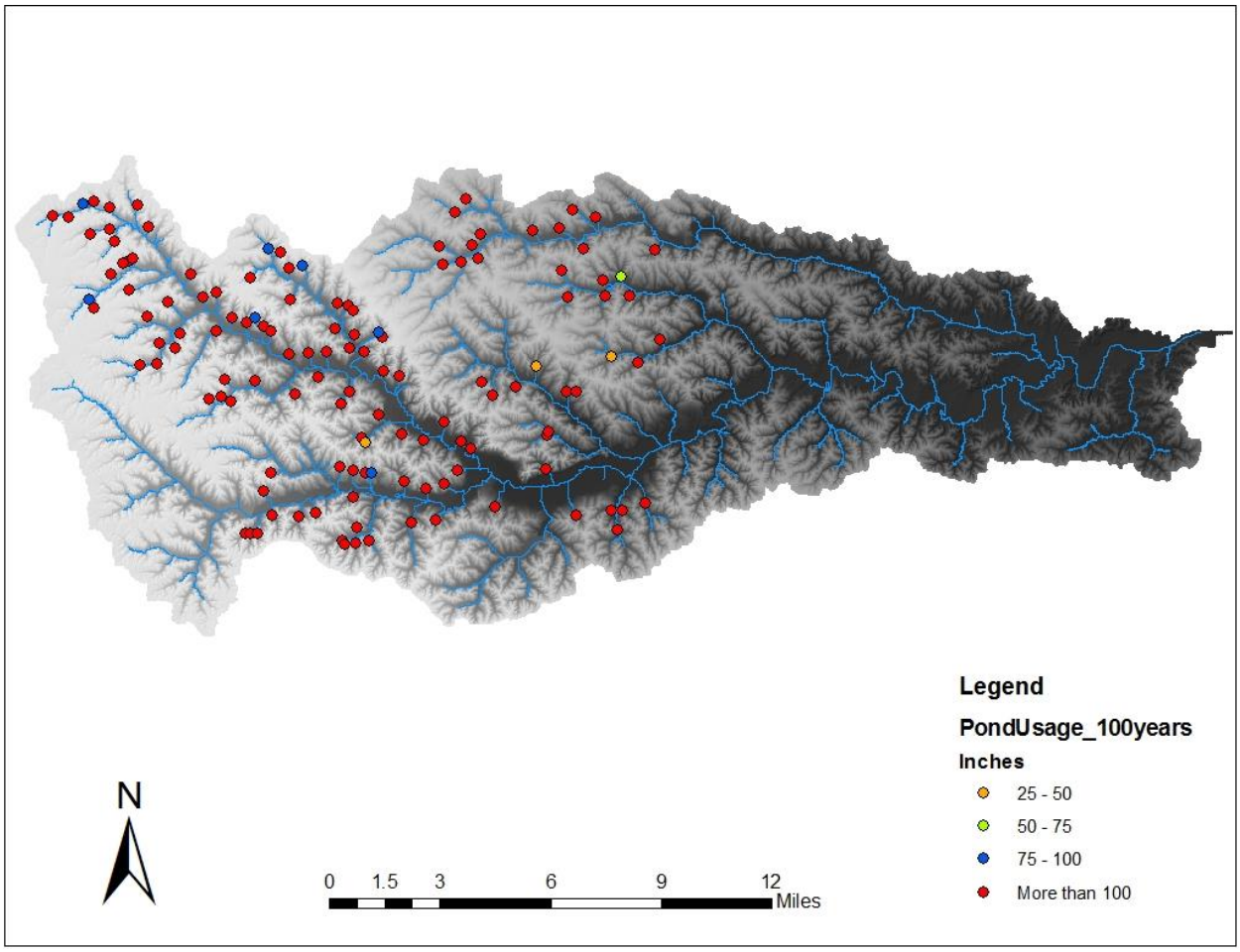

Figure 6.13 Percentage of storage each pond used for the 100-year 24-hour designs storm (6.96 inches).

6.2. Areas of High Runoff Potential

A sensible first step to implementing additional projects in the watershed in order to reduce flood peaks and minimize runoff is to identify areas of the watershed with higher runoff potential. Runoff potential can be estimated using the HEC-HMS model. To do this, we applied the same depth of rainfall to each subbasin and computed the percentage of rainfall that was converted to runoff. This runoff potential is driven primarily by the SCS Curve Number, which depends on the land use and soil types in the subbasin.

To evaluate the runoff potential, we simulated the runoff from each subbasin resulting

from the 25-year 24-hour storms. Figure 6.14 shows the runoff potential analysis by subbasin, and Figure 6.15 shows the runoff potential aggregated to the HUC 12 boundaries within the Soap Creek Watershed. As the figures demonstrate, almost all areas show that more than 50% of the rainfall was converted to runoff. Even though the two dominant land uses within the Soap Creek Watershed are forest (35%) and pasture/hay (35%), the entire watershed still has large runoff potential because of the soil type. As mentioned before, the majority of the soil within the Soap Creek Watershed consists of hydrologic soil groups C, C/D, and D, which are all poorly drained soils. From a hydrologic perspective, flood mitigation projects that can reduce runoff from these high runoff areas should be a priority.

Nevertheless, high runoff potential is but one factor in selecting locations for potential projects. Alone, it has limitations. Landowner willingness to participate is essential, and existing conservation practices or areas such as timber should not be disturbed. Stakeholder knowledge of places with repetitive loss of crops or roads/road structures is also valuable in selecting locations.

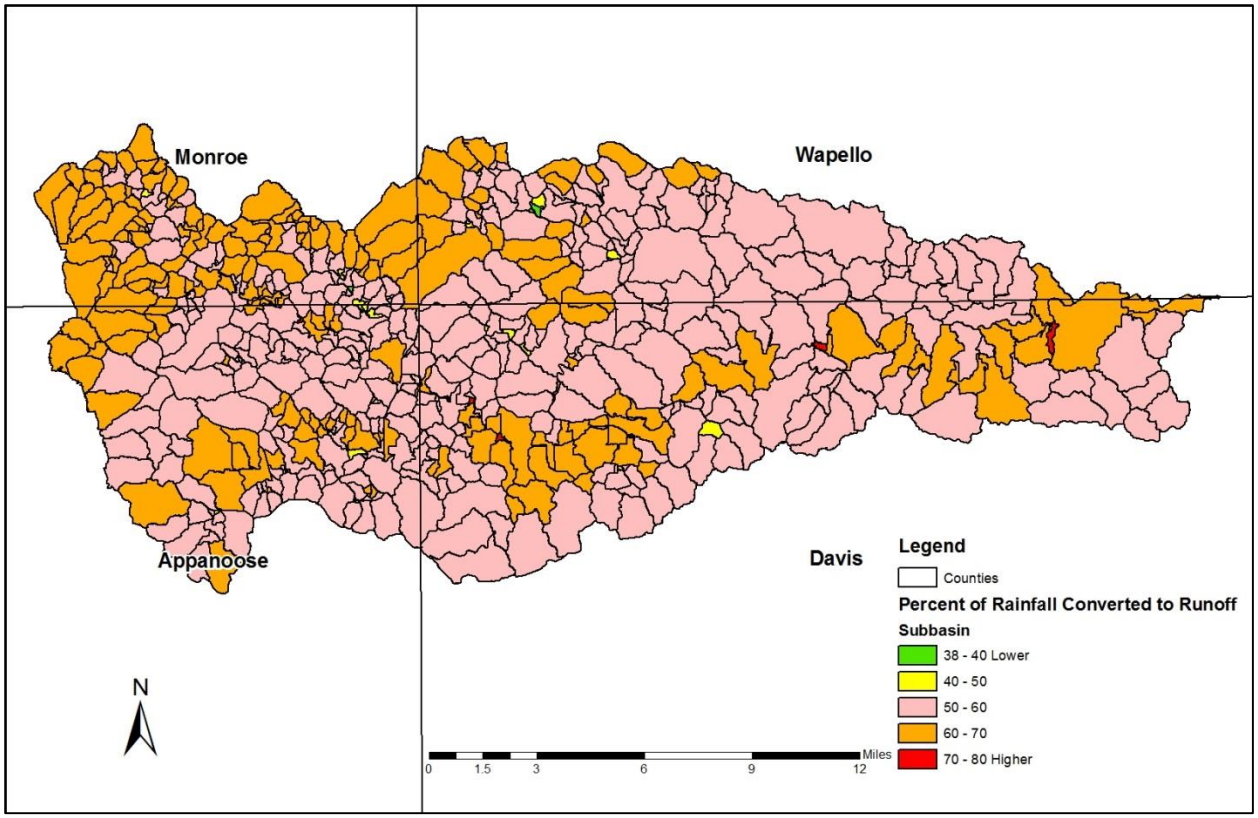

Figure 6.14 Runoff Potential Analysis Displayed by Subbasin Boundaries for the 25-year 24-hour storm (5.28 inches).

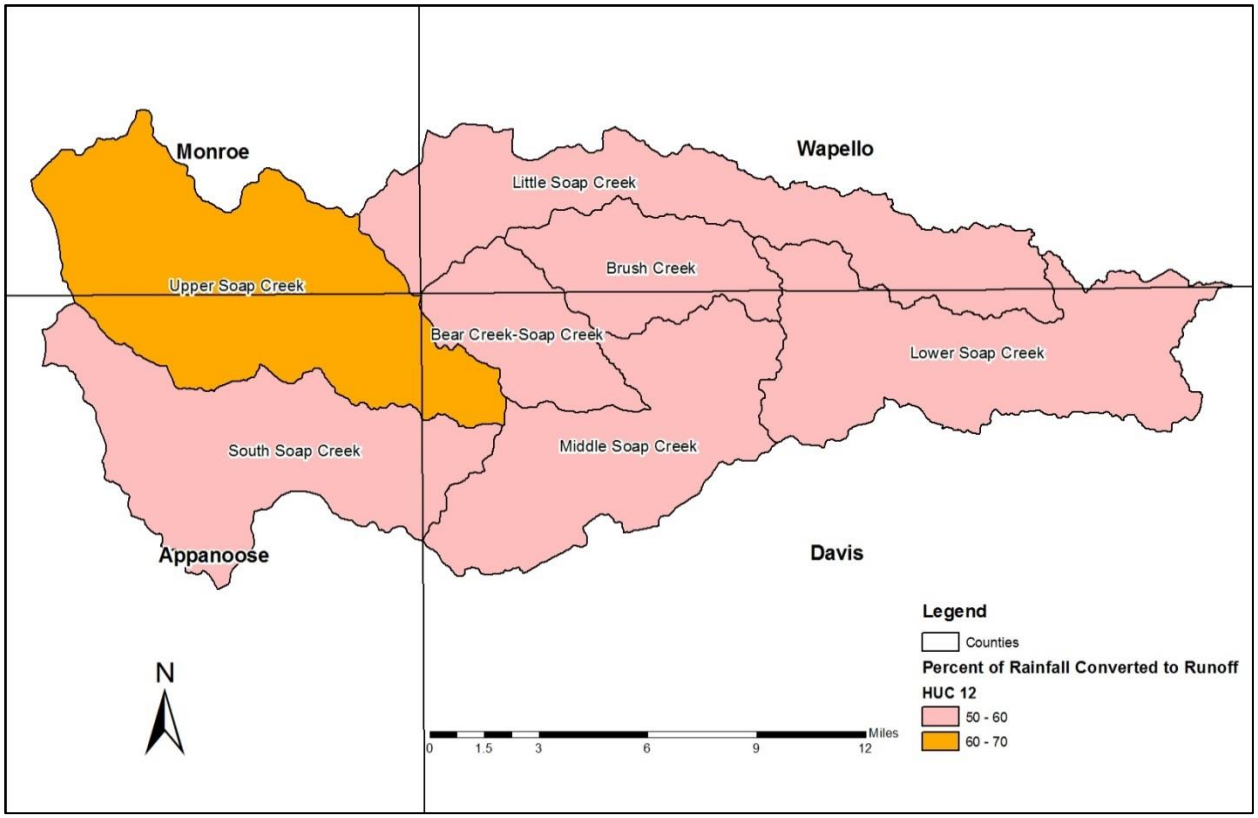

Figure 6.15 Runoff Potential Analysis Aggregated to HUC12 Boundaries for the 25-year 24-hour storm (5.28 inches).

6.3. Mitigating the Effects of High Runoff with Increased Infiltration

Reducing runoff from areas with high runoff potential may be accomplished by increasing how much rainfall infiltrates into the ground. Changes that result in higher infiltration reduce the volume of water that drains off the landscape during and immediately after the storm. The extra volume of water that soaks into the ground may later evaporate or slowly travel through the soil, either seeping into the groundwater storage or traveling beneath the surface to a stream. Increasing infiltration has several benefits. Even if the infiltration water reaches a stream, it arrives much later (long after the storm ends).

In this section, we examine two alternatives for reducing runoff. One is the conversion of row crop agriculture back to native tall-grass prairie within the Soap Creek Watershed, and the

other is improving soil quality. Both are hypothetical examples and are meant to illustrate the potential effects on flood reduction.

6.3.1. Hypothetical Increased Infiltration with the Watershed: Land Use Change

We performed an analysis to quantify the impact of human-induced land use changes on the flood hydrology of the Soap Creek Watershed. In this example, we converted all lands currently used for cultivated crops to native tall-grass prairie with much higher infiltration characteristics. While returning to this pre-settlement condition is unlikely to occur, this scenario provides an important benchmark to compare with any watershed improvement project considered.

We considered two methods to simulate the conversion to native tall-grass prairie with the HMS model. For both, we first adjusted the model parameters affecting runoff potential across the landscape (Curve Number) to reflect the tall-grass prairie condition. Specifically, we redefined existing agriculture land use, which accounts for 14% of the watershed area, as tall-grass prairie. We assigned new SCS Curve Numbers, reflecting the lower runoff potential of prairie, to each subbasin. For the first method, we used only changes to the Curve Numbers. Thus, this method only considers the reduction in runoff volume that resulted from the improved infiltration characteristics of the native prairie. However, changing land use can also alter how long it takes water to flow over the landscape. Therefore, for the second method, we also considered the effects of slower travel times across a prairie landscape and the resulting attenuation and delay in the timing of peak discharge that would be expected. To do this, in addition to changes to the Curve Numbers, we also altered model parameters affecting the travel time of runoff - the time of concentration and storage coefficient - to reflect a prairie landscape.

Following the assignment of new subbasin model parameters, we ran the HMS model with no ponds incorporated for a set of design storms and compared the current and tall-grass prairie simulations for the 10-, 25-, 50-, and 100- year return period 24- hour SCS design storms. Using design storms of different levels of severity illustrates how flooding characteristics change during more intense rainstorms. We used the same four index points described in Section 6.1 for comparison.

For the first method of representing a prairie landscape, Figure 6.16 compares simulated flood hydrographs for the current agricultural landscape (Baseline) to those for a native tall-grass prairie landscape (Scenario) for the 50-year return period 24-hour design storm (6.08 inches of rain in 24 hours). For all four locations shown (from upstream to the outlet of Soap Creek), a change to a prairie has little effect; the flood hydrographs and peak discharge rate are nearly the same for both cases (indeed, it difficult to distinguish between the two hydrographs in the plots). Overall, the percent reduction in peak discharge is less than 1% at all of these index points. The minimal difference for a prairie landscape is a result of the soil types within the Soap Creek Watershed. About 58% of the Soap Creek Watershed is type D and about 33% is type C. For type C and D soils, the Curve Number for a prairie landscape is not much less than for the existing landscape. Overall, the adjusted Curve Numbers for the prairie landscape decrease by only 0.4 % compared to the original Curve Numbers.

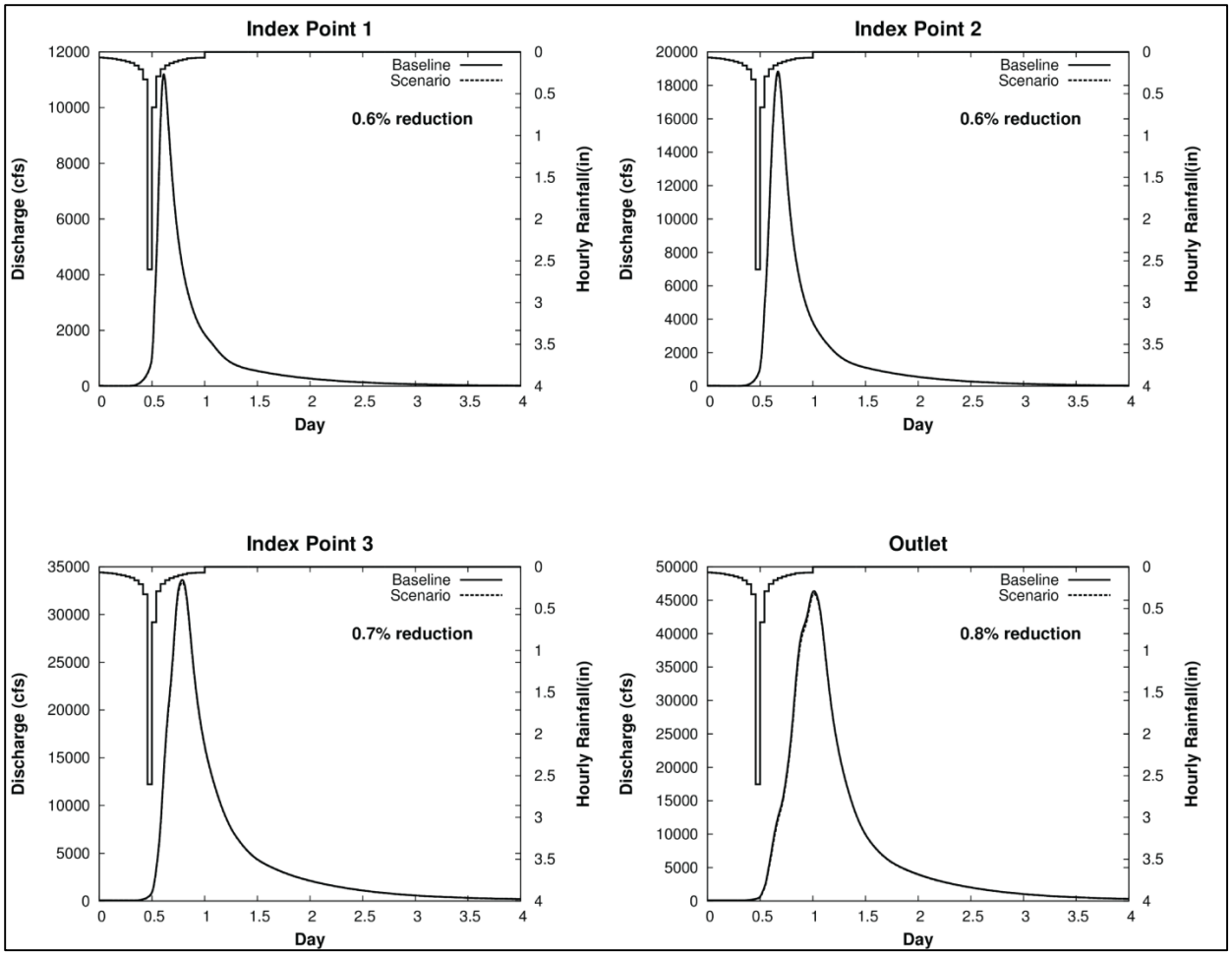

Figure 6.16 Hydrograph comparison at several locations for the increased infiltration scenario resulting from hypothetical land use changes (conversion of row crop agriculture to native prairie). Results shown are for the 50-year 24-hour storm (6.08 inches of rain).

Figure 6.17 shows the percent reductions in peak discharge resulting from this hypothetical tall-grass prairie at four index locations for four design storms. The restoration of native tall grass typically results in a peak discharge reduction of around 1%. The peak reduction is largest for the smallest design storm (10-year return period) and decreases with larger rainfall amounts (up to the 100-year return period). In other words, the runoff reduction benefits of increased infiltration are greater for smaller rainfall events. Note also that the percent reduction in peak discharge is fairly uniform at all locations.

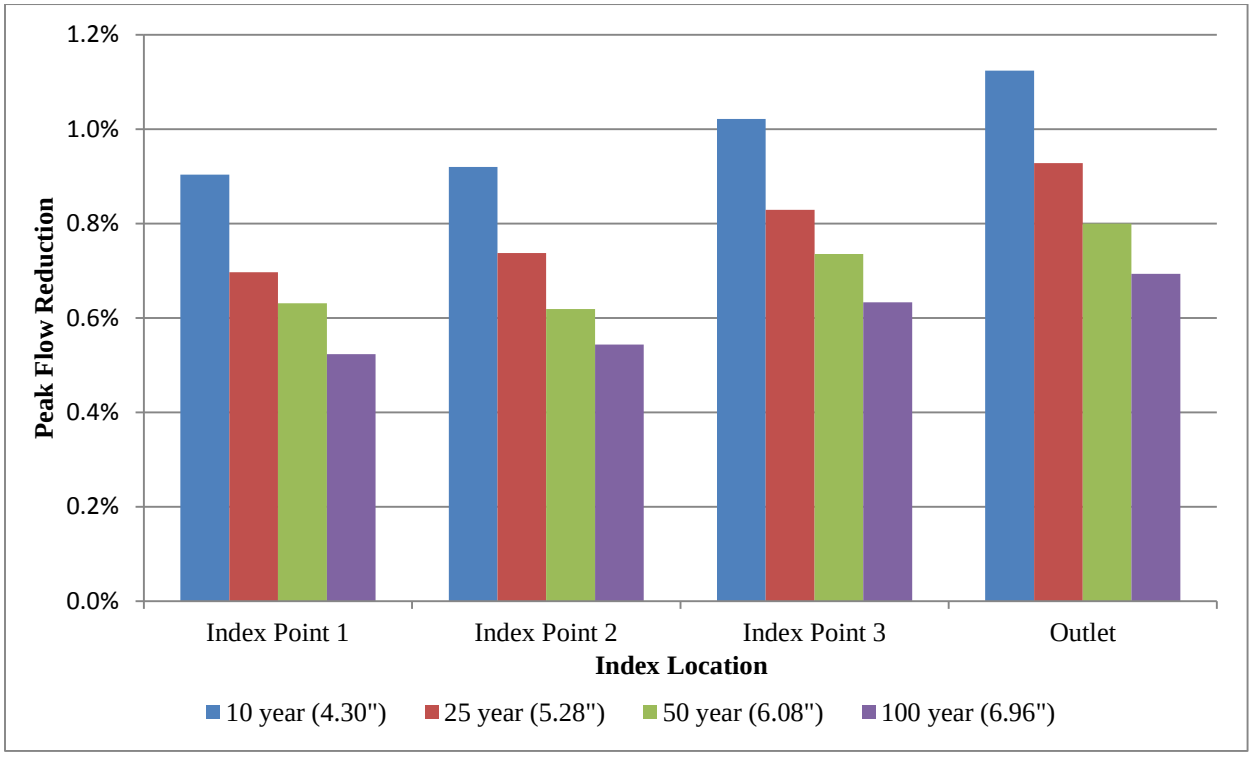

Figure 6.17 Percent reductions in peak flow for the increased infiltration scenario due to land use changes (conversion of row crop agriculture to native prairie). Peak flow reductions at four index points progressing from upstream (left) to downstream (right) are shown for four different 24-hour design storms.

The first method of representing a prairie landscape considers only changes in runoff potential. However, the second method considers both changes in runoff and the slower travel times of a prairie landscape. Figures 6.18 and 6.19 show similar comparisons between current land use and hypothetical prairie land use and considers the changes in both infiltration and travel time. The results are almost the same as for the first method. For the 50-year design storm (see Figure 6.18), the peak reduction effect is slightly higher upstream. At Index Point 1, when water travels more slowly across the prairie landscape (the second method compared to the first), the peak flow reduction increases from 0.6 to 1.0%. However, as the slower moving water

accumulates at downstream locations, the significance of changing the travel time decreases. As a result, at the outlet, the peak reduction effect simulated by the methods is virtually identical. The same trends are also observed for both smaller (10- and 25-year) and larger (100-year) design storm events (see Figure 6.19).

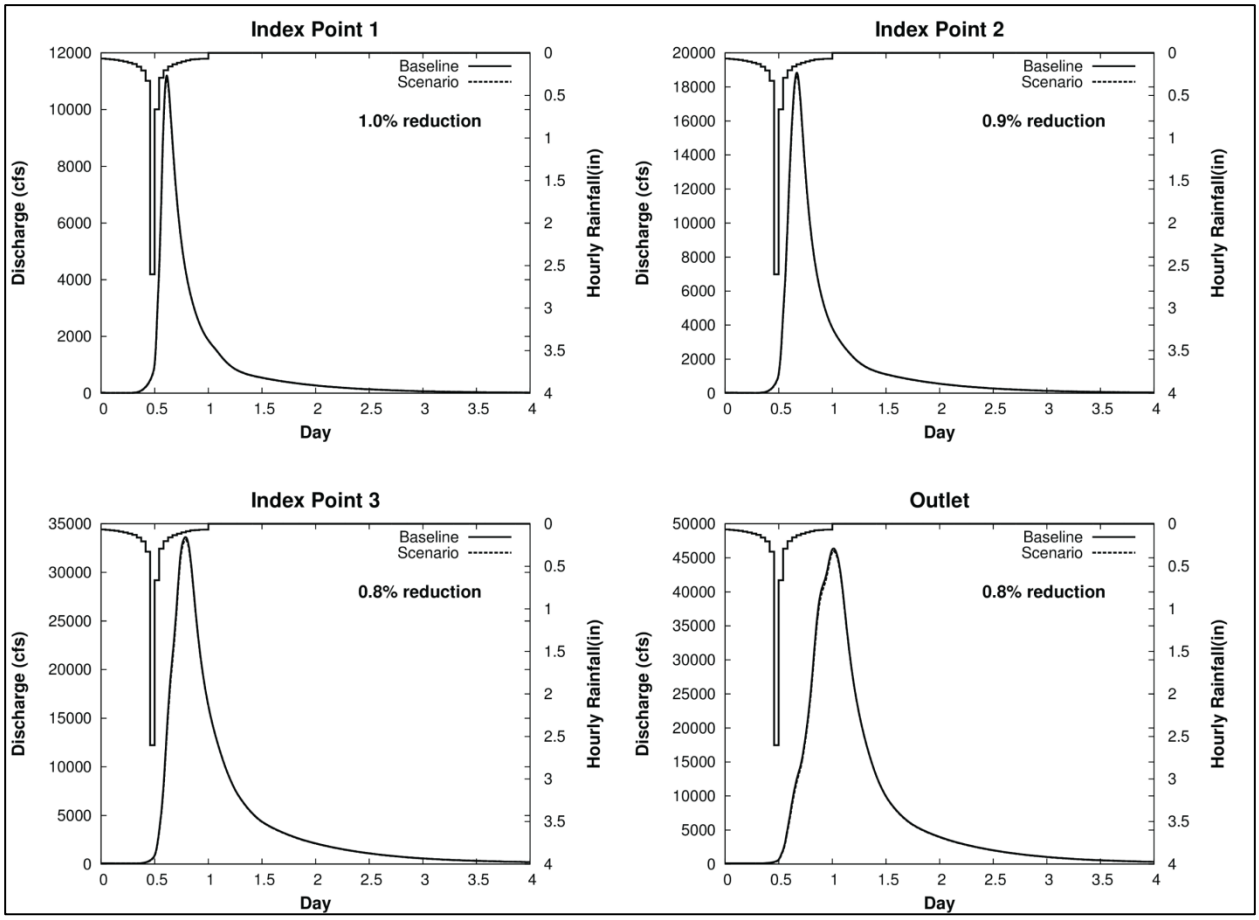

Figure 6.18 Hydrograph comparison at several locations for the increased infiltration scenario resulting from hypothetical land use changes (conversion of row crop agriculture to native prairie). Results shown are for the 50-year 24-hour storm (6.08 inches of rain).

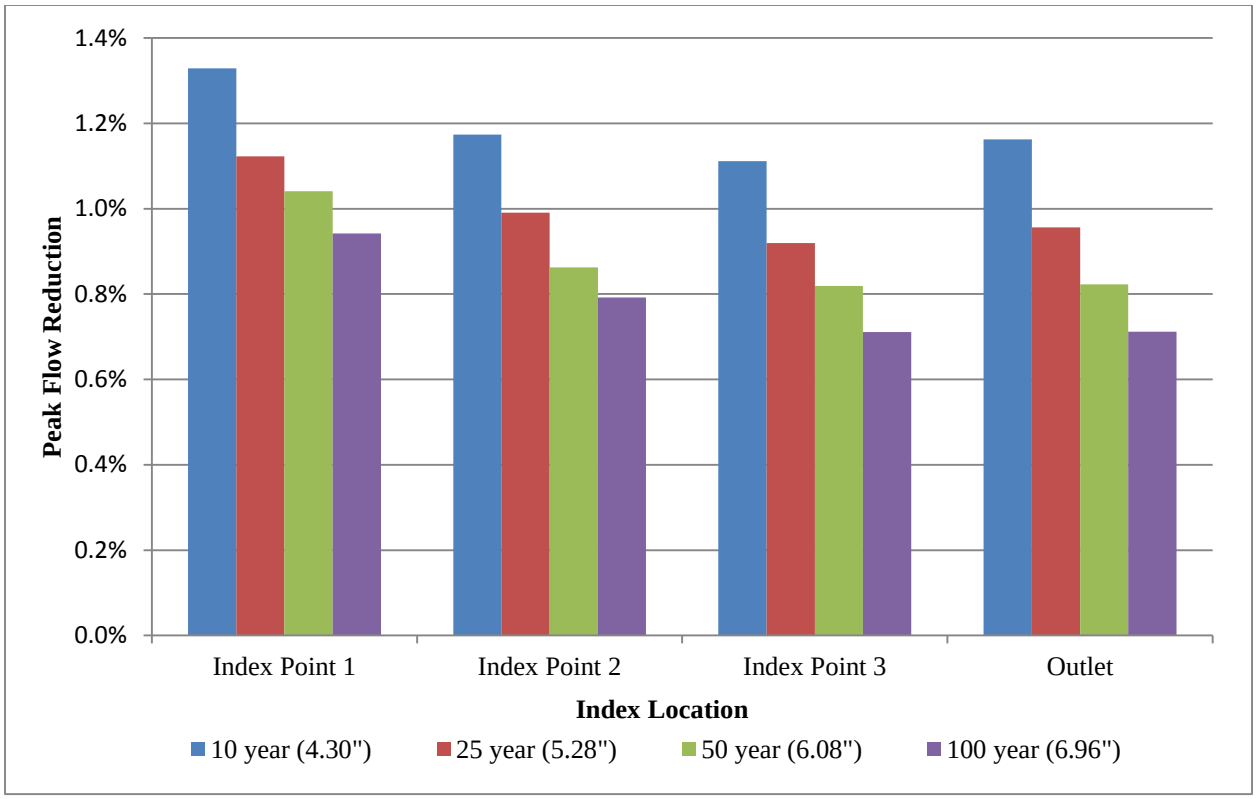

Figure 6.19 Percent reduction in peak flow for the increased infiltration scenario due to land use changes (adjusted other parameters estimated by CNs). Peak flow reduction at four index locations progressing from upstream (left) to downstream (right) are shown for four different 24-hour design storms.

6.3.2. Hypothetical Increased Infiltration within the Watershed: Improving Soil Quality

Another way to reduce runoff is to improve soil quality. Here, soil quality refers to the infiltration capacity of the soil. Better soil quality (increased soil infiltration characteristics) effectively lowers the runoff potential of the soil. If soil quality throughout the Soap Creek watershed were improved, it could potentially reduce flood damages.

To simulate improved soil quality with the HMS model, we hypothesize that improvements translate to changes in the NRCS hydrologic soil group. As discussed previously, NRCS rates the runoff potential of soils with four hydrologic soil groups (A through D). Type A

soils have the lowest runoff potential, and type D soils have the highest runoff potential. The NRCS relies primarily on three quantities to assign a hydrologic soil group: saturated hydraulic conductivity (the rate water flows through the soil under saturated conditions), which corresponds to the minimum infiltration rate, depth to an impermeable layer, and depth to the ground water table (Hoeft, 2007). Soils with a greater saturated hydraulic conductivity, or greater depth to an impermeable layer or ground water table, are assigned to a hydrologic soil group of lower runoff potential. To increase infiltration into the soil, one or more of these three quantities must be targeted. Obviously, the removal of all poorly draining soils throughout the watershed and replacement with higher infiltrating soils (e.g., sands and gravels) is unrealistic. However, certain conservation and best management practices, such as increasing the organic material content in the soil and the introduction of cover crops, could aid in improving soil infiltration to some degree.

In the HMS model of the Soap Creek Watershed, the effects of improved soil quality through conservation and best management practices are represented by changes in the NRCS hydrologic soil group. The most dominant soil type in the Soap Creek Watershed is Type D (including A/D, B/D, C/D), which makes up 58.4% of the area. In this case, improved soil quality is assumed to improve all Type D soils (clay) to Type C (loam containing silt and/or clay). Therefore, we generated a new Curve Number grid based on this new soil type and assigned it to each subbasin. Then, we ran the model with no ponds incorporated for a set of design storms and made comparisons between current and improved soil quality scenarios for the 10-, 25-, 50-, and 100- year return period 24-hour SCS design storm. As in the case of the prairie land use change, we used two methods to represent changes in soil quality. The first method considers only changes in runoff potential, and the second method considers both changes in

runoff and travel times with soil improvement.

For the first method, Figure 6.20 compares the simulated flood hydrographs for the current soil condition (baseline) to those for the soil improvement case (scenario) for the 50-year return period 24-hour design storm (6.08 inches of rain in 24 hours). For the 50-year design storm, the simulated soil condition infiltrates 0.33 inches more water into the ground than the current condition. For all four index locations shown–from upstream (Index 1) to the outlet of Soap Creek – the peak discharge reduction is relatively uniform (8.7% to 10.6%). The outcome reflects the relatively even distribution of Type D soils throughout the watershed. Figure 6.21 shows the percent reductions in peak flow that result from the first soil improvement case at the four index locations for all four design storms. The peak flow reduction is greatest for smaller storms and decreases systematically as rainfall increases. For the 10-year design storm, the peak reduction is between 12.1 and 14.7%. For the 100-year design storm, the peak reduction drops to between 7.8 and 9.2%.

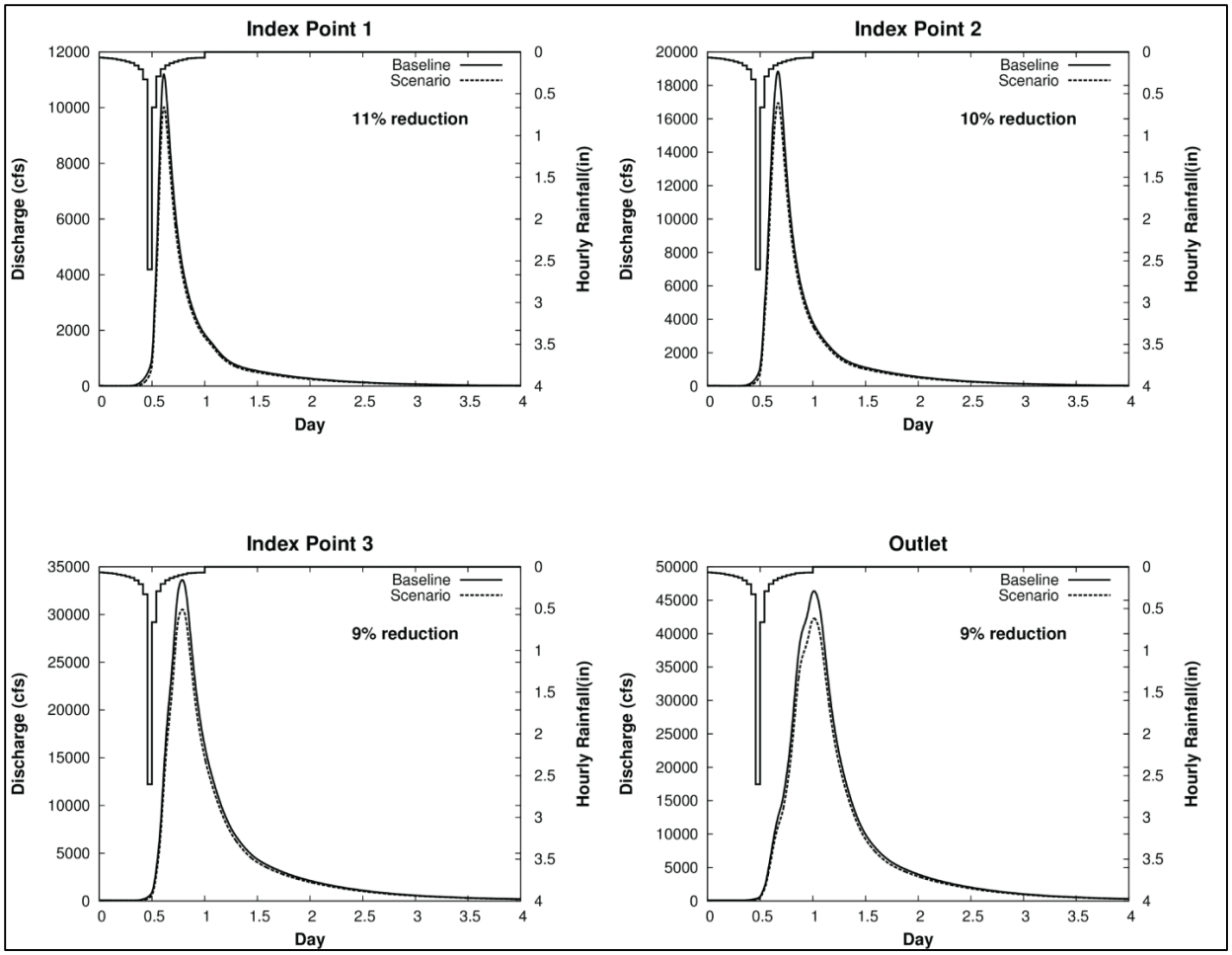

Figure 6.20 Hydrograph comparison at several locations for the increased infiltration scenario due to soil improvements (changes in runoff potential only). Improved soil quality was represented by converting all Hydrologic Group D (includes A/D, B/D and C/D) to C. Results shown are for the 50-year 24-hour storm (6.08 inches of rain).

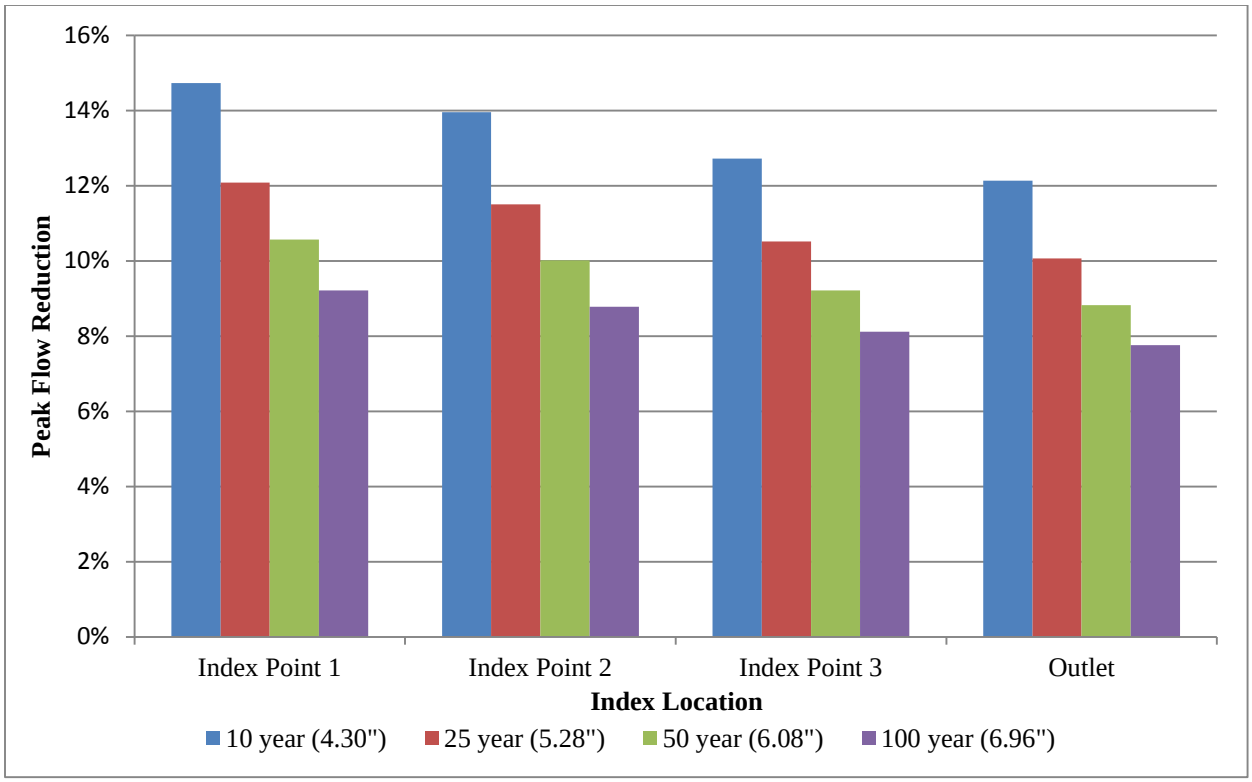

Figure 6.21 Percent reductions in peak flow for the increased infiltration scenario due to soil improvements (changes in runoff potential only). Improved soil quality was represented by converting all Hydrologic Group D (also includes A/D, B/D and C/D) to C. Peak flow reductions at four locations progressing from upstream (left) to downstream (right) are shown for four different 24-hour design storms (6.08 inches).

Figures 6.22 and 6.23 show the comparison results created by the second method, which accounts for both changes in runoff potential and travel times with soil quality improvements. Similar to the results seen for the transformation to a prairie landscape, adding the effects of travel time to the simulation has a small impact at upstream locations only. As Figure 6.22 shows, the peak flow reduction at Index Point 1 increases from 10.5 to 16.4%. There is also a slight reduction at Index Point 2. However, at the two downstream locations, the slower moving water produces no significant peak flow reduction. The same trends are also observed for both smaller (10- and 25- year) and larger (100-year) design storm events (see Figure 6.23).

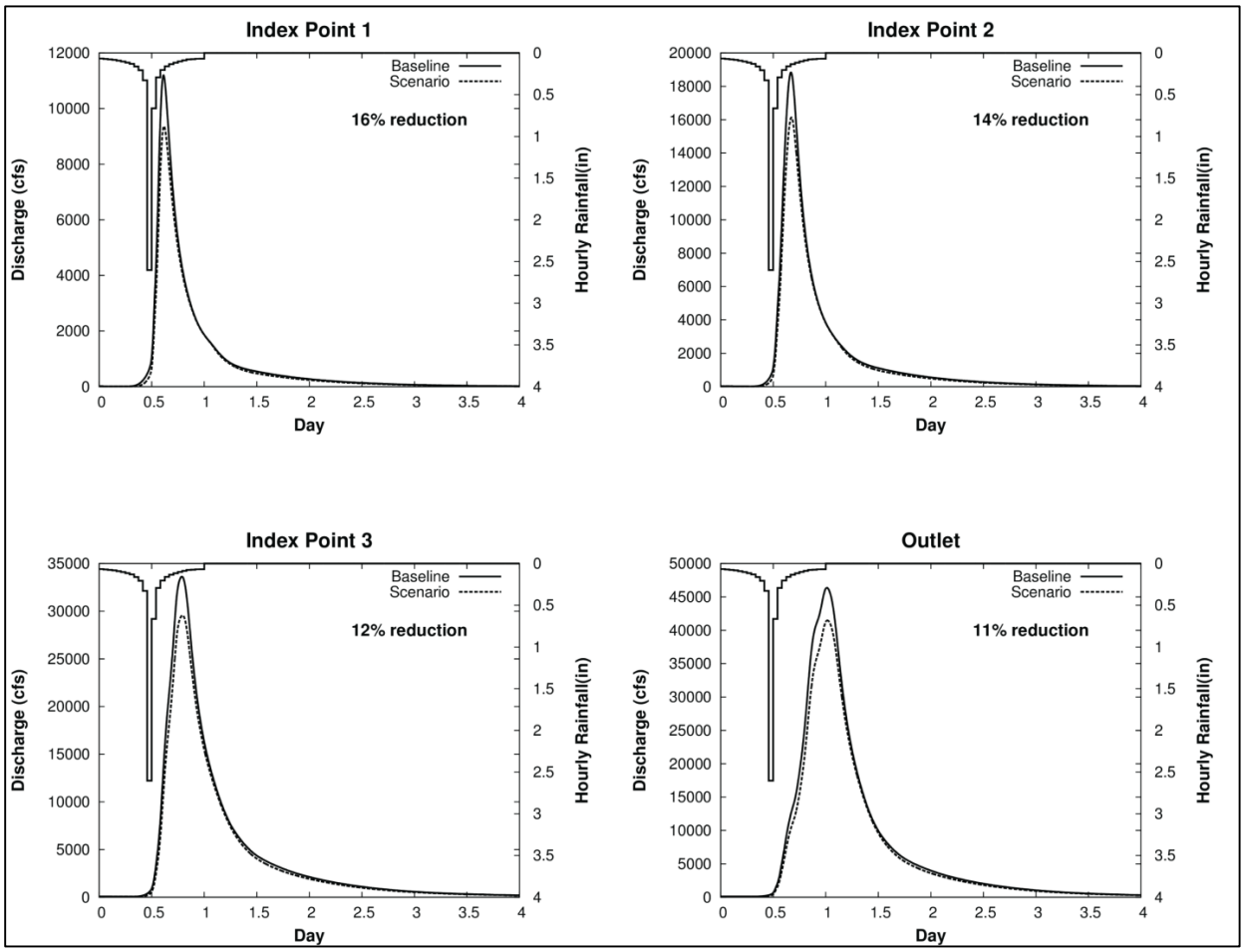

Figure 6.22 Hydrograph comparison at several locations for the increased infiltration scenario due to soil improvements (changes in runoff potential and travel times with soil quality improvements). Improved soil quality was represented by converting all Hydrologic Group D (includes A/D, B/D and C/D) to C. Results shown are for the 50-year 24-hour storm (6.08 inches of rain).

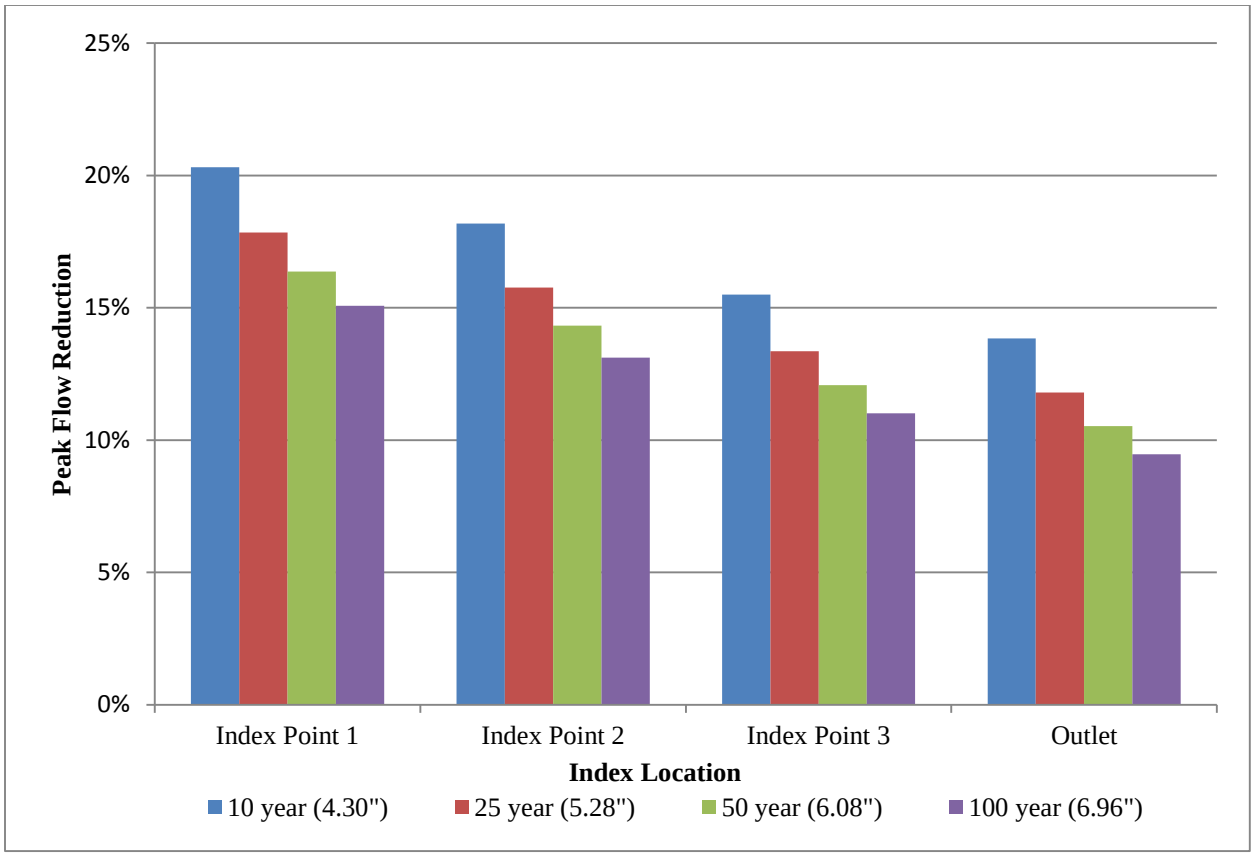

Figure 6.23 Percent reductions in peak flow for the increased infiltration scenario due to soil improvements (changes in runoff potential and travel times with soil quality improvements). Improved soil quality was represented by converting all Hydrologic Group D (including A/D, B/D, and C/D) to C. Peak flow reductions at four locations progressing from upstream (left) to downstream (right) are shown for four different 24-hour design storms (6.08 inches).

6.4. Comparison of Results Generated from HEC-HMS and HEC-RAS Models

The comparison of results produced by the HEC-HMS and the HEC-RAS models is meant to illustrate how the different routing methods will affect the hydrograph predictions. Recall that flow routing is the process of predicting the shape of a hydrograph at a particular location downstream when given an upstream hydrograph (see Figure 6.24). The HEC-HMS and HEC-RAS use the hydrologic and hydraulic routing methods, respectively.

The hydrologic routing method, known as the Muskingum routing method, uses only the

continuity equation but makes simplified assumptions. On the other hand, the hydraulic routing method uses the continuity equation as well as the momentum equation, which accounts for the actual physics of water movement in the channel.

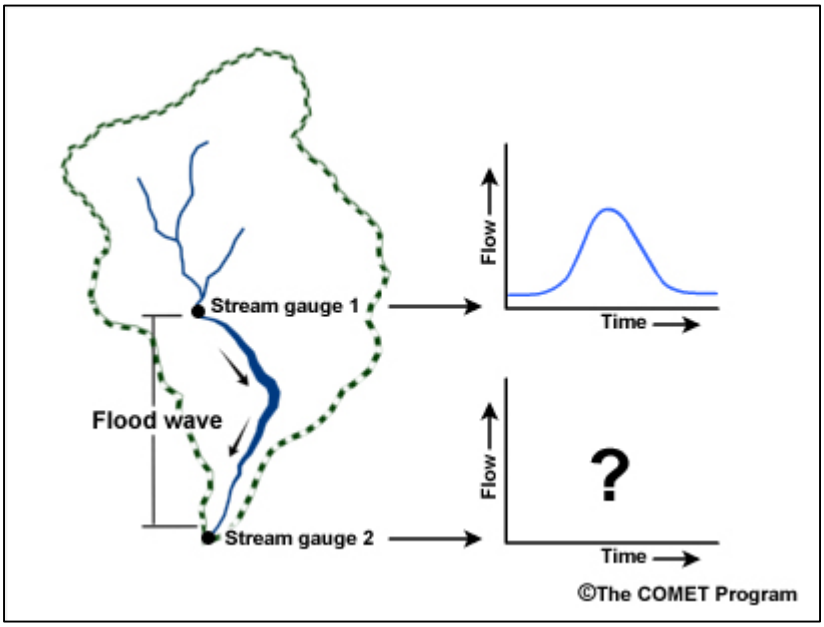

Figure 6.24 Concept of general flow routing (produced by the COMET Program).

In order to identify how different the results could be from hydrologic and hydraulic routing methods, we selected two storms for this study: one is the 100-year 24-hour design storm (6.96 inches of rainfall), and the other is the historic storm that occurred during the April 17-20, 2013 time period. After running the simulations with the HEC-HMS model with 132 ponds incorporated, the flow hydrographs resulting from each simulation can be exported as a DSS format and be read directly by the HEC-RAS model as boundary conditions.

Table 6.6 shows the drainage area of locations where the IFC stream stage sensors are installed (see Figure 3.8). This table also lists the peak discharges, volumes, and peak time differences computed by the HEC-HMS and the HEC-RAS models for the 100-year 24-hour

design storm (6.96 inches). The volumes indicated describe the total volume of water passing through these four locations during the simulation. The water volume under both HEC-HMS and HEC-RAS hydrographs has to be conservative before making any comparison between them. The volume of water passing through a given location does not match perfectly between the two programs. There are two main reasons. First, the base flows we assumed for the HEC-HMS and HEC-RAS models are slightly different. As we described in the Chapter 5, the base flows in the HEC-RAS model were set up with higher values than the ones in the HEC-HMS model in order to prevent drying and numerical instability during the simulation. Second, the drainage areas defined for each location in these two models are slightly different. The HEC-HMS model provides the hydrographs for a given point, while the HEC-RAS provides the hydrographs for a given cross section. Therefore, two representing a given sample point hydrographs are not precisely collocated. As a result, there are some slight differences in volume between the two models. At all four locations considered, differences in total volume were less than 1%, which is negligible.

Table 6.6 Results comparison at four different locations for the 100-year 24-hour storm (6.96 inches).

		HEC-HMS		*HEC-RAS*		*Results Comparison*		
Location	Drainage Area (acre)	Peak Flow (cfs)	Volume (ac-ft)	Peak Flow (cfs)	Volume (ac-ft)	Peak Time	Volume Difference (%)	Peak Flow Difference (%)
LTLSOAP01	27,591	8,680	9,461	6,213	9,479	3 hours 29 mins delayed	0.20	28.4
SOAPCR01	137,113	34,651	52,322	19,767	52,489	9 hours 44 mins delayed	0.32	43.0
SOAPCR02	79,863	22,828	31,383	16,700	31,375	5 hours 47 mins delayed	-0.02	26.8
SOAPCR03	24,971	10,167	10,002	8,153	100,10	1 hour 11 mins delayed	0.08	19.8

We compared the hydrographs associated with the 100-year 24-hour storm generated from the HEC-RAS model to those computed by the HEC-HMS model at four different locations

(see Figure 6.24). The hydrographs computed from the hydraulic routing method are much flatter, have lower peaks, and have a delayed time-to-peak relative to the hydrologic routing. The largest difference in peak discharge, 43.0%, is at SOAPCR01. The smallest difference in peak discharge, 19.8%, occurs at SOAPCR03. The peak discharged reduction increases as the water moves downstream because water that has to travel longer in the stream channel results in more attenuation.

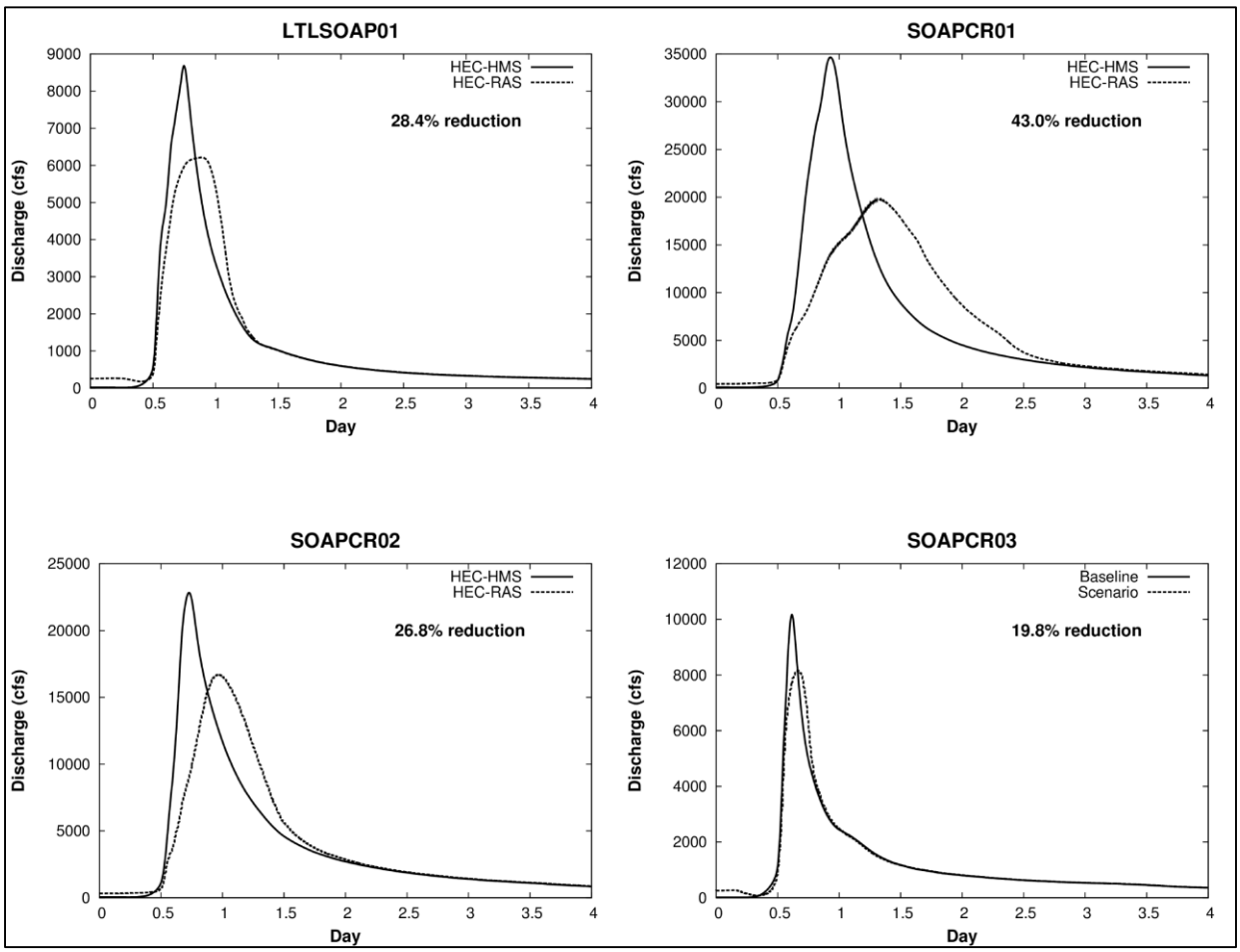

Figure 6.25 Hydrograph comparison at several locations for the Soap Creek river system - 100-year 24-hour storm (6.96 inches of rain).

We also simulated another storm, which happened during April 17-20, 2013, with the HEC-RAS and HEC-HMS models. Figure 6.25 shows the flow hydrographs generated from

these two models as well as the stage hydrographs recorded by the IFC stage sensors during the event. Table 6.7 summarizes the peak discharge, direct runoff volume, and time of peak simulated by these two models. The volume differences also remained under 1%.

Table 6.7 Results comparison at four different locations for the April 17-20, 2013 storm.

		HEC-HMS		*HEC-RAS*		*Results Comparison*		
Location	Drainage Area (acre)	Peak Flow (cfs)	Volume (ac-ft)	Peak Flow (cfs)	Volume (ac-ft)	Peak Time	Volume Difference (%)	Peak Flow Difference (%)
LTLSOAP01	27,591	3,532	4,705	3,387	4,735	2 hours 38 mins delayed	0.63	-4.1
SOAPCR01	137,113	16,312	27,487	10,038	27,274	6 hours 19 mins delayed	-0.78	-38.5
SOAPCR02	79,863	10,213	16,924	8,295	19,998	9 hours 3 mins delayed	0.43	-18.8
SOAPCR03	24,971	3,330	4,921	3,228	4,961	8 hour 8 mins delayed	0.82	-3.1

Similar to the 100-year 24-hour design storm simulation, the HEC-RAS model also predicted smaller peak discharges than the HEC-HMS model. However, the differences at LTLSOAP01 and SOAPCR03 are very small, 4.1% and 3.1%, respectively. As Figure 6.25 shows, the discharge hydrographs generated from the HEC-HMS and HEC-RAS models aligned very well at LTLSOAP01 and SOAPCR03 because these two sensors are located in the upstream area of Soap Creek. As a result, water travels a shorter distance and leads to less attenuation of the peak discharge. Figure 6.25 also plots the observed stage hydrographs and demonstrates that the peak time of hydrographs computed by the HEC-HMS model show a better match with the observed stage hydrograph as compared to the hydrographs computed with the HEC-RAS model. These results demonstrate that the average velocity of flow computed by the hydraulic routing method is underestimated.

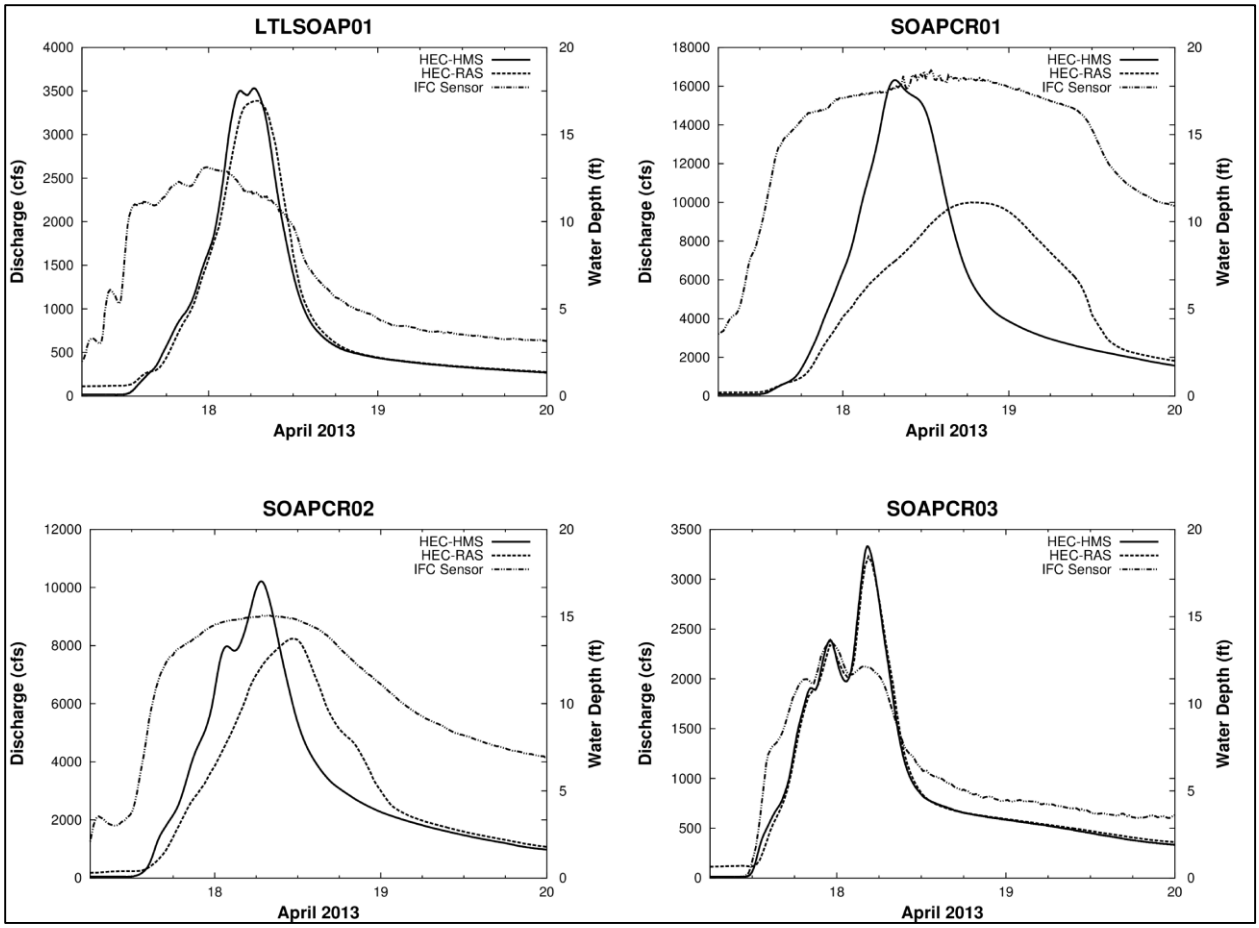

Figure 6.26 Hydrograph comparison at several locations for the Soap Creek river system and the stage hydrograph recorded by the IFC gages for the April 17-20, 2013 storm.

One objective of this study is to evaluate the benefits that a system of detention basins could bring to the downstream area of the Soap Creek Watershed. We accomplished this goal by using the HEC-HMS model. However, in this chapter, we learned that the hydrographs predicted by the hydraulic routing method are different from the ones resulting from the hydrologic routing method. Theoretically speaking, the hydraulic routing method should perform better than the hydrologic routing method, as it incorporates physical characteristics of the channels. Therefore, it is valuable for us to evaluate the benefits of the pond system that are estimated by the HEC-RAS model. Figure 6.26 compares the flood hydrographs that are simulated by the HEC-RAS

model for the no ponds condition (Without Ponds) to those with 132 built ponds (With Ponds) for the 100-year 24-hour design storm (6.96 inches). The peak flow reduction ranges from 23%-37%.

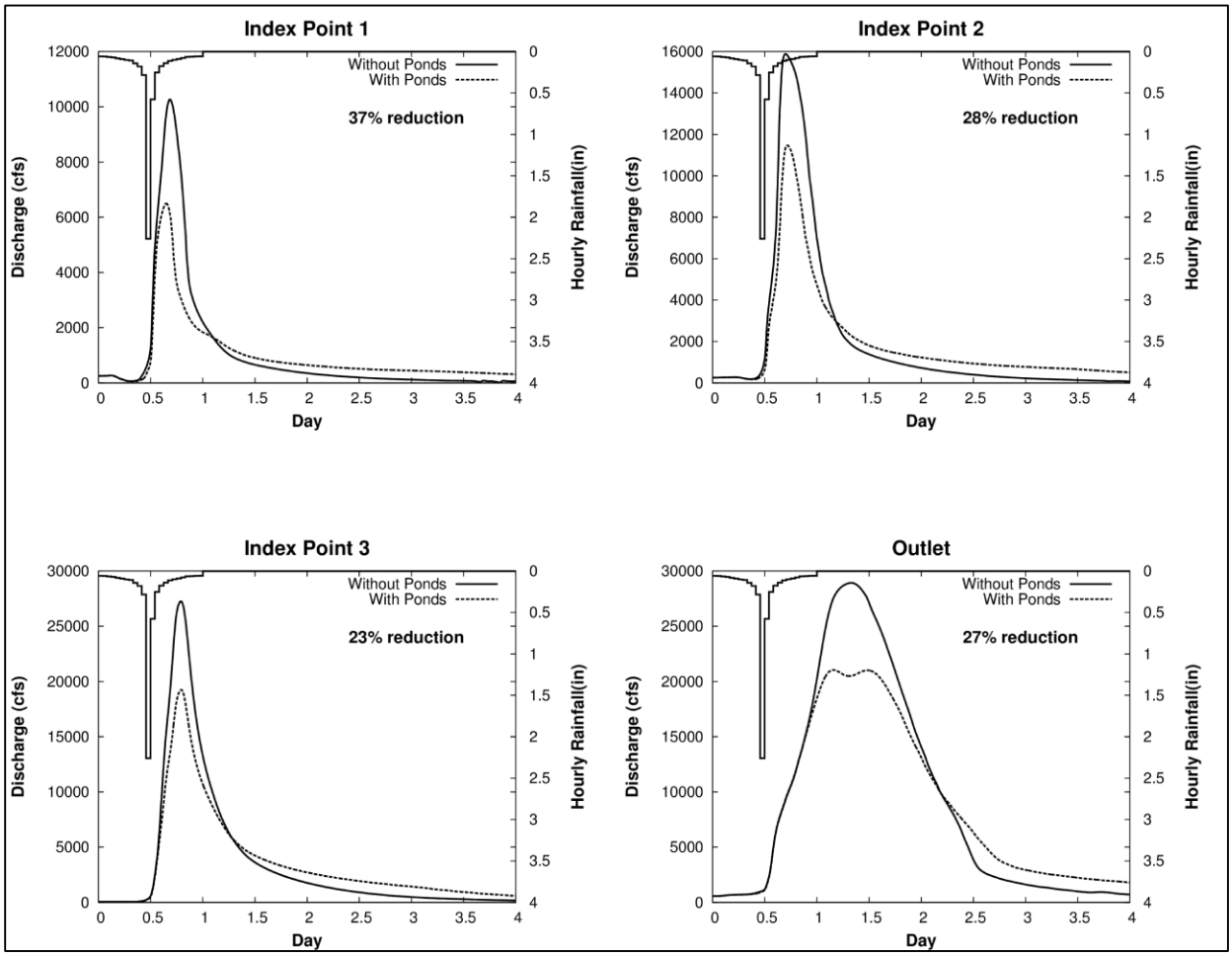

Figure 6.27 Hydrograph comparisons with 132 ponds and without ponds for the 100-year 24-hour design storms (6.96 inches) computed by the HEC-RAS model.

Figure 6.27 shows that peak discharge reductions result from the 132 ponds at the four index points for the 100-year 24-hour design storm computed by the HEC-HMS and the HEC-RAS models. The results from the HEC-HMS and the HEC-RAS models are similar and prove that these 132 detention ponds can significantly reduce the peak discharges into the downstream area of the Soap Creek Watershed.

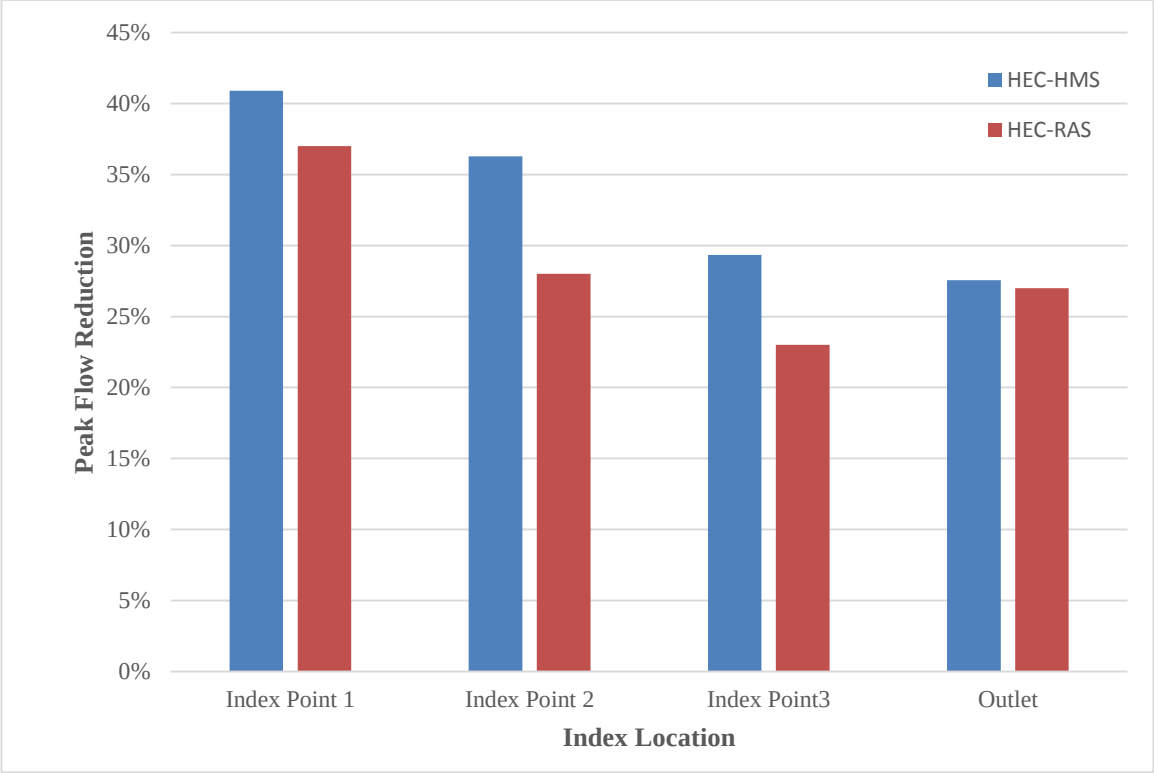

Figure 6.28 Peak discharge reductions for the HEC-HMS model with ponds and the HEC-RAS model with ponds built before 2013 for the 100-year 24-hour design storm (6.96 inches).

6.5. Chapter Summary

This chapter introduced several ways to make use of the HEC-HMS and HEC-RAS models for the Soap Creek Watershed. We used the HEC-HMS model to better understand the flood hydrology of the Soap Creek Watershed and to evaluate potential flood mitigation strategies. We first assessed the flood mitigation effects of the ponds that have been constructed within the Soap Creek Watershed. We then simulated flow throughout the watershed for the 10-, 25-, 50-, and 100-year recurrence interval 24-hour design rainfalls. These events correspond to rainfall amounts of 4.30, 5.28, 6.08, and 6.96 inches in 24 hours over the entire Soap Creek Watershed. The simulation results shows that pond construction can significantly reduce the

peak discharges for 10-, 25-, 50-, and 100-year 24-hour design storms. The peak flow reduction ranges from 28 – 40% at four index point locations for all four design storms. The simulation results also indicate that the ponds' effectiveness varies based on their sizes and locations. We also used the HEC-HMS model to identify high runoff potential areas in Section 6.2. Additional pond construction in these areas has the greatest potential downstream flood benefits.

We also evaluated two hypothetical flood mitigation strategies: restoring the majority land use of the Soap Creek Watershed (agriculture) back to the primitive prairie and improving the soil quality of the Soap Creek Watershed by converting all of the type D soil with high runoff potential to type C soil with lower potential runoff. We also simulated the effects of these two strategies for the four design flood events: 10-, 25-, 50-, and 100-year recurrence interval 24-hour design rainfalls. The simulation results illustrated that changing the land use within the Soap Creek Watershed will not significantly reduce the peak discharges. Land use changes only resulted in a less than 1.0% reduction in peak discharges. Hypothetical improvements to soil quality had better performance, resulting in an approximately 10% reduction of peak discharges.

The last section of this chapter compared results from the HEC-HMS model with those from the HEC-RAS model in order to illustrate the difference between the hydrologic and the hydraulic routing methods. We simulated two storms: the 100-year 24-hour design flood event and a real event that occurred in April of 2013. The simulation results demonstrate that the hydraulic routing method cause more attenuation as compared to the hydrologic routing method. In addition, we also used the HEC-RAS model to estimate the benefits that the 132 detention ponds bring to the downstream areas of the Soap Creek Watershed. The results estimated by the HEC-RAS model are consistent with those estimated by the HMS-HMS model, which indicates that the ponds are very effective in reducing flooding throughout the watershed.

CHAPTER 7. SUMMARY AND CONCLUSION

This thesis presents the development of HEC-HMS and HEC-RAS models for the Soap Creek Watershed and their various applications. We developed the HEC-HMS model, a hydrologic model that simulates event-based watershed-scale rainfall runoff processes, as part of the Iowa Watersheds Project. The HEC-HMS model incorporates several data sources, including Lidar DEM with 1-meter resolution, land use, soil type, and radar rainfall data produced by NCEP. Due to limited historical flow data, the calibration of the HEC-HMS model of the Soap Creek Watershed was challenging. Since no USGS stream gages are present in the watershed and IFC stage sensors have only recently been installed, we could not calibrate the model to historical observations. In order to calibrate this model, we created another HEC-HMS model for the Fox River Watershed, which has similar hydrologic characteristics. The Fox River Watershed has one USGS stream gage with a six-year period of record. We used six historical storm events occurring between June 2008 and May 2013 to calibrate and validate the Fox River Watershed model. We then transferred the calibrated Fox River Watershed parameters to the Soap Creek Watershed model and used the Soap Creek Watershed model to assess the cumulative benefits a series of ponds could bring to the watershed, to identify the runoff potential areas, and to evaluate the effectiveness of alternative flood mitigation strategies. We simulated four different design storms in the model: 24-hour duration storms for return periods of 10, 25, 50, and 100 year rainfall events, which correspond to rainfall depths of 4.30”, 5.28”, 6.08”, and 6.96”, respectively. Furthermore, instead of using the traditional 5-day antecedent rainfall total, we used the more flexible API in our research to more accurately represent soil moisture conditions before the storms.

Another important objective of this project was to compare hydrologic and hydraulic

routing methods. We developed a HEC-RAS hydraulic model for several major streams in the Soap Creek Watershed and used it to simulate the unsteady flow throughout the river network. We then compared the HEC-HMS and HEC-RAS results as well as the observed data from the IFC Stage Sensors for the 100-year 24-hour design storm and the April 17-20, 2013 historical storm.

7.1. Effects of Existing Ponds

The simulation results for the pond scenarios demonstrate their efficiency and effectiveness as a flood mitigation strategy. The ponds are highly effective in reducing flood peaks throughout the watershed and are most effective in reducing flood peaks immediately downstream of their locations. Further downstream, flood detention in the ponds is also realized, although with less impact. Floodwaters originating from watershed areas with and without ponds arrive at significantly different times. The result is that the storage effect from controlled areas is spread out in time instead of being concentrated at the time of highest flows. Hence, as one moves further downstream in the watershed, the flood peak reduction of storage ponds slowly diminishes. Owing to their hydraulic design, the ponds were equally effective in reducing peak discharge for the smallest (10-year) and largest (100-year) design storms that were simulated. Peak reductions ranged from 40% at the most upstream site to about 28% at the outlet. For the 100-year design storm, almost all of the ponds (121 out of 132) completely utilize all their flood storage and flow over their emergency spillways. Therefore, one could anticipate that for floods much larger than the 100-year design storm, the peak reduction effect of the system of ponds might begin to decrease.

7.2. Increased Infiltration in the Watershed: Land Use Changes

The changes in land use due to human activity significantly affect hydrological processes because they affect watershed infiltration. In a hypothetical simulation, all row crop agricultural land use, which accounts for 14% of the landscape, was converted to native-tall grass prairie. From the simulation results, changing agricultural lands to native tall-grass prairie is not an effective strategy for reducing peak flows in the Soap Creek Watershed. Simulated peak flow reductions range from about 0.7% (at the outlet) to about 1.2% (at index point 1). Only a relatively small portion of the current landscape has agricultural land use, and the basin's soils have naturally high runoff potential; as a result, changing from agricultural lands to tall-grass prairie do not significantly enhance infiltration. However, for very small drainages within the Soap Creek Watershed where the land use is predominately agricultural, there could be beneficial localized reductions in peak flows with upstream changes to prairie land use.

7.3. Increased Infiltration in the Watershed: Improve Soil Quality

Even without changes to land use, the storage capacity of the soil could be increased by improving soil quality to enhance infiltration. The hypothetical improved soil quality scenario suggests that it is a much more effective strategy than land use change. For the 50-year design storm, the improved soil quality scenarios predict an increased infiltration of 0.36 inches. The peak flow reduction effect of improved soil quality is greatest for smaller storms and decreases systematically as storm rainfall increases. For the 10-year design storm, the peak reduction is between 13.8 and 20.3%. For the 100-year design storm, the peak reduction drops to between 9.5 and 15.1%. For the Soap Creek Watershed, with its current mix of forest, undeveloped, and agricultural lands, efforts to improve soil quality can be an effective part of a watershed-wide flood mitigation strategy.

7.4. Comparison between hydrologic and hydraulic routing methods

The hydrologic and the hydraulic routing methods are two different ways to predict the movement of water through the channel networks. We simulated a 100-year return period 24-hour design storm and the April 2013 historical storm and then used the HEC-HMS model to generate hydrographs for these two storms. We then used the output from HEC-HMS to provide inflow boundary conditions to the HEC-RAS model. Generally, the hydraulic routing method predicted lower peak discharges and a longer time base of the hydrograph than the hydrologic routing method. The percent change in peak discharges from the HEC-HMS model to the HEC-RAS model ranges from 19.8%-43.3% for the 100-year 24-hour design storm and ranges from 3.1%-38.5% for the April 17-20, 2013 event. However, these results are only applicable to our case, because the HEC-RAS results are depend upon the HEC-HMS results. This means that if we assumed a lower flow velocity for the hydrologic routing method, the comparison results might be completely different. We also used the HEC-RAS model to estimate the benefits that these 132 detention ponds bring to the Soap Creek Watershed. Similar to the HEC-HMS model simulation results, the HEC-RAS model also proves that the detention pond system can reduce the peak discharges significantly throughout the Soap Creek Watershed, which range from 23%-37%.

7.5. Future Work

As a final note, it is important to recognize that the modeling scenarios evaluate the hydrologic effectiveness of the flood mitigation strategies and not their effectiveness in other ways. For instance, while certain strategies are more effective from a hydrologic point of view, they may not be more effective economically. As part of the flood mitigation planning process, it is necessary to consider factors such as the cost and benefits of alternatives and landowners'

willingness to participate in addition to considering the hydrology.

Due to the lack of reliable observed stage hydrographs, we could not successfully calibrate the Soap Creek HEC-RAS model in this study. Future work can be done to collect reliable data, such as the stream bed elevations, at the four IFC Stage Sensors, which can then be used for model calibration. In addition, in this study, the HEC-RAS model is only calibrated to the Manning's roughness coefficient and the CNs. Future work should also evaluate the effects of other parameters, including the flow velocity assumed for the HEC-HMS model and the contraction and expansion coefficients of the bridges.

REFERENCES

Bárdossy, A. (2007) "Calibration of Hydrological model parameters for ungauged catchments." Copernicus GmbH on behalf of the European Geosciences Union.

Beck, Hylke E., Richard A. De Jeu, Jaap Schellekens, Albert I. Van Dijk, and L. A. Bruijnzeel. (2009). "Improving Curve Number Based Storm Runoff Estimates Using Soil Moisture Proxies." *IEEE Journal of Selected Topics in Applied Earth Observations and Remote Sensing* 2.4: 250-59.

Chow, V. T., Maidment, D., and Mays, L. (1988). *Applied Hydrology*. McGraw-Hill, Inc.

Emerson, C., Welty, C., and Traver, R. (2005). "Watershed-Scale Evaluation of a System of Storm Water Detention Basins." *J. Hydrol. Eng.*, 10(3), 237–242.

Frans, C., Istanbulluoglu, E., Mishra, V., Munoz-Arriola, F., and Lettenmaier, D. P. (2013). Are climatic or land cover changes the dominant cause of runoff trends in the Upper Mississippi River Basin? Geophysical Research Letters, Vol. 40 (17), doi:10.1002/grl.50262, 2013.

Gupta, H., Sorooshian, S., and Yapo, P. (2010). "Toward improved calibration of hydrologic models; Multiple and noncommensurable measures of information." *Water Resources Research*. 34(4), 751-763.

Huff, F. A., and Angel, J. R. (1992). *Rainfall Frequency Atlas of the Midwest*. Illinois State Water Survey, Champaign, Bulletin 71.

Hjelmfelt, A. T., Jr, Kramer K. A., and Burwell R. E. (1982). Curve numbers as random variables. In *Proceeding, International Symposium on Rainfall-Runoff Modelling*, Singh V. P. (ed.). Water Resources Publication: Littleton, CO; 365–373.

Kult, M. J. (2013). "Regionalization of hydrologic response in the Great Lakes Basin: Considerations of Temporal Variability." *Thesis and Dissertations*. Paper 124.

Kokkonen, T. S., Jakeman, A. J., Young, P. C., and Koivusalo, H. J. (2003). "Predicting daily flows in ungauged catchments: Model regionalization from catchment descriptors at the Coweeta Hydrologic Laboratory." North Carolina. *Hydrological Processes*, 17(11), 2219-2238.

Kaini, P., Artita, K., and Nicklow, J. (2007). "Evaluating Optimal Detention Pond Locations at a Watershed Scale." World Environmental and Water Resources Congress 2007: pp. 1-8. Doi:10.1061/40927(243)170.

May, L. W. (2010). *Water Resource Engineering*, John Wiley & Sons, Inc.

Larson, L. W. (1993). "The USA Flood of 1993." *Natural Disaster Survey Report*, National Weather Service, Kansas City, Missouri.

Linhart, S. M., Nania, J. F., Sanders, C. L., Jr., and Archfield, S. A., (2012). Computing daily mean streamflow at ungauged locations in Iowa by using the Flow Anywhere and Flow Duration Curve Transfer statistical methods: U.S. Geological Survey Scientific Investigations Report 2012-5232, 50 p.

Linsley, R. K., Kohler, M. A., and Paulhus, J. L. H. (1982). *Hydrology for engineers*. McGraw-Hill, New York, NY.

Madment, D. R. (1993). Handbook of Hydrology. McGraw-Hill, Inc. P10.1.

Madsen, H. (2003). "Parameter estimation in distributed hydrological catchment modeling using automatic calibration with multiple objectives." *Water Resources*. 26, 205-216.

Merz, R., and Blöschl, G. (2004). "Regionalisation of catchment model parameters." *Journal of Hydrology*, 287(1-4).

Meierdiercks, K. L., Smith, J. A., Baeck, M. L., and Miller, A. J. (2010). "Analyses of Urban Drainage Network Structure and its Impacts on Hydrologic Response," *Journal of American Water Resources Research*, 14(4), pp. 416-424.

Mejia, Ai. I., and Moglen, G. E. (2010). "Impact of the Spatial Distribution of Imperviousness on the Hydrologic Response of an Urbanizing Basin," *Hydrologic Processes*, 24, pp. 3353-3373.

Mora, C., Abby G., Frazier, A. G., Longman, R. J., Dacks, R. S., Walton, M. M., Tong, E. J., Sanchez, J. J., Kaiser, L. R., Stender, Y. O., Anderson, J. M., Ambrosino, C. M., Fernandez-Silva, I., Giuseffi, L. M., and Giambelluca, T. M. (2013). The projected timing of climate departure from recent variability, Nature, Vol 502(7470).

Oudin, L., Andreassian, V., Perrin, C., Michel, C., and Le Moine, N. (2008). "Spatial proximity, physical similarity, regression and ungaged catchments: A comparison of regionalization approaches based on 913 French catchments." *Water Resources Research*, 44(3), W03413.

Perica, Sanja, et al. "NOAA Atlas 14 Point Precipitation Frequency Estimates: IA." B *Hydrometeorological Design Studies Center: Precipitation Frequency Data Server*. NOAA, 2013. Web. Nov. 2013. <http://hdsc.nws.noaa.gov/hdsc/pfds/pfds_map_cont.html?bkmrk=ia>.

Perica, Sanja, et al. "NOAA Atlas 14 Point Precipitation Frequency Estimates: IA." *Hydrometeorological Design Studies Center: Precipitation Frequency Data Server*. NOAA, 2013. Web. Nov. 2013.

Ravazzani, G., Gianoli, P., Meucci, S., and Mancini, M. (2014). "Assessing Downstream Impacts of Detention Basins in Urbanized River Basins Using a Distributed Hydrological Model." *Water Resources Management*, (28)4, pp. 1033-1044.

Ryberg, K. R., Lin, W., and Vecchia, A. V. (2012). "Impact of Climate Variability on Runoff in

the North Central United States," Journal of Hydrologic Engineering, doi: 10.1061/(ASCE)HE.1943-5584.00000775.

Schilling, K. E., Chan, K-S., Jha, M. K., Zhang, Y-K., and Gassman, P. W. (2008). "Impact of Land Use and Land Cover Change on the Water Balance of a Large Agricultural Watershed: Historical Effects and Future Directions," Water Resources Research, 44, doi: 10.1029/2007WE006644.

Schilling, K. E., Chan, K-S., Liu, K-S., Zhang, Y-K., and Gassman, P. W. (2008). "Quantifying the Effect of Land Use Land Cover Change on Increasing Discharge in the Upper Mississippi River," J. Hydrology 387, pp. 343-345.

Schottler, S. P., Ulrich, J., Belmont, P., Moore, R., Lauer, J. W., Engstrom, D. R., and Almendinger, J. E. (2013). Twentieth century agricultural drainage creates more erosive rivers, Hydrol. Process. DOI: 10.1002/hyp.9738.

Singhofen, P. J., P.E. (2001). Calibration and Verification of Stormwater Models, http://www.streamnologies.com/support/pdfs/Calibration.pdf (December 27, 2013) Website 1: http://www.lakesundown.com/sundown/map.html.

Linhart, S. M., Nania, J. F., Sanders, Jr., C. L., and Archfield, S. A. (2010). Computing Daily Mean Streamflow at Ungaged Locations in Iowa by using the Flow Anywhere and Flow Duration Curve Transfer Statistical Methods: U.S. Geological Survey Scientific Investigations Report 2012-5232, 50 p.

Sanborn. (February 20, 2013.). LiDAR Products. Retrieved from Sanborn Total Geospatial Solutions: http://www.sanborn.com/products/lidar.

Scharffenberg, W. A., and Fleming, M. J. (2010). HEC-HMS User's Manual 3.5. August 2010.

Takle, E. S. (2010). "Was Climate Change Involved?" Chapter in A Watershed Year: Anatomy of the Iowa Floods of 2008, C. Mutel (editor), University of Iowa Press, Iowa City, IA. pp. 111 – 116.

The Iowa Department of Natural Resources - Iowa Geological &Water Survey (2014), http://www.igsb.uiowa.edu/browse/landform.htm.

United States Department of Agriculture-National Resource Conservation Service (December 1988). Soap Creek Watershed: Appanoose, Davis, Monroe &Wapello Counties, Iowa, pp.7-16.

United States Department of Agriculture-National Resource Conservation Service (2007). National Engineering Handbook. Part 630. Chapter 7. May 2007. http://directives.sc.egov.usda.gov/OpenNonWebContent.aspx?content=17757.wba.

Urbonas, B., and Glidden, M. W. (1981). "Potential effectiveness of detention policies." *Flood Hazard News,* Urban Drainage & Flood Control District.

Villarini, G., Smith, J. A., Baeck, M. L., and Krajewski, W. F. (2011). Examining Flood Frequency Distributions in the Midwest. *U.S. Journal of the American Water Resources Association* (JAWRA) 47(3): 447-463. DOI: 10.1111/j.1752-1688.2011.00540.x.

Wu, Y., Liu, S., Sohl, T. L., and Young, C. J. (2013). Projecting the land cover change and its environmental impacts in the Cedar River Basin in the Midwestern United States, Environmental Research Letters, 8(2).

Appendix A - Incorporated Structures

Table A.1 Structural Data of 132 Structured Ponds

Project	Drainage Area (mi^2)	Flood Storage (ac-ft)
26-127	0.531	85.74
26-32	0.146	15.51
26-33	0.077	8.18
26-34	0.469	67.68
26-36	0.525	79.30
26-37A	0.541	53.07
26-37B	0.198	17.88
26-38	0.471	84.40
26-39	0.412	62.83
26-44	0.488	188.94
26-49	0.360	54.88
26-51B	0.761	122.45
26-51C	1.147	198.35
26-52	0.377	64.05
26-53	0.193	16.76
26-55	1.784	769.24
26-58	0.427	70.91
26-63	1.853	307.43
26-64	0.237	28.97
26-65	1.942	308.81
26-66	0.235	23.60
26-67	0.219	30.07
26-68	0.328	40.35
26-71	0.375	54.13
26-73	0.102	10.65
26-74	0.344	48.58
4-109	0.245	34.97
4-110	0.780	118.68
4-111	0.273	35.85
4-112	0.371	51.63
4-113	0.764	122.23
4-114	0.194	30.90
4-31	1.831	319.25
4-35	0.464	66.39
4-36	0.230	31.47
4-37	0.121	16.14
4-38A	0.427	64.48

4-39	0.313	47.46
4-40A	0.298	46.13
4-40B	0.225	30.09
4-40C	0.156	17.41
4-44	0.250	40.13
4-48	0.100	10.62
4-53	0.098	9.04
4-54	0.144	14.70
4-55	0.098	9.11
4-55X	0.053	9.29
4-56	0.413	63.86
4-57A	0.216	126.11
4-57B	0.861	32.56
4-58	0.349	49.23
4-73	0.312	38.82
4-74	0.116	14.73
4-77	0.402	60.07
4-78	0.113	18.65
4-79	0.346	52.24
4-81	0.420	64.10
4-84	0.384	35.59
4-86	0.399	55.90
4-87	0.238	32.00
4-88	0.069	7.28
4-89	0.165	16.89
4-90A	0.500	78.74
4-90B	0.105	11.16
4-91	0.121	16.87
4-92	0.134	15.22
4-93	0.273	36.85
4-94	0.271	41.20
4-98	1.063	341.21
4-99	0.441	72.00
68-114A	0.138	17.51
68-114C	0.186	35.26
68-29	0.099	8.50
68-31	0.218	33.73
68-32	0.441	69.16
68-33A	1.293	295.22
68-33B	0.241	40.84
68-35	0.449	66.75

68-36	0.301	41.61
68-42	0.217	32.87
68-44	0.111	20.80
68-47	0.248	40.42
68-49	0.187	25.94
68-50	0.136	26.64
68-53	0.133	14.99
68-54	1.501	269.30
68-56	0.804	148.19
68-58A	0.100	9.58
68-58B	0.093	11.26
68-58C	0.070	6.37
68-58D	0.124	14.39
68-60	0.113	12.94
68-61	0.332	50.74
68-62	0.211	26.85
68-63	0.204	31.25
68-64A	0.189	24.01
68-64B	0.029	4.55
68-65	0.046	4.77
68-66	1.087	298.89
68-68	0.062	12.33
68-69B	0.198	22.66
68-70	0.099	15.55
68-71A	0.737	141.48
68-72	0.087	18.85
68-74	0.367	67.00
68-76A	0.183	26.88
68-76B	0.201	29.29
68-77	0.251	35.32
68-78	0.213	27.21
68-80	1.905	303.77
68-88	0.784	79.29
68-89	0.538	79.29
90-102	0.390	42.90
90-112	1.208	262.85
90-113	0.433	74.36
90-70	0.178	22.30
90-73	0.434	117.59
90-74	0.337	39.30
90-75	0.840	115.19

90-79B	1.363	260.11
90-79C	0.327	35.68
90-83	2.570	462.81
90-84	2.537	503.57
90-85	2.342	485.99
90-86	0.125	16.62
90-87	0.275	40.55
90-88	0.192	22.92
90-91	0.312	54.46
90-92	0.250	32.47
90-94	0.077	8.85
90-95	0.508	74.73
90-97	0.178	19.67

Appendix B – Maps for the Fox River Watershed

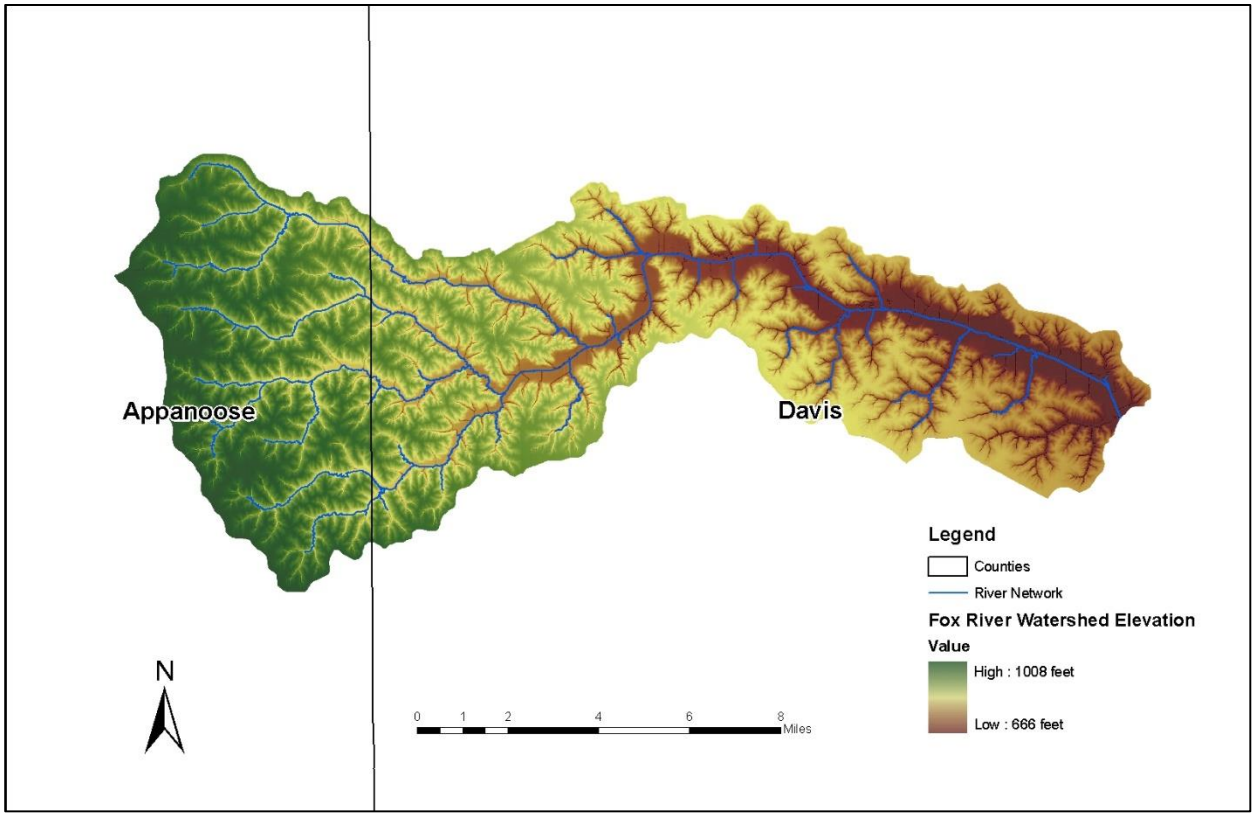

Figure B.0.1 Topography of the Fox River Watershed.

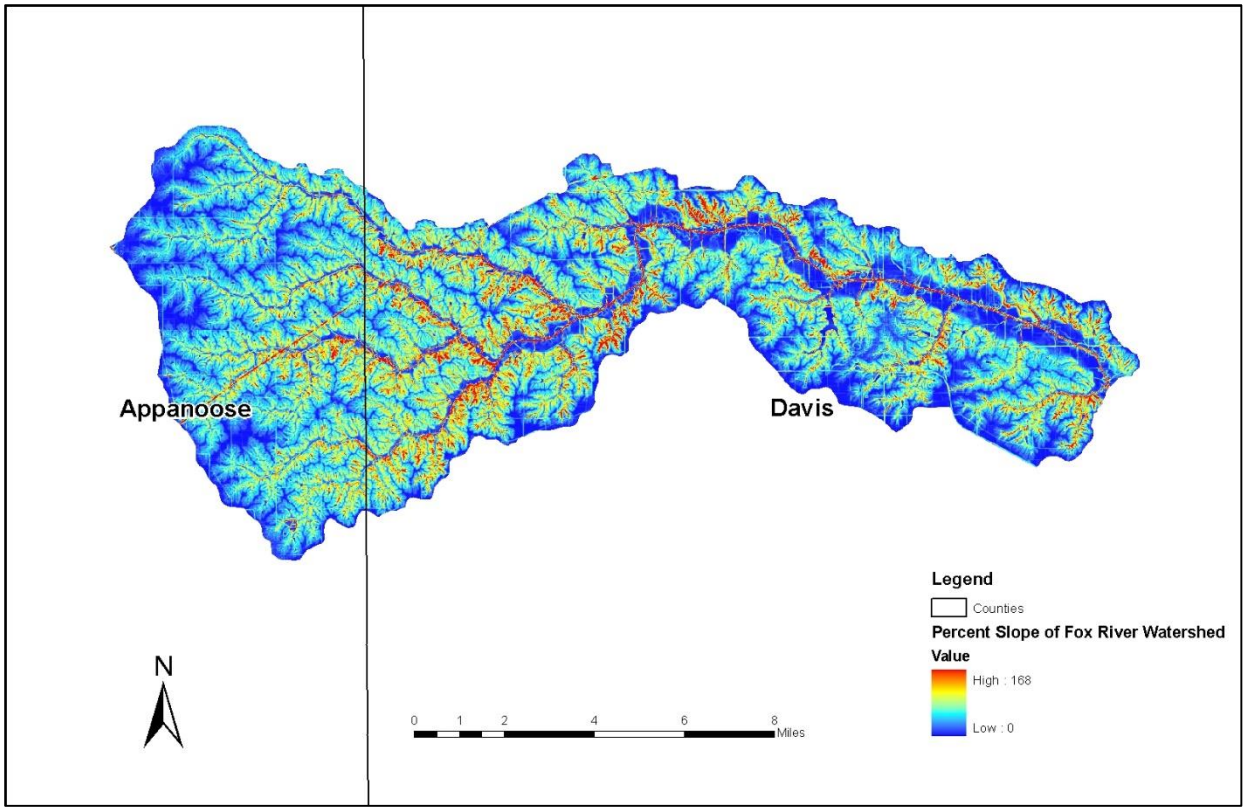

Figure B.0.2 Slope of the Fox River Watershed, Ranges from 0 to 168%.

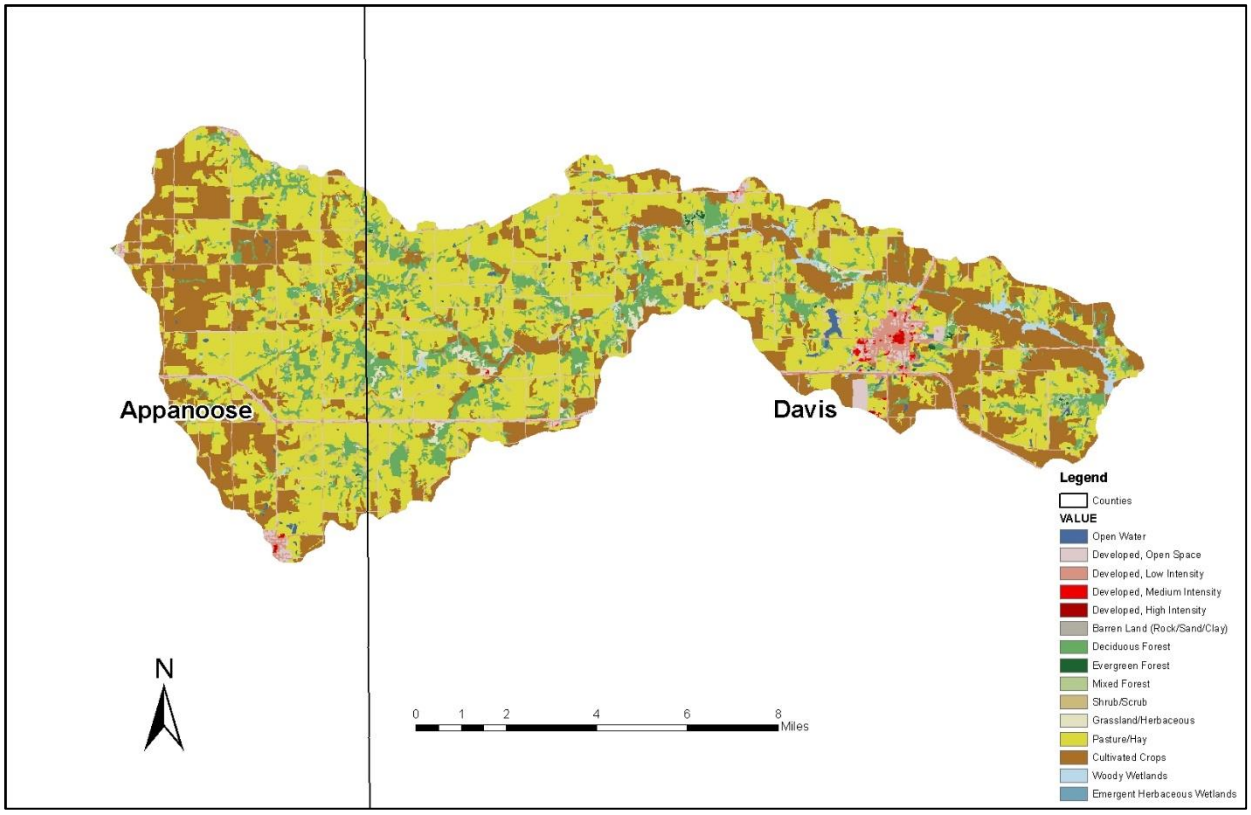

Figure B.0.3 Soil Distribution of the Fox River Watershed.

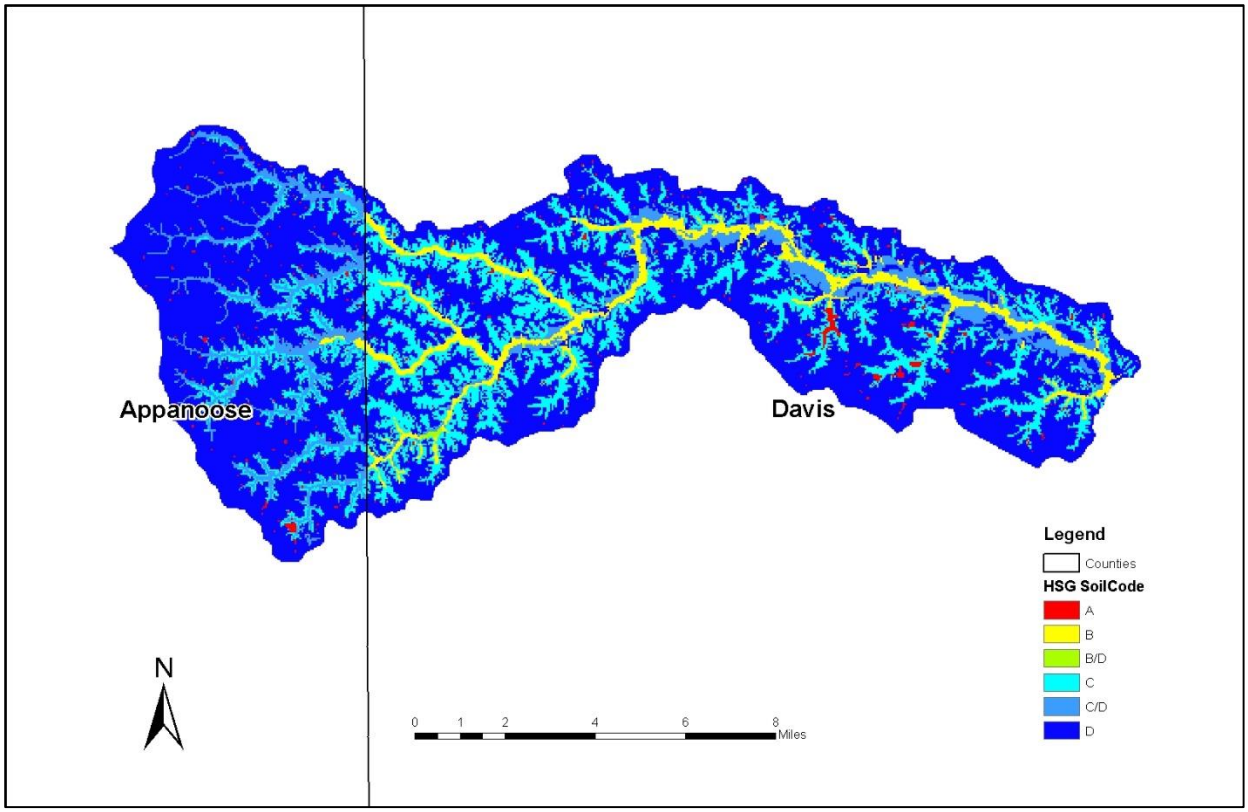

Figure B.0.4 Land Use Composition in the Fox River Watershed.

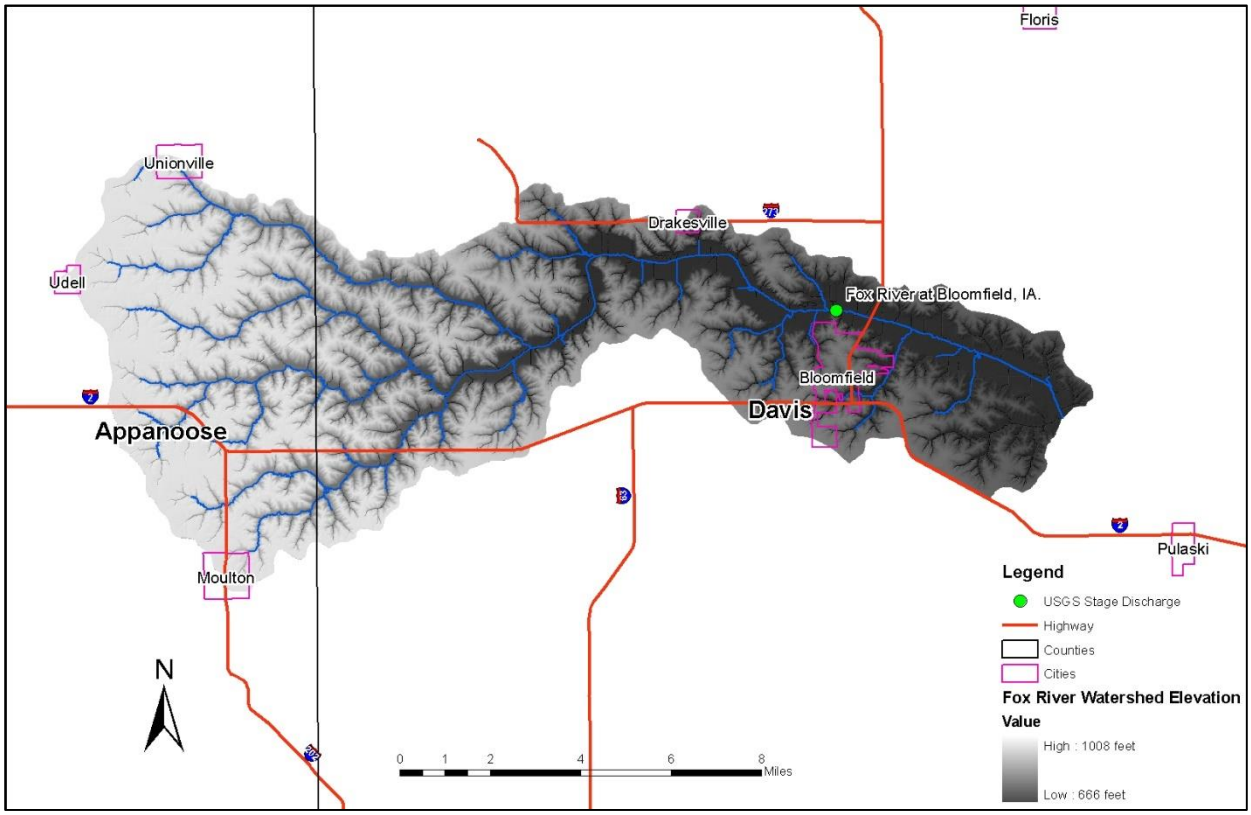

Figure B.0.5 USGS Stream Gage at Bloomfield in the Fox River Watershed.

Table B.2 Comparison of Elevation between the Soap Creek and Fox River Watersheds.

Elevation Comparison		
	Soap Creek	Fox River
Range	600 – 1023 feet	666 – 1008 feet

Table B.3 Comparison of Watershed Slope between the Soap Creek and Fox River Watersheds

Watershed Slope Comparison		
	Soap Creek	Fox River
Range	0% - 161 %	0% - 168 %

Table B.4 Comparison of Soil Type between the Soap Creek and Fox River Watersheds.

	Area Percentage of each soil type (%)	
Soil Type	Soap Creek	Fox River
A	~0	~0
A/D	~0	~0
B	8.9	5.4
B/D	0.3	0.1
C	32.7	21.8
C/D	10.0	8.5
D	48.1	64.2

Table B.5 Comparison of Land Use between the Soap Creek and Fox River Watersheds.

Original percentage of each land cover (%)		
Land Use Description	Soap Creek Watershed	Fox River Watershed
Open Water	1.1	0.6
Developed, Open Space	3.3	4.5
Developed, Low Intensity	0.6	1.9
Developed, Medium Intensity	~0	0.2
Developed, High Intensity	~0	~0
Barren Land (Rock/Sand/Clay)	~0	~0
Deciduous Forest	34.9	10.3
Evergreen Forest	0.4	0.2
Mixed Forest	3.6	1.2
Shrub/Scrub	1.5	1.2
Grassland/Herbaceous	4.6	0.9
Pasture/Hay	34.7	50.6
Cultivated Crops	13.9	27.2
Woody Wetlands	1.3	1.2
Emergent Herbaceous Wetlands	0.1	0.1